UNIVERSITEIT GENT

Faculteit Bio-ingenieurswetenschappen

Academiejaar 2013 – 2014

Linking plant-water relations to wood anatomical features of *Maesopsis eminii* under different water conditions to assess its drought resilience

Janne Van Camp

Promotors: Prof. dr. ir. Kathy Steppe
Prof. dr. ir. Joris Van Acker

Tutors: dr. ir. Hans Verbeeck
Msc. Jackie Epila

Masterproef voorgedragen tot het behalen van de graad van
Master in de bio-ingenieurswetenschappen: bos- en natuurbeheer

UNIVERSITEIT GENT

Faculteit Bio-ingenieurswetenschappen

Academiejaar 2013 – 2014

Linking plant-water relations to wood anatomical features of *Maesopsis eminii* under different water conditions to assess its drought resilience

Janne Van Camp

Promotors: Prof. dr. ir. Kathy Steppe
Prof. dr. ir. Joris Van Acker

Tutors: dr. ir. Hans Verbeeck
Msc. Jackie Epila

Masterproef voorgedragen tot het behalen van de graad van
Master in de bio-ingenieurswetenschappen: bos- en natuurbeheer

Ghent, June 2014

……

Prof. dr. ir. Kathy Steppe
Promotor

……

Prof. dr. ir. Joris Van Acker
Promotor

……

Janne Van Camp
Author

ACKNOWLEDGEMENTS

Graag zou ik enkele mensen bedanken die mij hebben bijgestaan en geholpen bij het realiseren van dit werk. Allereerst wil ik de docenten bedanken die mij tijdens mijn masterjaren vaak wisten te interesseren en inspireren. Een bijzonder dankwoord gaat naar mijn promotors Prof. dr. ir. Kathy Steppe en Prof. dr. ir. Joris Van Acker. De werking van planten en in het bijzonder bomen intrigeert mij enorm. Tijdens de lessen ecofysiologie ontdekte ik hoe je de processen die het fundamentele leven van deze organismen sturen kan bestuderen en zelfs modeleren. De lessen hebben me geïnspireerd bij de keuze van een thesisonderwerp. Ik wilde ook heel graag naar het Zuiden trekken in de hoop dat mijn thesis daar enige maatschappelijke relevantie zou hebben. Het onderzoek dat werd aangeboden, zou deze ecofysiologische aspecten omvatten. Zelf wilde ik heel graag ook de hout-anatomische kant van het verhaal bekijken, aangezien ook dit mij zeer sterk aanspreekt. Dankzij de samenwerking die ontstond tussen Prof. Kathy Steppe en Prof. Joris Van Acker kon ik mijn wetenschappelijke interessegebieden op een synergetische manier combineren. Het geplande veldwerk vond plaats in Uganda in de zomer van 2014. Bij het voorbereiden van zo een avontuurlijke onderneming werd ik met veel goede raad bijgestaan door dr. ir. Hans Verbeeck..

I would like to thank Msc. Jackie Epila and her family to welcome me in their house during my stay in Uganda. After long days of measurements I could always enjoy a tasteful Ugandan meal and sleep in a nice bed which I both deeply appreciate. The nice walks through the neighbourhood were always very welcome and relaxing moments. Although the field campaign was not always convenient, I am grateful for the opportunity I received to perform my first research abroad.

Wanneer ik een beetje teleurgesteld terugkeerde van de veldcampagne, gingen Prof. Kathy Steppe en dr. ir. Hans Verbeeck onmiddellijk akkoord om een nieuw experiment op te zetten en zij wisten mij meteen terug te motiveren zodat ik terug vol interesse in het onderwerp aan de slag kon gaan. Mijn tutor zat nog in het buitenland maar gelukkig kon ik rekenen op de vele enthousiaste doctoraatstudenten van het Labo Plantecologie. Ik denk hierbij in het bijzonder aan Elizabeth, Jasper en Jochen. Jochen heeft mij heel veel van de praktische kant van het onderzoek bijgeleerd en stond steeds om mijn vragen te beantwoorden en hulp te bieden. Ook de techniekers, Philip en Geert, wil ik heel graag bedanken. Nog voor ik zelf wist dat een extra experiment mogelijk was, stonden zij al in de serre alles voor te bereiden. Mijn dank gaat ook uit naar dr. ir. Jan Van den Bulcke bij wie ik terecht kon voor het houtanatomische gedeelte en het scannen van de staaltjes (en allerlei beeldverwerkingsproblemen op mijn niet-krachtige laptop en goede raad).

Ik wil ook mijn kotgenoten en mijn klasgenoten bedanken. We zaten in hetzelfde schuitje, hoorden elkaars verhalen aan en sleurden elkaar er wel door. Op kot moesten we dit jaar allemaal hard zwoegen en toch hebben we ons goed geamuseerd. Ik bedank ook mijn vrienden, die mij hebben gesteund en opgebeurd wanneer het even niet zo vlot ging.

Ik ben mijn ouders dankbaar om mij steeds te steunen. Dankzij hen kreeg ik de kans om te studeren en te worden wie ik wou. Zij ondersteunen mij in ieder avontuur dat ik onderneem. Ik bedank mijn ouders en mijn broers voor de vele aanmoedigingen doorheen het jaar.

Ten slotte wil ik mijn lief, Michiel, enorm bedanken. Vooral om in mij te blijven geloven, zeker op momenten dat ik dat zelf even niet deed. Maar ook voor het luisteren naar theorieën, mee redeneren, nalezen van grote brokken thesis en samenwerken tijdens de vroege tot heel late meetdagen in de serre.

TABLE OF CONTENTS

ABBREVIATIONS

A: cross-sectional area of the stem
c_s: specific heat of xylem sap
CT: computed tomography
DC: direct current
DD: diameter variation
DOY: day of year
dpi: dots per inch
dT: rise in sap temperature, ie temperature gradient over the sap flow sensor heater
e_a: actual vapour pressure
e_s: saturation vapour pressure
G: gravitational potential
IPCC: Intergovernmental Panel on Climate Change
K_{sh}: sheet condutance, ie thermal conductance for a specific gauge installation
K_{st}: thermal conductivity of the stem
LVDT: linear variable differential transformer
M: matric potential
MDS: maximum daily shrinkage
PAR: photosynthetic active radiation
P_{in}: power input
Q_d: downwards vertical conduction
Q_f: flow convection
Q_H: constant amount of heat supplied to the heater
Q_r: radial conduction
Q_u: upwards vertical conduction
Q_v: vertical conduction
R: resistance
RH: relative humidity
ROS: reactive oxygen species
r_s: stomatal resistance
SF: sap flow
SHB: stem heat balance
T_a: air temperature
UGCT: Centre for X-ray Tomography of the Ghent University
V: potential difference
VDC: volts of direct current
VPD: vapour pressure deficit
WC: water content
ΔV: volume difference
ΔW: weight difference
Π: pressure potential
ψ: water potential
ψ_{soil}: soil water potential
ψ_l: leaf water potential
ψ_x: xylem water potential
Ω: osmotic potential

SUMMARY

Experts on climate change predict longer periods of drought for extensive parts of the southern hemisphere. Already, more frequent and severe droughts have been recorded and the situation is still expected to deteriorate. The impact of this phenomenon on forests is uncertain. Forests ecosystems, serve as a source of subsistence and revenue for many people. This can be directly as shelter and via the products they deliver or indirectly for the entire world population through the manifold ecosystems they provide. To predict the impact of drought on tree and forest degradation, the fundamental effects of drought stress on the water relations and the anatomy of the plants need to be elaborated. *Maesopsis eminii*, the species selected for this research, is a key timber tree species in Uganda and is planted for firewood and other purposes in many other parts of the world. Drought stress, meaning that there is less water available in the soil, leads to numerous physiological and structural responses. Stomatal closure is an efficient short-term reaction to prevent a critical water loss. Under prolonged drought conditions water potential will continue to decrease leading to xylem embolism. The ecophysiological features are monitored on 14 juvenile *M. eminii* trees in a greenhouse experiment using specialised instrument. Seven of the trees were subjected to absolute drought during 14 days. Stomatal closure occurred rapidly after drought inducement, followed by the deactivation of the photosynthetic apparatus, wilting and eventually, leaf shedding. The inducement of drought caused a net decrease in diameter during the first days of drought. Remarkably, from the fourth day of drought a net swelling of the diameter was observed. Explanation of this occurrence was found in the daily course of stem diameter variation and sap flow of under control conditions. The observation of considerable predawn sap flow rates without sound indications of night time transpiration, suggests the capacity of *M. eminii* to use root pressure to build up notable sap flow rates. This root pressure is assumed to be an important drought resistance mechanism of *M. eminii* and it is believed to have caused the diameter swelling during drought stress. The stem heat balance method that was used to measure, appeared to be insufficient to monitor low sap flow rates during the night and during water limitation. However, indications of low sap flow dynamics were observed in the raw signals of the sensor. The wood anatomical drought response was analysed using the pinning method in combination with X-ray tomography. Pinning, where a thin needle is used to wound the cambium, was a suitable method to chronologise wood formation in *M. eminii*. Wood growth was coupled to the physiological findings to assess the drought resilience. To some degree, *M. eminii* showed resilience towards the drought stress that was imposed during this experiment. Further research on the impact of actual droughts (and their complexity) on *M. eminii* and other tree species is required to confirm, adjust and complete the findings of this report. The combination of methodologies used in this experiment was innovative and could be ground-breaking. The outcome was promising for following research on the drought resilience of tropical tree species.

SAMENVATTING

Klimaatexperten voorspellen steeds langere droogteperiodes voor grote delen van het zuidelijk halfrond. De laatste jaren werden reeds frequentere en ernstigere periodes van droogte vastgesteld en de situatie wordt niet verwacht te verbeteren. De impact van de klimaatsverandering op bossen is nog onzeker. Bosecosystemen zijn van essentieel belang in het leven van vele mensen, ze dienen als bron van inkomsten en zijn belangrijk voor het levensonderhoud. Voor lokale bevolking is dit vaak rechtstreeks, als onderdak of via de producten die ze gebruiken of verkopen. Het kan gesteld worden dat de totale wereldbevolking onrechtstreeks afhankelijk is van bossen. Ze bieden immers talrijke en unieke ecosysteemdiensten. Om de invloed van klimaatsverandering op bosdegradatie in te schatten, moet kennis vergaard worden over de fundamentele effecten van droogte op de waterrelaties en de anatomie van planten. De tropische boom *Maesopsis eminii* werd geselecteerd voor dit onderzoek. *Maesopsis eminii* is een sleutelsoort voor houtproductie in Oeganda en wordt aangeplant voor brandhout en andere doeleinden in verscheidene landen. Droogtestress, waarbij bodemwater niet beschikbaar is voor de plant, leidt tot allerlei fysiologische en structurele reacties in de plant. Het sluiten van huidmondjes is een efficiënte kortetermijnstrategie om te voorkomen dat de plant een kritieke hoeveelheid water zou verliezen. Bij langdurige droogte blijft de waterpotentiaal dalen wat kan lijden tot embolie in de transportvaten. De fysiologie van 14 *Maesopsis eminii* zaailingen werd opgevolgd tijdens een serre-experiment. Zeven bomen werden onderworpen aan absolute droogte gedurende 14 dagen. Het sluiten van de stomata werd snel waargenomen, gevolgd door de uitschakeling van het fotosyntheseapparaat, verwelking van de bladeren en ten slotte ook bladval. Het opleggen van droogte zorgde voor een netto afname in diameter tijdens de eerste dagen van de droogte. Na vier dagen werd echter opnieuw een netto zwelling van de stammen waargenomen. De verklaring voor deze observatie werd gevonden in het dagelijkse patroon van diametervariatie en sapstroom tijdens controle omstandigheden. Er werd sapstroom waargenomen voor zonsopgang en omdat er geen aanwijzing was dat de planten ’s nachts transpireerden, wordt aangenomen dat *M. eminii* in staat is worteldruk te gebruiken om een kleine maar aanzienlijke sapstroom op te bouwen. De worteldruk werd beschouwd als een van de belangrijkste weerstandsmechanismen tegen droogte en heeft vermoedelijk de zwelling tijdens de droogteperiode veroorzaakt. De *stem heat balance* methode was niet geschikt om lage sapstromen te meten. Niettemin gaven de ruwe signalen van de sensor aan dat er enige dynamiek in watertransport werd waargenomen. Het effect van de droogte op de houtanatomische structuur van *M. eminii* werd geanalyseerd met behulp van de pinning methode. Deze methode, waarbij het cambium verwond wordt met behulp van een fijne naald, bleek geschikt om houtvorming in *M. eminii* te dateren. Groei kon gekoppeld worden aan de fysiologische waarnemingen om de veerkracht van *M. eminii* ten opzichte van droogte te beoordelen. Tot op zeker niveau, bleek *M. eminii* resistent tegenover de droogte die werd opgelegd. Verder onderzoek op de impact van reële droogte (in al hun complexiteit) op *M. eminii* en andere soorten zou de bevindingen van dit onderzoek kunnen bevestigen, aanpassen en vervolledigen. De combinatie van methodes die in dit experiment gebruikt werd, was vernieuwend en grensverleggend. De uitkomst is veelbelovend voor verder onderzoek naar de droogteresistentie van tropische bomen.

INTRODUCTION

GENERAL INTRODUCTION – PLANTS, THE BIO-ENGINEERS FROM NATURE

When people mow their grass, water their houseplants or take a walk between the trees in the forest, they tend to forget how astonishing these creatures are. Plants are able to transform the very basic elements (earth, water, air and sunlight) into complex and diverse structures. With the least effort they seem to develop from, for example, a small seed into a 30 m tall tree with numerous branches, not to mention the countless leaves. However, one should be careful to consider plant growth as something simple or effortless. Plants have designed ingenious structures and processes to develop themselves and to persist whether or not under variable conditions. The question of where a plant gets its material to grow was already the subject of early plant physiology studies in the beginning of the 17th century (Coruzzi and Bush 2001). Based on his famous willow-experiment, the Belgian researcher Jan Van Helmont decided that plants gathered all material for their building-blocks from water (Pagel 2002). He planted a 2.3 kg willow stem in a pot filled with 90 kg of soil and gave it nothing but rain water. In five years, the stem became a well formed tree of 77 kg. Since only 57 g of the soil seemed to have disappeared he decided that only the rain water could have brought the material for the tree to grow. Four centuries later, scientists have managed to unravel a great deal of the life processes in plants. Still, water is considered to have an indispensable role in the life of plants. Carbon dioxide, the other basic resource for biomass production was found in the ostensibly empty atmosphere. Although the understanding of plant physiology extended considerably, there are still a lot of astounding phenomena to declare. Moreover, we will be faced with new research questions within the light of climate change. An example to illustrate the latter could be how a tree species such as *Maesopsis eminii* will cope with the predicted changing climate.

JUSTIFICATION

The research on the link between physiological and anatomical properties of *Maesopsis eminii* under different water conditions is ground-breaking on three levels:

(1) There have been few studies specializing on the physiological behaviour of *M. eminii*. In general, most ecophysiological studies focus on temperate tree species. This research evaluates a broad range of physiological features on a tropical species.
(2) Little is known about the anatomy of *M. eminii*.
(3) Research on linking physiological data to wood anatomical features is still mostly an unexplored frontier and this research will be the first to establish this link for *M. eminii*.

Maesopsis eminii is a relevant timber tree in several parts of the world. In the light of predicted climate change and its inherent increased duration and intensification of droughts, the resilience of key tree species to drought is a hot topic.

OBJECTIVES

The main goal of this research was to link physiological features of *Maesopsis eminii* to its anatomical features under limited water availability in order to assess its drought resilience. However, since it is one of the first (drought) experiments on the species, many aspects could be observed for the first time and these observations formed objectives per se. This narrowed down to the following specific objectives:

(1) Monitor a broad range of physiological features of *M. eminii* under optimal and suboptimal (dry) water conditions to assess their response to drought and how the interactions between them determine the resilience to drought of the whole plant;
(2) Evaluate the wood anatomical structure of *M. eminii* under optimal and suboptimal (dry) water conditions;
(3) Link the results of (1) and (2) to fully assess drought resistance of *M. eminii* and its relevance in the framework of climate change;
(4) Evaluate if the combination of physiological measurements and the pinning method is adequate for such research on this tropical species.

1 LITERATURE REVIEW

The first part of the literature review will put the research subject in a broader perspective. One can only get a satisfying insight in the object, a tropical tree species, if its environment is considered as well. Therefore first forests will be regarded, highlighting their importance, its threats and the species *Maesopsis eminii*. The second part of this section will focus on the growth of plants in general, with special attention to plant-water and plant-carbon relations. The latter fits neatly into the final part of this literature study, which discusses the link between plant physiology and wood formation.

1.1 FORESTS

1.1.1 IMPORTANCE OF FOREST ECOSYSTEMS

Almost one third of the terrestrial biosphere is covered with forest ecosystems. One billion people depend on these forests of which 60 million indigenous peoples directly use the forest as a source of subsistence and revenue (Food and Agriculture Organisation of the United Nations 2012). Forests are multifunctional as they deliver products and resources such as timber, rattan, fibre, food, fodder and medicine, and have a social function in everyday life as they provide shelter next to having aesthetic, scientific and/or religious values (Montagnini et al. 2005, Government of Uganda 2007, Food and Agriculture Organisation of the United Nations 2012). Furthermore forests are ecosystems with an important environmental function. The high biological habitats contain most of terrestrial biodiversity. Half of terrestrial net primary production takes place in forest ecosystems, providing the air with oxygen and extensively contributing to carbon sequestration. Forests take up one third of anthropogenic carbon emission and store about two third of all terrestrial carbon (Montagnini et al. 2005, Bonan 2008, den Ouden et al. 2010). With their low surface albedo and their contribution to the hydrological cycle, *i.e.* evapotranspiration followed by cloud forming and precipitation, forests have a climate buffering and regulating function and prohibit global warming (Bonan 2008). Also, they protect soil from erosion since plant roots have an anchoring function and surface run-off is retarded. The evasion of a fast and harmful run-off by vegetation cover is threefold. First, the forest canopy diminishes the energy of precipitation impact on the soil, preventing soil compaction and evading fast run-off. Secondly, roots maintain the porosity and permeability of the soil, allowing a better infiltration. Evapotranspiration, in turn, prevents saturation of the soil. It can be concluded that the importance and value of forest ecosystems are immense.

Tropical forests play an important role in this story. Notwithstanding they only cover 6% of the earth's terrestrial surface, experts estimate they may be home to about two third of all animal and plant species on earth (Montagnini et al. 2005, Pimm et al. 2013). Also, in some tropical forests indigenous stems live in very close relationship to the forest on which they exclusively depend for their subsistence. Although these societies seem to be disappearing (Montagnini et al. 2005), they count more than 60 million individuals spread over different parts over the world (United Nations 2009, Food and Agriculture Organisation of the United Nations 2012). They suffer from discrimination and political exclusion and their homes are under constant and extensive threat by deforestation (United Nations 2009). However, even though these peoples have without a doubt the strongest bond with the forest, they are not the largest group of people that are closely related to the forest. Many people living in or close to tropical forest fell trees, cut rattan, collect food, use the vegetation as fodder for their livestock, plant crops, produce medicines from forest products and

many more. The products are used both for sustenance and trade on local and international markets. The people in development countries who are directly depended on forest products are often among the poorest and most vulnerable of society (Sunderlin et al. 2005). The ongoing disappearance of forests (Food and Agriculture Organisation of the United Nations 2012) leads to loss in income. Since they often live in remote areas far away from changing socio-economic systems and development (Sunderlin et al. 2005), adaptation of other money-making activities is often ruled out. A total of about 350 million of the world less fortunate people depend on forests for their livelihood and income.

Many of the above mentioned functions and values of (tropical) forest ecosystems can be contributed to its impressive inhabitants: trees. These often remarkable mastodons and their distribution determine the general appearance of forests. Together with other vegetation such as lianas (Schnitzer and Bongers 2002) and herbaceous vegetation, they all contribute to the forest value in their own way. Sustainable timber harvest combines the environmental and productive function as it ensures carbon storage and biodiversity on the long term and produces good and sustained quantities of qualitative timber (Pearce et al. 2003). In this respect, the African key timber species *Maesopsis eminii* was selected for this research. *M. eminii* is a fast-growing tree species (Herawati 2010) and therefore suitable to grow in the setting of a pot experiment. The species is discussed in detail under chapter 1.1.3.

1.1.2 FORESTS UNDER THREAT

Forests have been cut and converted into land for housing or cultivating by our societies from the earliest times. Ancient civilizations often overexploited these natural resources (Mcneely 1994). Growing human population and economic activity enlarges the pressure on natural ecosystems. The effect of the astonishing population increase is amplified by a higher individual consumption of energy and resources (Mcneely 1994). Worldwide deforestation by mankind is the largest scaled anthropogenic change of the earth's appearance (Food and Agriculture Organisation of the United Nations 2012). Even though currently deforestation takes place mostly in the tropics, the driving engines are often Western economies. Forest must give way for large industrial agricultural fields and plantations to produce food and energy for Western countries (Laurance and Peres 2006). Also what is under the forest floor may be of interest to large multinationals. Open mining and oil drilling threaten forests, their biodiversity and their inhabitants (Laurance and Peres 2006). Finally the trees themselves are often illegally logged in the tropics, leading to impoverishment and disappearance of forests (Food and Agriculture Organisation of the United Nations 2012).

A more indirect and uncertain threat that is gaining scientific interest, is the effect of climate change on forest ecosystems (Bush et al. 2011). Forests mitigate climate change (Bonan 2008) but may also undergo changes and degradation due to the changing climate. Because the impact of climate change could be severe and lead to tree mortality (Allen et al. 2010), the phenomenon of climate change and its impact on forest ecosystems is described in the next section.

1.1.2.1 CLIMATE CHANGE

The Intergovernmental Panel on Climate Change (IPCC) states that climate is indisputably warming. Worldwide observations showed increases in average air and ocean temperatures, melting of snow and ice, and a rising sea level (Alley et al. 2007, Allen et al. 2010). There is no doubt that human influences have tremendously contributed to climate change. Human activities in the past and

present have changed the composition of the atmosphere. In particular concentrations of carbon dioxide, methane and nitrous oxide have increased considerably since 1750. The former can be primarily contributed to the use of fossil fuel and secondarily to land use changes such as deforestation. The latter two increases are predominantly driven by agricultural activities. Together these increases cause a radiative forcing[1] of + 2.30 W m^{-2}. In combination with other anthropogenic contributors such as the emission of aerosols (cooling effect), emissions of ozone-forming chemicals, changes in halocarbons and changes in surface albedo due to land cover changes a net anthropogenic radiative forcing can be estimated as + 1.6 ±1 W m^{-2}. More and more consistent evidence reveals that these changes in solar radiation could cause surface temperature changes (Alley et al. 2007). Furthermore there is a growing consensus among scientists that increasing emissions of greenhouse gasses have caused the recent global temperature rise and have changed the earth's hydrological cycle (Allen et al. 2010). What is more, a further rise in global mean temperature in the range of 1.4 to 5.8 degrees centigrade together with more frequent and severe droughts, hot extremes and heat waves is predicted during the period 1990 to 2100 (Alley et al. 2007, Allen et al. 2010). Although large fluctuations of rainfall are characteristic for semi-arid regions in Africa, recent droughts have been more frequent and consequences are becoming more severe for the continent (Nicholson 1989). In eastern Africa rainfall patterns became more intense and dipole, meaning that rainfall over the northern part increased and that the southern part received smaller amounts of rain (Boko et al. 2007). It can be concluded that climate change and its inherent weather extremes will mostly affect one of the most vulnerable continents: Africa and its developing countries. For example in Uganda, a country that is representative for wet and dry tropical environments, drought frequency and intensity have already increased (Government of Uganda 2007). The impact of climate change on (tropical) forests is not yet clear (Allen et al. 2010). However, based on observations it can be assumed that forests are already responding to climate change. Forests appear to be vulnerable for higher temperatures and more harsh droughts, leading to tree mortality and loss in carbon sequestration with a positive feedback to the atmosphere resulting in further warming (Allen et al. 2010). Therefore gaps in the information and scientific understanding to predict climate induced tree and forest degradation must be filled. Additionally to worldwide monitoring and inventory systems, the fundamental effect of climate change and in particular drought stress on the plant water relations and the anatomy of the plants needs to be elaborated.

1.1.3 MAESOPSIS EMINII

Maesopsis eminii, in English known as Umbrella tree, belongs to the family of the Rhamnaceae in the order of the Rosales. It originates from the African lowland rain forest zone (Hall 1995). As shown on Figure 1.1, its native range can be found from tropical West to Central Africa and some regions of Eastern Africa (Orwa et al. 2009). Due to its fast growth *M. eminii* is widely planted for fuel wood, timber production and sometimes for fibre yield. It is planted both within and outside its natural range. The latter made that nowadays the species can be found in different places around the world such as Costa Rica, Fiji, India, Indonesia, Malaysia and Puerto Rico (Orwa et al. 2009). In Uganda *Maesopsis* is the only native fast-growing timber species and therefore regarded as a high potential quality timber species (Buchholz et al. 2010). It is called *musizi*, *musinde* or *muside* in the local language Luganda.

[1] *Radiative forcing* is a measure of the influence that a factor has in altering the balance of incoming and outgoing energy in the Earth-atmosphere system and is an index of the importance of the factor as a potential climate change mechanism. Positive forcing tends to warm the surface while negative forcing tends to cool it. In this report, radiative forcing values are for 2005 relative to pre-industrial conditions defined at 1750 and are expressed in watts per square metre (W m^{-2}). (definition from Alley et al. (2007))

Figure 1.1 Native distribution of *Maesopsis eminii* according to Orwa et al. (2009). Countries are filled if they comprise regions where *M. eminii* populations are native. These regions can be small and not covering the whole country.

While reaching only 25 m height in the western regions of occurrence, *M. eminii* can exceed 40 m in Uganda and Tanzania (Hall 1995). The stem is straight with a pale grey to grey-brown bark. Mature trees have a clear bole of 15 m. The crown is open and spreading. Leaves are simple, opposite, subopposite or alternate (Orwa et al. 2009). In tropical regions with a severe dry season *Maesopsis* is deciduous whereas in constant humid areas, leaf shedding does not always occur (Hall 1995).

Figure 1.2 *Maesopsis eminii* line planting in Kifu © Thomas Raussen, worldagroforestryorg.com

Maesopsis eminii is a typical light demanding colonizing species (Hall 1995). Under suitable conditions and limitation of competition or fire-risk, *M. eminii* is known to gregariously colonize

grasslands and forest gaps (Hall 1995, Viisteensaari et al. 2000). Optimal growth occurs on deep, well drained soils that are not prone to drought stress (Hall 1995). Trees start flowering and fruiting after 10 years, forming large seeds every year and often every six months (Orwa et al. 2009). The fruiting period can be up to six weeks, ensuring a good dispersal. The seeds are dispersed by silvery-cheeked hornbills (*Bycanistes brevis*) and monkeys such as the blue monkey (*Cercopithecus mitis*) and chimpanzees (*Pan troglodytes*) (Hamilton and Bensted-Smith 1989, Hall 1995).

In conservation areas, national parks and forest reserves, *Maesopsis* fruits are on the menu of endangered species such as chimpanzees (Newton-Fisher 1999). In agroforestry *Maesopsis* is often used as a shade tree for coffee (*Coffea spp.*) and banana (*Musa spp.*) plantations and home gardens. When maturity is reached, *Maesopsis* is felled for timber. Because of its fast-growing capacity *M. eminii* is often planted as fuel wood (Orwa et al. 2009). More often, but mainly and almost exclusively in Uganda, *Maesopsis* is harvested for its timber (Buchholz et al. 2010). It is felled in natural forests whether or not in accordance with sustainable management principles (Plumptre 1995, Baranga 2007). Natural forest area is scarce and under constant pressure (Food and Agriculture Organisation of the United Nations 2012). That is where *Maesopsis* reveals its opportunities. As a light demanding and fast-growing species it lends itself to plantation forestry on abandoned lands (Hall 1995, Buchholz et al. 2010). Timber wood of *M. eminii* is known under the trade names *mutere* or *musizi* and is described by Ani and Aminah(2006) and Orwa (2009). The sapwood is light coloured yellowish and darkens during drying. The distinguishable heartwood is darker brown to dark red. With a density between 0.38 and 0.65 g cm^{-3} wood of *Maesopsis eminii* is classified as a light hardwood timber under the Malaysian Grading Rules for Sawn Hardwood Timber. The wood dries easily and relatively rapidly. Untreated wood is vulnerable for termite attacks end moisture induced decay. Therefore it is mostly used for indoor construction purposes. However, it is easily treatable with preservatives. It's cylindrical shaped bole and interlocked grain makes *Maesopsis* an interesting species for plywood applications with a good visible figure. The species is also used for making poles, for packaging material as boxes and crates, carpentry and timber constructions. There are few detailed descriptions on the wood anatomical features of *M. eminii.* Ani and Aminah (2006) empirically concluded that parenchyma are paratracheal to aliform and moderately abundant around reasonably small to large vessels.

1.2 PLANT GROWTH

1.2.1 PLANT-WATER RELATIONS

1.2.1.1 THE SUBSTANTIAL ROLE OF WATER IN PLANTS

Water plays an important role in plant development, subsistence and growth. This can be enlightened by the functions it fulfils as described by Kramer and Boyer (1995). Firstly, water is the main component of plants since it constitutes 80 to 90% of herbaceous plants and 50% of woody plants. Secondly, as a reactant in the photosynthesis processes, it is an essential resource for biomass production. In other processes it may serve as a reactant or substrate as well. Water makes the plant able to build turgor pressure which is indispensable to stand up and keep shape. The hydrostatic pressure contributes significantly to the plants resilience and elasticity. Besides, turgor pressure is crucial for cell elongation, mitosis and therefore growth. Lockhart (1965) developed a model that describes irreversible growth as function of the pressure potential when a threshold for pressure potential is exceeded (Steppe et al. 2006). Finally, turgor is as well a driver for the opening as for the closing of stomata. Plant water is a solvent for gasses, minerals and other solutes. It is responsible for

the storage and transport of these solutes throughout the whole plant. Lastly transpiration of water at leaf level has a cooling effect so that even under high incoming radiation leaf temperature can approximate air temperature (Porporato and Laio 2001).

1.2.1.2 WATER TRANSPORT IN PLANTS

Water in plants is a dynamic feature since every day considerable amounts of water are lost to the atmosphere by transpiration while water uptake from the soil is necessary to sustain this stream and to replenish reserves. Moreover the amount of water stored in plants is low relative to the flux that transpires daily (Ritchie 1981). Water flows through the plant in the soil-plant-atmosphere continuum (SPAC, Cowan 1965). As illustrated in Figure 1.3, the sap flow pathway consists of diverse conductive elements and the interfaces between them (Leuning et al. 2004). In the rhizosphere, water moves through the hairs into the roots and into the root xylem. Next, water is transported to the central cylinder of the stem and raised upwards through a complex of xylem vessels and tracheids to the leaf veins. Finally, the sap reaches the substomatal cavities where it evaporates and diffuses through small pores at the leaf surface, called stomata.

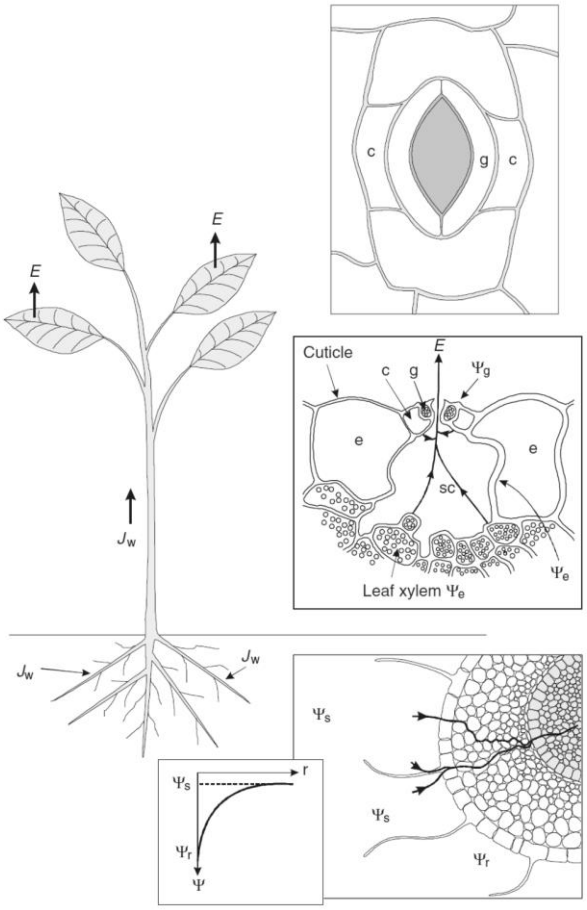

Figure 1.3 Water flow through the soil-plant-atmosphere-continuum. Transpiration (E) and water flux (J_W) are indicated with arrows. Water potentials at the level of the soil (Ψ_s) root (Ψ_r) and leaf xylem (Ψ_e) are represented. The middle drawing illustrates how water evaporates from the mesophyll cells into the stomatal cavity (sc) through the stomata. The stomata with its guard cells (g) and companion cells (c), is embedded in the leaf epidermis (e). (Leuning et al. 2004)

The driving force behind water transport is the decrease in water potential (ψ) over the SPAC (Tyree and Ewers 1991). The water potential is a term to express the availability of water (Porporato and Laio 2001) or the potential of the water molecules to deliver work. The work of a force field acting on the water molecules to move them from soil to top is determined only by the beginning and end position and does not depend on the path. ψ is the difference in free potential energy per unit volume compared to the reference level which is free and pure water where the potential is zero. Different types of energy contribute to the potential of water in plants (eq. [1], Porporato and Laio 2001).

$$\psi = \mathrm{M} + \Pi + \Omega + \mathrm{G} \qquad [1]$$

where M is the matric potential that is linked to capillary and adhesive forces. Π is the pressure potential that is the positive pressure of the liquid water in living cells and the negative suction pressure in xylem sapwood. The osmotic potential Ω depends on the solute concentration. Water moves to higher concentrations which correspond with more negative osmotic potentials. The latter, the gravitational potential G, is the potential energy of water molecules at a certain height and is only of great importance in tall trees. Each position of the SPAC has a corresponding water potential. Spontaneous water flow occurs in the direction of decreasing water potential (Tyree and Ewers 1991, Porporato and Laio 2001). The potential energy of water vapour in the air determines the water potential of the atmosphere. The value of the atmosphere water potential is very low, depending on the relative humidity of the air (RH). At a RH of 40% water vapour potential can be as low as -100 MPa (Porporato and Laio 2001). The relative humidity in the substomatal cavity is much higher (>95%) because most leaves are covered with a thin cutin layer that is impermeable for water and water loss mostly occurs through the stomata. Due to a major drop in water potential towards the atmosphere the water vapour overcomes this stomatal resistance (r_s) and diffuses into the atmosphere. Therefore new water molecules will evaporate from surrounding the mesophyll cells into the substomatal cavity. The surface tension on the water molecules is translated through the whole stem since it pulls the water column upwards with the strong cohesion forces between water molecules. The theory that describes this phenomenon is known as the cohesion-tension theory (C-T theory) and was first described by Dixon and Joly (1894). In 1948, van den Honert extended the theory by describing the SPAC as an analogue of Ohm's law (van den Honert 1948, Cowan 1965, Tyree 1997). As illustrated in Figure 1.4 and equation [2], stationary flow is assumed to be determined by the potential difference across the plant and the conductivity of the transport elements.

$$\mathrm{J} = \Delta\psi \cdot \mathrm{K}_{\mathrm{liquid}} = \frac{\Delta\psi}{\mathrm{R}_{\mathrm{liquid}}} \qquad [2]$$

where J is the flux density of sap flow, $\Delta\psi$ the potential difference over the plant and $\mathrm{K}_{\mathrm{liquid}}$ and $\mathrm{R}_{\mathrm{liquid}}$ are the total plant conductance and resistance for the liquid water, respectively.

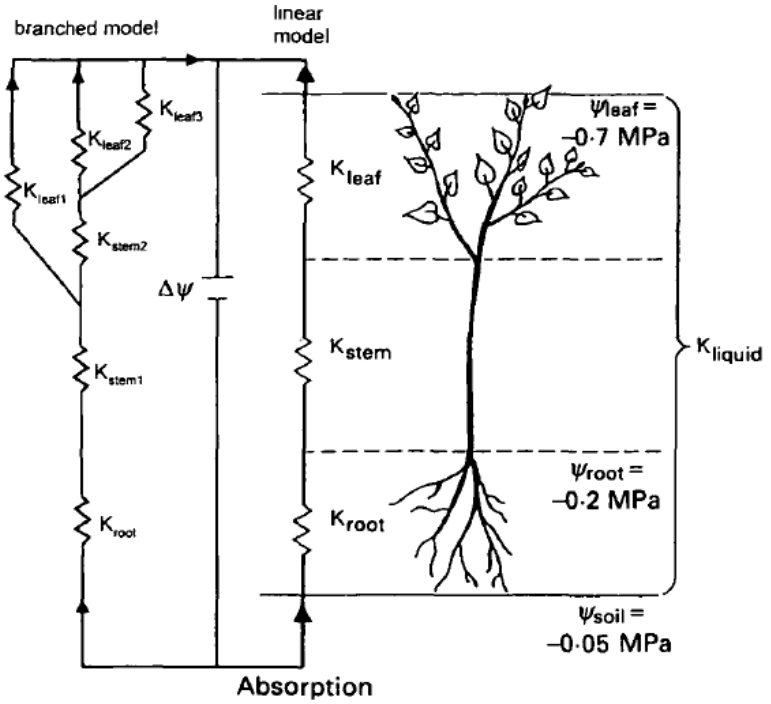

Figure 1.4 Van den Honert's Ohm's law analogy. Conductances (K) and water potentials (Ψ) are represented with an index that indicates the section in the SPAC (Tyree 1997).

Although the van den Honert concept is very valuable for the quantification and clarification of the C-T theory it has some drawbacks due to the simplification of reality. Firstly the flow equation is only valid for water in the liquid phase. Hence, for the leaf stomatal resistance, a diffusion analogue should be used. Secondly, the model considers the stem as a pipe with the sap flow as a steady flow. However, studies on the daily dynamics of water uptake, sap flow and transpiration show that reality is more complicated than the assumed continuous steady flow (Schulze et al. 1985, Goldstein et al. 1998, Steppe et al. 2002). In the morning the water uptake at root level can lag hours behind on the start of the transpiration at leaf level. At midday the latter may already decrease while sap flow has not yet reached its maximal range. At sunset, water uptake continues, while transpiration rates are close to zero. Thus, to answer the water demand of transpiration before water take-up is started, the plant needs to mobilise its internal reserves which are replenished by the continued sap flow in the evening (Herzog et al. 1995, Zweifel et al. 2001). These water storages can be implemented in the electrical Ohm's analogue models by the use of capacities (Lhomme et al. 2001). This is illustrated in Figure 1.5. Diurnal dynamics of transpiration, sap flow and soil water uptake can also be approached as dynamic hydraulic systems that take into account stem radius variation to include storage changes (Zweifel et al. 2001). For elaborate description of such a model is referred to Steppe et al. (2006), Steppe and Lemeur (2007), Steppe et al. (2008) and De Pauw et al. (2008).

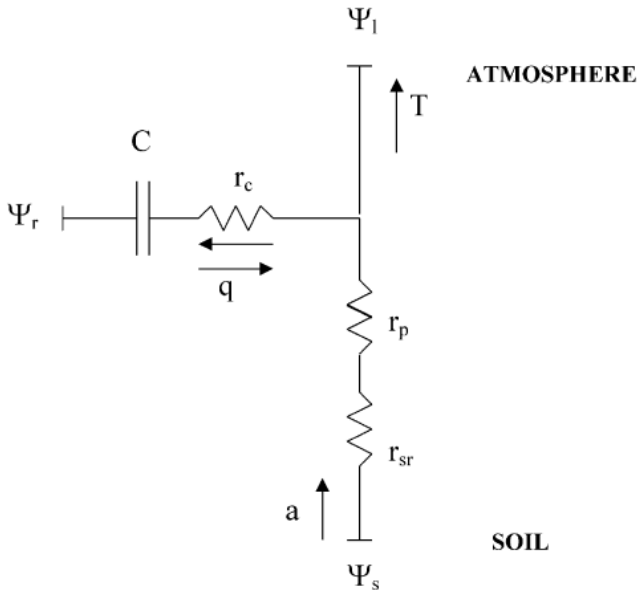

Figure 1.5 Dynamic sap flow model based on the electrical analogue. In this model, the transpiration rate (T) does not necessarily equal the absorption rate (a) since part of the current can be stored by the hydraulic capacitance (C). Resistances (r) and potentials (Ψ) of the different plant sections are indicated by their index, where s is the soil, sr the soil-root interface, p the plant and r the plant-reservoir (Lhomme et al. 2001).

1.2.1.3 STOMATAL CONTROL OF WATER USE

Most leaves are covered with a thin cutin layer that is water repellent and impermeable for carbon dioxide. Therefore, plants have developed small gateways on the leaf surface through which water loss and CO_2 uptake takes place (Kramer and Boyer 1995b). These openings are called stomata. The diffusion of gasses is thus controlled by the opening and closing of these stomata. At short term stomatal opening is regulated by atmospheric moisture content but moreover stomatal closure is expected to occur quickly after a decrease in cell water potential due to drought (Porporato and Laio 2001). Therefore, it can be considered as a responsive safety mechanism to evocate dehydration and cavitation. Cavitation occurs when the water column is under large suction pressure over a too high resistance and breaks. Embolisms enter the xylem vessels and the affected water transport route is interrupted. The drawback of this safety measure is the loss in photosynthetic activity. Indeed, when stomata are closed to prevent water loss, inwards diffusion of CO_2 cannot take place either (Leuning et al. 2004).

1.2.2 PLANT-CARBON RELATIONS

Plants are photosynthetic autotrophs meaning that they convert simple molecules from their environment into complex organic compounds using light as energy source (Lawlor 1993). After water, carbon is the main element that constitutes plants. Carbon can be found in many organic molecules such as sugars, lipids and carbohydrates. Most carbon is absorbed from the atmosphere as carbon dioxide and converted into carbohydrates by the photosynthesis process (Edwards and Walker 1983). Photosynthesis, where carbon dioxide and water are converted into sugars and oxygen takes place in the green parts of the plants, more specific in chloroplasts which are the most abundant in the cytoplasm of leaf mesophyll cells (Edwards and Walker 1983). Indeed, the reactants and the energy source of the photosynthesis reactions are sufficiently present in this environment: leaves can intercept the incoming sunlight while CO_2 is supplied through the stomata (Collatz et al.

1991). Next, the produced sugars can be permanently incorporated in the plant structure. In trees, one of the most straightforward expressions of this structural biomass production is wood formation by the cambial initials. Other organic molecules are used to maintain numerous biochemical reactions and are transported throughout the plant. Like other living creatures plants consume O_2 for their growth and maintenance (Nobel 1983). The respiration process takes place in the mitochondria where carbon molecules are oxidised for the synthesis of the energy carrier ATP. During this reaction CO_2 is released. At night or in stress situations when the photosynthesis rate is diminished, CO_2 flux towards the atmosphere may exceed CO_2 influx (Nobel 1983).

Both photosynthesis and respiration strongly depend on the plant water status. Carboxylation is limited due to declined CO_2 influx after stomatal closure occurs. But above all drought hinders carboxylation because many other processes besides CO_2 supply are damaged (Farooq et al. 2009). For example water deficit lessens Rubisco activity and leads to a higher production of reactive oxygen species (ROS). When cell dimensions are reduced, viscosity increases with a higher risk of aggregation and denaturation. Drought induced reduction of respiration also leads to a decrease in ATP production. Therefore the growth, the maintenance and even the survivability of the plant could be at risk during periods of drought stress (Porporato and Laio 2001, Farooq et al. 2009).

1.2.3 LINK TO WOOD ANATOMICAL FEATURES

In earlier studies knowledge on xylem structure primarily has been obtained from comparative studies between species or within one species growing in different environmental sites (Bryukhanova and Fonti 2012). Little is known about the direct link between wood anatomical features and physiological water relations (Bryukhanova and Fonti 2012). However, wood formation as a dynamic process is considerably influenced by environmental conditions such as the water status, nutrient and carbon availability (Arend and Fromm 2007). One of the major threats to wood production is drought stress, which may affect growth either directly or indirectly. The first refers to cell growth and development since cell expansion and cell wall synthesis strongly depend on the cell water status (Lockhart 1965, Hsiao 1973, Steppe et al. 2006). Additionally, cambial activity is strongly driven by the availability of photoassimilates (Krabel 2000) and thus indirectly by the photosynthetic activity and translocation of the assimilates (Arend and Fromm 2007).

Unlike chronological physiological data, changes in wood structure are much more difficult to date, especially in tropical species without annual rings. To obtain these latter time series several methods have been developed. The pinning method is the most successful and therefore the most frequently used method to observe cambium dynamic over a precise time period (Yoshimura et al. 1981, Seo et al. 2007, Robert et al. 2010). In this method a thin needle is inserted into the outer stem in order to wound the cambium (Figure 1.6). Because of this wounding, wood formation stops within a constricted zone around the canal made by the needle (Schmitt et al. 2004). Further away from the pinning canal the cambium remains active but it forms diversified xylem that can be microscopically distinguished from the xylem formed prior to the pinning (Schmitt et al. 2004). Thus, the method allows examining the wood that is developed in a specific time period*, i.e.* the period between two pinnings. However, cambial wounding and pinning mostly have been performed on temperate softwood (Yoshimura et al. 1981, Schmitt et al. 2004, Gricar et al. 2007, Seo et al. 2007), to a lesser extent on temperate hardwood (Schmitt et al. 2004) and only a few examples of pinning on tropical species are known (Bauch and Dunisch 2000, Robert et al. 2010). All these studies concerned mature trees and periods between subsequent pinnings ranged from one week to a few months. When

performing the pinning method on a new tree species, comprehensive knowledge on its anatomical response to cambial wounding is highly necessary (Gricar et al. 2007).

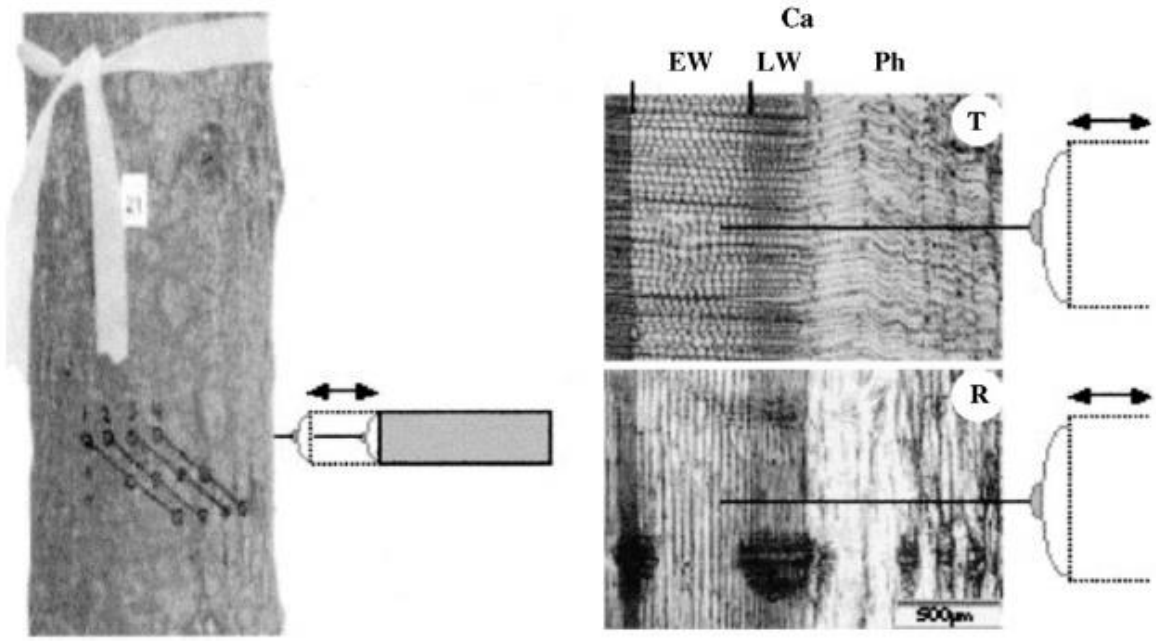

Figure 1.6 Pinning on Scots pine trees (*Pinus sylvestris)*. Pinnings are repeated three times per pinning series in a helix formation with vertical and horizontal spacing of 2-3 cm. On the transverse (T) and radial (R) section can be observed that the pin was inserted through the phloem (Ph), into the cambium (Ca) and reached through the latewood (LW) into the earlywood (EW) (Seo et al. 2007).

2 MATERIALS AND METHODS

2.1 EXPERIMENTAL SETUP

Fourteen juvenile *Maesopsis eminii* trees were placed in a greenhouse of the Plant Science Unit of The Institute for Agricultural and Fisheries Research (ILVO). At the beginning of the experiment the trees were 1.5 year old (diameter = ± 14 mm) and grown in plastic pots measuring 28 cm in height, 17 cm in lower diameter and 22 cm in upper diameter.

The trees were placed in two rows of seven trees and labelled from 1 to 14 as shown in Figure 2.1. Plants 7 and 14 were situated south-east and received the first sunlight in the morning.

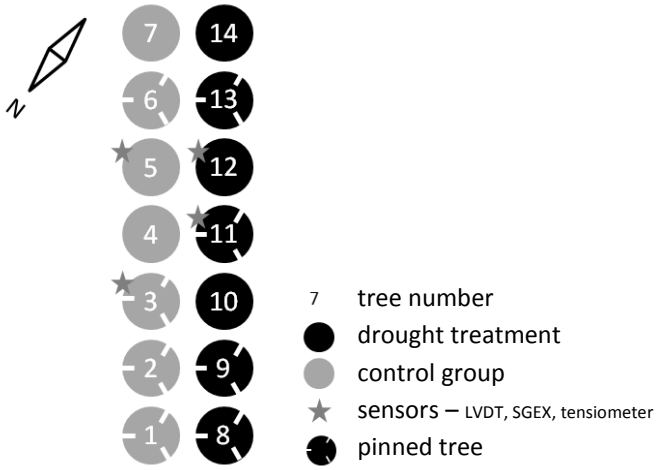

Figure 2.1 Experimental setup: Trees 1 to 7 were allocated to the control treatment and trees 8 to 14 to the drought treatment. Trees equiped with automatic sensors are designated with a star. The trees on which wood anatomical features were examined are indicated as pinned trees. Orientation of the set up is indicated by the compass rose.

Water was supplied by means of automatic drip irrigation. Two emitters were placed in each pot. All trees were irrigated during the first month of the experiment. During this stabilisation period the trees could acclimatise under the greenhouse conditions and under adequate water availability. The drip irrigation system daily released 1200 mL in three irrigation sessions of 400 mL at 9:00, 13:00 and 21:00. On 20 November 2013 (DOY 324) drought was imposed by closing the irrigation line of trees 8 to 14 while the control group continued to receive 1200 mL per day. At the moment of leaf drop of the drought treated trees, the irrigation channel was reconnected to the water supply. The drought period lasted for about two weeks, from 20 November till 3 December 2013 (DOY 324-337).

Trees 3 and 5 from the control group and trees 11 and 12 from the drought treatment group were equipped with different sensors which are described in detail in the next sections. Tensiometers were placed in the containers of these trees. The linear variable displacement transducer (LVDT) dendrometer was installed at approximately 4 cm above the soil. The sap flow sensor was situated 15 cm higher on the stem. Sensors on one of the trees are depicted on Figure 2.2.

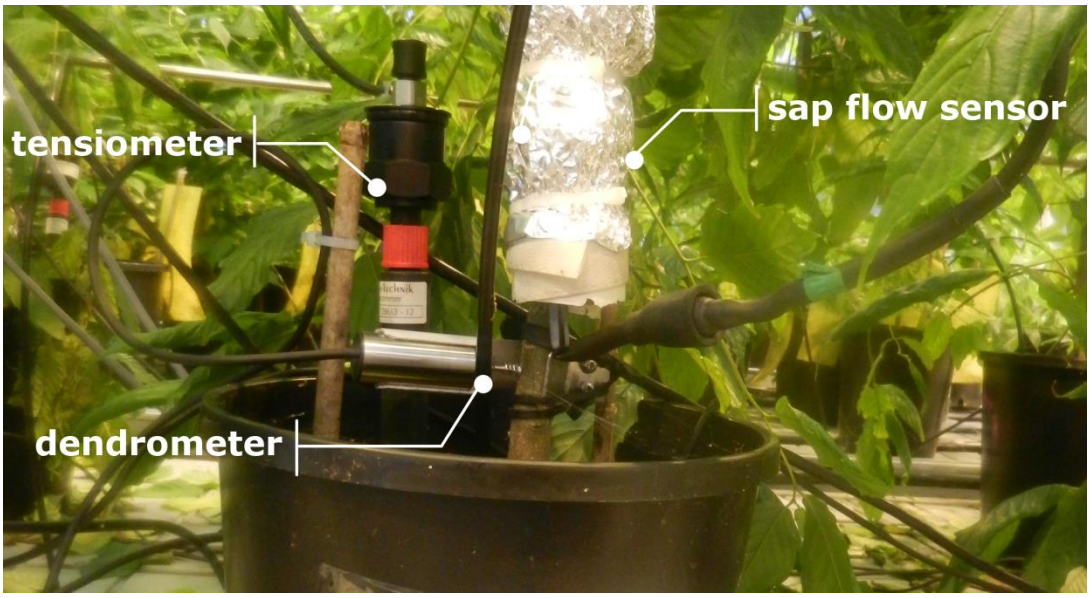

Figure 2.2 Stem and soil sensors installed on tree 3 of the experiment

2.2 ENVIRONMENTAL CONDITIONS

2.2.1 CLIMATIC SETTINGS

Climatic conditions in the greenhouse were monitored, controlled and regulated via a greenhouse climate controller connected with a computer.

Air temperature (T_a) at night was set at 18 °C. Between 8:00 and 9:15 this target temperature rose to 22 °C and declined again to the night temperature between 20:00 and 21:15 in the evening. Ventilation was automatically turned on when temperature exceeded 24 °C. Between 8:00 and 20:00 the greenhouse was illuminated with assimilation lights. The activation and deactivation of the lights will be referred to as sunrise and sunset respectively, analogous with natural conditions. The minimum and maximum radiation of these lights were programmed at respectively 300 W m^{-2} and 500 W m^{-2}.

2.2.2 METEOROLOGICAL DATA

During the experiment three meteorological parameters were measured. The self-constructed meteo-station was placed between the two rows of plants and measured radiation, air temperature and relative humidity. The sensors scanned the environment every 20 seconds and 5 minutes averages were logged. Photosynthetic active radiation (PAR) was measured above the crowns of the trees using a LI-190S Quantum Sensor (Li-COR, Lincoln, NE, USA). PAR could be measured with an accuracy of ± 5%. Air relative humidity (RH) and temperature sensors (Type EE08, E+E Elektronik Ges.M.B.H., Engerwitzdorf, Austria) were placed between the trees approximately at mid height of the crowns. Relative humidity could be recorded between 0 and 100% RH with an accuracy of ± 2%. The temperature measurements could range between -40 and 80 °C with an accuracy of ± 0.2 °C. To evaluate the water vapour conditions in the greenhouse vapour pressure deficit (VPD) was derived from air temperature and relative humidity. VPD is a more sensitive indicator for the moisture conditions of the air since it varies strongly with temperature changes and indicates evaporation better than relative humidity does (Anderson 1936). For calculation of VPD the equations as presented by Allen et al. (1998) were used. Vapour pressure deficit (VPD, kPa) is the difference

between the total amount of moisture that the air can contain when it is saturated, i.e. saturation vapour pressure (e_s, kPa), and the actual vapour pressure (e_a, kPa) (eq. [3]). Saturation vapour pressure is related to air temperature (T_a, °C) and can be calculated from T_a as presented in equation [4]. Actual vapour pressure can be derived from the relative humidity (RH, %) and RH is the quotient of actual and saturated vapour pressure at the same temperature, expressed in percentage of air moisture saturation (eq. [5]).

$$\mathrm{VPD} = \mathrm{e_s} - \mathrm{e_a} \quad [3]$$

$$\mathrm{e_s} = 0.6108\exp\left[\frac{17.27\mathrm{T}_a}{\mathrm{T}_a + 237.3}\right] \quad [4]$$

$$\mathrm{RH} = 100\frac{\mathrm{e_a}}{\mathrm{e_s}} \quad [5]$$

2.2.3 Soil water potential

The soil water potential (ψ_{soil}) was monitored in the four containers of the trees that carried plant sensors (Figure 2.1) using electronic tensiometers (Type: TT-1531 Tensiotrans, ceramic tube 1252-22 (steck-tensio keramik LK-GL), bambach GbR, Tensio-Technik, Geisenheim, Germany). The measuring range for the sensor was between 0 and 1000 hPa.

2.3 Physiological data

2.3.1 Continuous measurements of stem diameter and Sap flow

On four trees stem diameter variation (DD) and sap flow rates (SF) were measured every 20 seconds and logged 5 minutes (Figure 2.1, Figure 2.2). A very sensitive dendrometer was used to monitor both daily shrinkage and swelling due to changes in internally stored water and irreversible growth of the stems (Zweifel et al. 2001, Steppe et al. 2006, Deslauriers et al. 2011). Linear variable displacement transducers (LVDT) are known to accurately measure diameter variation. The LVDT (type DF5.0, Solartron Metrology, Bognor Regis, UK) was mounted in a stainless steel holder just above the broader base of the trunk which more or less corresponded with a distance of 4 cm above the soil. On Figure 2.3 is shown how the sensor was attached to the stem. The measuring range of the sensor was ± 5 mm.

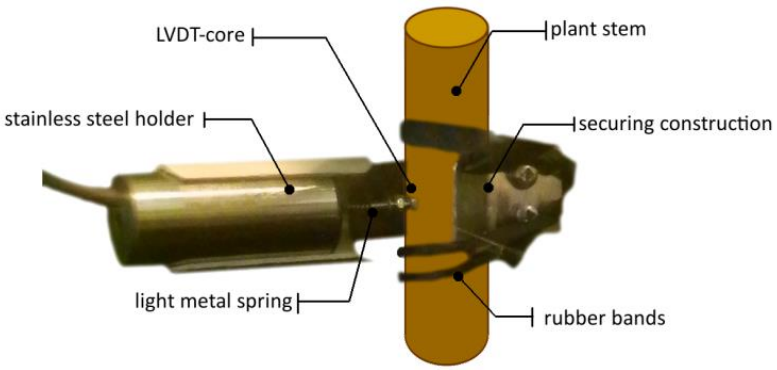

Figure 2.3 Linear variable displacement transducer.

Sap flow was monitored using the stem heat balance method (SHB). Dynagage sap flow sensors (SGA10, Dynamax Inc., Houston, TX, USA) were placed around the stem 15 cm above the LVDT sensor. A straight and smooth stem section was selected and lubricated wit EEG gel to improve conductance from the sensor to the stem. Low density polyethylene (LDPE) plastic was supplied between the stem and the sensor. The sensor was surrounded with an isolation layer and wrapped in reflective aluminium foil to prevent external temperature influences (Figure 2.2).

Since the data processing of the sensor output requires user settings, parameter and filter choices, the stem heat balance will be described briefly, highlighting those specific settings. The theory described is based on the Dynagage sap flow sensors manual (Dynamax Inc 2005).

2.3.1.1 STEM HEAT BALANCE THEORY AND PRACTICE

The heater band around the stem provides a steady state and constant energy input. Figure 2.4 illustrates how the delivered heat is dissipated through conduction and convection.

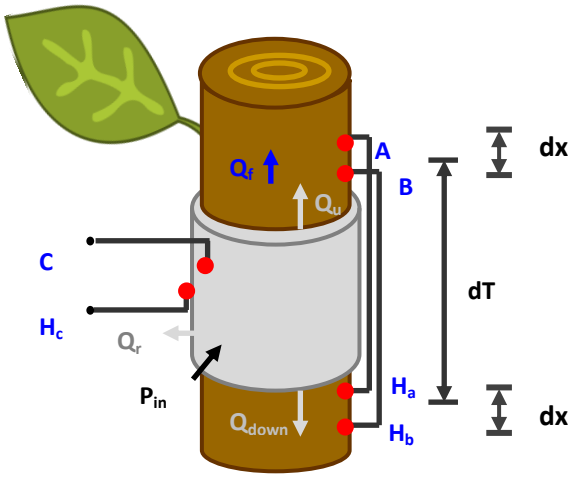

Figure 2.4 Schematic drawing of the stem heat balance. Symbols are used analogous with symbols used in text and formulas.

A DC supply provides a power input (P_{in}, W) to the stem from the heater which is the equivalent for the constant amount of heat Q_H, delivered to the stem. Part of the heat is conducted. Q_r (W) is the radially conducted heat whereas Q_u (upward, W) and Q_d (downward, W) are the components of the axial conducted heat Q_v. The heat that is carried away by the sap flow is the axial convection Q_f (W). Since all other factors of the energy balance are measured, the convection factor can be calculated (eq. [6]).

$$P_{in} = Q_r + Q_v + Q_f \qquad [6]$$

Using Ohms law (eq. [7]) power input can be calculated from the potential difference (V, mV) and the resistance of the heater (R, Ω)

$$P_{in} = \frac{V^2}{R} \qquad [7]$$

The potential difference of the heater was scanned every 20 seconds and a 5 minutes average is logged. R values for the four sensors are tabulated in Table 1.

The upward and downward components of the vertical conductance can be derived as demonstrated in equation [8] and [9]. Their sum is the vertical conductance (eq. [10]).

$$Q_u = K_{st} A \frac{dT_u}{dx} \quad [8]$$

$$Q_d = K_{st} A \frac{dT_d}{dx} \quad [9]$$

$$Q_v = Q_u + Q_d = \frac{K_{st} A}{dx}(dT_u + dT_d) \quad [10]$$

where K_{st} is the thermal conductivity of the stem (W m^{-1} K^{-1}), A the stem cross-sectional area (m^2), dT_u/dx and dT_d/dx the temperature gradients (K m^{-1}) and dx the spacing between thermocouple junctions (m) as indicated in Figure 2.4. K_{st} of a woody stem is given as 0.42 W m^{-1} K^{-1} (Steinberg 1989).

The AH channel measures the potential difference between A and H_a (mV). Channel BH measures the difference in potential between B and H_b (mV). Subtraction of these two signals gives equation [11] (mV)

$$BH - AH = (B - H_b) - (A - H_a) = (B - A) + (H_a - H_b) = dT_u + dT_d \quad [11]$$

This can be combined with [10] and a conversion factor of 0.040 mV °C^{-1} (Dynamax Inc 2005) to convert the thermocouple potential differential signals to Celsius degrees:

$$Q_v = \frac{K_{st} A}{dx}(dT_u + dT_d) = \frac{K_{st} A}{dx}\left(\frac{BH - AH}{0.040}\right) \quad [12]$$

AH and BH signals were scanned every 20 seconds and 5 minutes averages are logged.

The radial component of the stem heat balance is determined from the radial temperature difference between C and H_c.

$$Q_r = K_{sh} CH \quad [13]$$

K_{sh} is the thermal conductance for a specific gauge installation and is unknown. It needs to be calculated from the radial temperature difference CH. When there is no sap flow, Q_f is zero, Q_v can be determined as described and K_{sh} can be derived from the heat balance (eq. [6]). Since K_{sh} depends on all the materials surrounding the heater and stem diameter a new minimal K_{sh} value was calculated every day. Apparent K_{sh} was computed continuously for all 5 minutes data. The lowest predawn values when sap flow was assumed zero were used (Steinberg 1989). The part of the day

when these conditions were met for most of the days in the experiment was selected. The first data-analysis showed that this period was found from 0:00 to 1:55. During this period minimal K_{sh} was withhold as the daily minimum. Every 5 minutes it was determined what the lowest daily minimum was within the 36 previous and the 36 following hours. That K_{sh} was used for sap flow calculation at that time.

Because all other components of the heat balance (eq. [6]) are known, sap flow rate per unit of time (SF, g s^{-1}) can be derived (eq. [15]). The residual value of the balance in watt (Q_f) is divided by the increase in temperature of the sap (dT, °C) and the specific heat of the sap (c_s, J g^{-1}°C^{-1}). The latter value is assumed to be the same as that of water at 20 °C (4.186 J g^{-1} °C^{-1}, Vandegehuchte and Steppe 2012). The temperature increase of the sap, dT (eq. [16]), is calculated as the average of the AH and BH signals (mV) and converted to °C by dividing by the thermocouple temperature conversion constant (0.040 mV °C^{-1})

$$Q_f = P_{in} - Q_v - Q_r = SF \cdot c_s dT \quad [14]$$

$$SF = \frac{P_{in} - Q_v - Q_r}{c_s dT} \quad [15]$$

$$dT = \frac{AH + BH}{2} \cdot \frac{1}{0.040} \quad [16]$$

This sap flow rate was computed every 5 minutes and theoretically impossible outcomes, such as sudden extreme high or extreme low flows, were rejected. The convective heat flow (Q_f), the radial heat flow (Q_r) or the K_{sh} value may not be negative. Extra energy supply of the environment toward the sensor can cause a negative CH signal and consequently a negative Q_r. When Q_f, Q_r or K_{sh}, where negative, sap flow, was set -0.0001 g h^{-} as a flag value. At very low sap flow rates another filter was required. Indeed a low sap flow rate corresponds with a small temperature difference dT. Equation [15] is not defined if dT = 0, while F should approach zero. Moreover when |dT| approaches zero, large differentiations are expected in the eventually calculated sap flow resulting in considerable errors in the calculation of the sap flow rate. Low convective flows and small temperature differences are therefore filtered out. Corresponding with the company's technical notes on the Dynagage sap flow sensors (Dynamax Inc 2005), sap flow is set to zero when both convective flow is very low ($Q_f < 0.2\ P_{in}$) and temperature differences are small ($|dT| < dT_{min}$). The minimal temperature difference dT_{min} was set at 0.75 °C. Both conditions must be met to set the filter because high sap flow may result in small temperature differences as well when sap velocity is too high to assimilate heat from the heater.

Note that a serious drawback of the SHB method is the uncertainty in determination of K_{sh}. The assumption of predawn zero sap flow was preliminary and therefore could be incorrect (Smith and Allen 1996). Zero flow is difficult to assure (Vandegehuchte and Steppe 2012) and some plants are known to have night-time water uptake (Zweifel and Häsler 2001, Vandegehuchte and Steppe 2012).

Table 1 Installation properties of the sap flow sensors: resistance (R), diameter at the time of installation (D) and thermocouple distance (dx).

	Stem 3	Stem 5	Stem 11	Stem 12
R, Ω	145.8	148.6	147.7	134.7
D, mm	13.543	14.650	13.315	13.725
dx, m	0.004	0.004	0.004	0.004

2.3.2 TOTAL LEAF AREA

Development of total leaf area was determined in order to assess the effect of drought on the plants biomass. Furthermore leaf area is a required dimension for the extrapolation of photosynthetic rates from the measurement unit (µmol m^{-2} s^{-1}) to total plant photosynthesis. Evolution of total leaf area of the plants that were equipped with continuous sensors was estimated by assessing average leaf area and surveying leaf quantities. Therefore the amount of leaves on the plants was counted before and during the experiment. Counts were performed on DOY 312, 325, 326, 329 and 332 for the drought treatment and on 312 and 326 for the control treatment. At the end of the experiments the trees were cut for wood analysis. At that time of harvest, 520 leaves were collected randomly to quantify their surface. Leaves were placed on a flatbed scanner and covered with a white paper to have a background with sufficient contrast. Scans were taken at a resolution of 300 dpi. The image processing package Fiji (Schindelin et al. 2012) was used to analyse the scans (Figure 2.5). The digital images were manually processed: after adjusting the contrast levels leaves could by segmented from the background by setting a threshold. Pixels were counted, areas were converted to cm² using the resolution and average leaf area was calculated. Next total leaf area of the plants was approximated by multiplying the average leaf area with the number of leaves per plant.

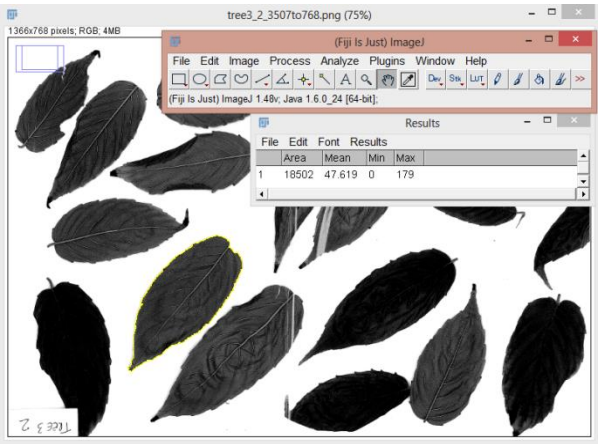

Figure 2.5 Image processing and area calculation with Fiji.

2.3.3 LEAF WATER POTENTIAL

The water status of leaves can be used as a feature to assess the plants dehydration condition. The instrument that is most frequently used to determine the water potential of leaves is the Scholander pressure chamber (Scholander et al. 1964, Cochard et al. 2001). The instrument was developed by P.F. Scholander to examine the negative water potentials in tree canopies that make them capable to pump water to impressive heights. For this experiment a portable pressure chamber (PMS Instrument Company, Corvallis, OR, USA) was used to measure leaf water potential (Figure 2.6). The

instrument consists of a thick walled chamber with a lead cover to withstand high pressure. In the opening of the lid a rubber band is fixed where a leaf petiole can be inserted and clamped. When a leaf petiole is cut, the sap is retracted in the xylem vessels due to the loss of two sided tension and the negative water potential in the apoplast (Cochard et al. 2001). Next the petiole is pierced through the rubber sealing in this way that leaf can be placed in the pressure camber and the cut surface can be observed outside the chamber with a magnifier. Pressure in the camber is increased gradually so that the sap within the petiole is forced to the surface. The amount of pressure build in the chamber at the moment that sap appears at the surface can be read from the gauge. At that moment the pressure in the chamber equals the tension in the xylem before the leaf was cut. The pressure potential in the apoplast and consequently the pressure chamber technique does not take into account the osmotic potential of the xylem sap. Although the osmotic potential typically is considerably less negative than the pressure potential and the error should be marginal, nevertheless the user should be aware of this disadvantage (Cochard et al. 2001). Another source of error is the fact that it is not evident to capture the exact moment when the water column reaches the surface. In order to have comparable results it is preferable that all measurements are performed by the same person.

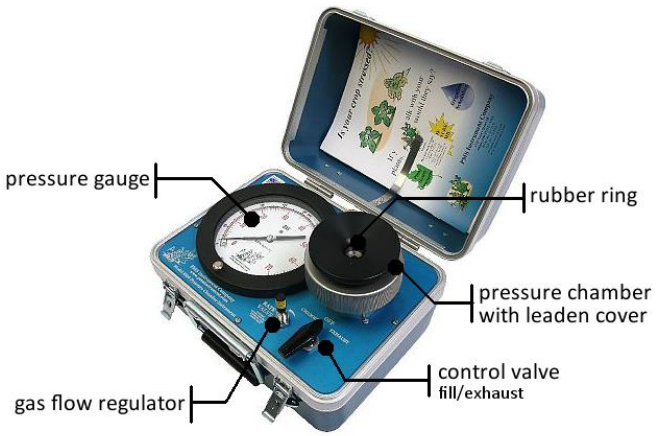

Figure 2.6 Portable Scholander pressure bomb

Since the method is destructible the number of measurements was kept to a minimum. Leaf water potential was assessed in blocks of 14 measurements where first one leaf of all even trees was evaluated and consecutively of the uneven trees in order to measure water potential of the drought and the control treatment in the same time span. A normal measurement day consisted of three measurement series around 9:00; 14:00 and 18:00. This routine was followed on DOY 325, 326, 329 and 332. On DOY 323 measurement series of leaf water potential were conducted consecutively throughout the day. In this way the diurnal course of water potential in the leaves of the *Maesopsis* plants could be outlined. There was only one measurement series on DOY 324, 331 and 333 where on the latter day predawn leaf water potential was measured.

2.3.4 STOMATAL RESISTANCE – POROMETRY

As described in the literature review (1.2.1.3), the degree of stomatal regulation provides information about both the level of water use control and photosynthetic capacity. Hence, it is an inevitable feature to evaluate in the assessment of a plant's response to drought. As stomatal opening or closing respectively permits or limits the diffusion of gasses through the leaf surface it can

be expressed as diffusive resistance and is measured in m s^{-1}. The instrument that is used in this experiment to measure stomatal resistance (r_s) is a diffusion porometer. There are two types of diffusion porometers, depending on their principle of operation. The steady state and the dynamic diffusion porometer are described and compared by Bell and Squire (1981). For both types a chamber is placed on or around the leave. A steady state diffusion parameter supplies a modifiable stream of dry air to the leaf chamber while relative humidity inside the chamber is monitored. When steady state humidity is reached, diffusive resistance can be derived from the relative humidity, leaf temperature, cup area and the flow rate that sustains the steady state. The dynamic type operates in measuring cycles and is therefore also called a cycling porometer. This type was used during the measurements. A typical cycle is illustrated in Figure 2.7. The cycle starts with the pumping of dry air into the leaf chamber. When relative humidity is 5% lower than the pre-set value for humidity, which is preferable just above ambient RH, pumping stops and the RH inside the chamber will start rising. An internal counter times how long it takes before the RH is 2.3% above the pre-set RH and logs it as the transit time (Figure 2.7, δt_m). At this point dry air is pumped into the chamber again as this is the start of a new cycle. Cycles are repeated until a stable transit time is found. Before each measuring session a calibration is performed using a calibration plate. This perforated plated has six series of holes. Since their dimensions are known, their resistance can be calculated. Hence, by performing a calibration under equal ambient conditions as the measuring session with the identical pre-set target RH, δt_m can be correlated to the diffusion resistance.

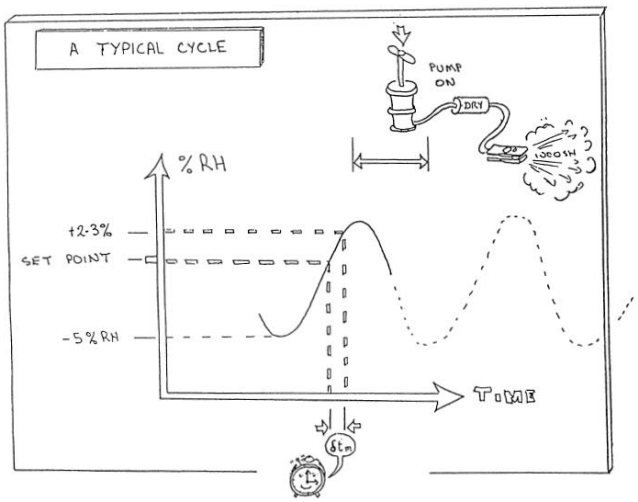

Figure 2.7 Representation of a cycle of the AP4 porometer from the very illustrative user manual (Webb et al. 1990, illustrations by Webb and Simpson).

In this experiment r_s was evaluated with a dynamic AP4 diffusion porometer (Delta-T Devices Ltd, Cambridge, UK). The porometer and its components are shown on Figure 2.8. Porometer measurements are non-continuous and manual. They were combined with other manual measurements of leaf water potential and photosynthesis and are therefore performed only when no other manual measurements had priority. Leaf stomatal resistance was measured between 12 and 16 h on the day before drought was imposed (DOY 223) and intensively throughout the day on the first day of drought (DOY 324).

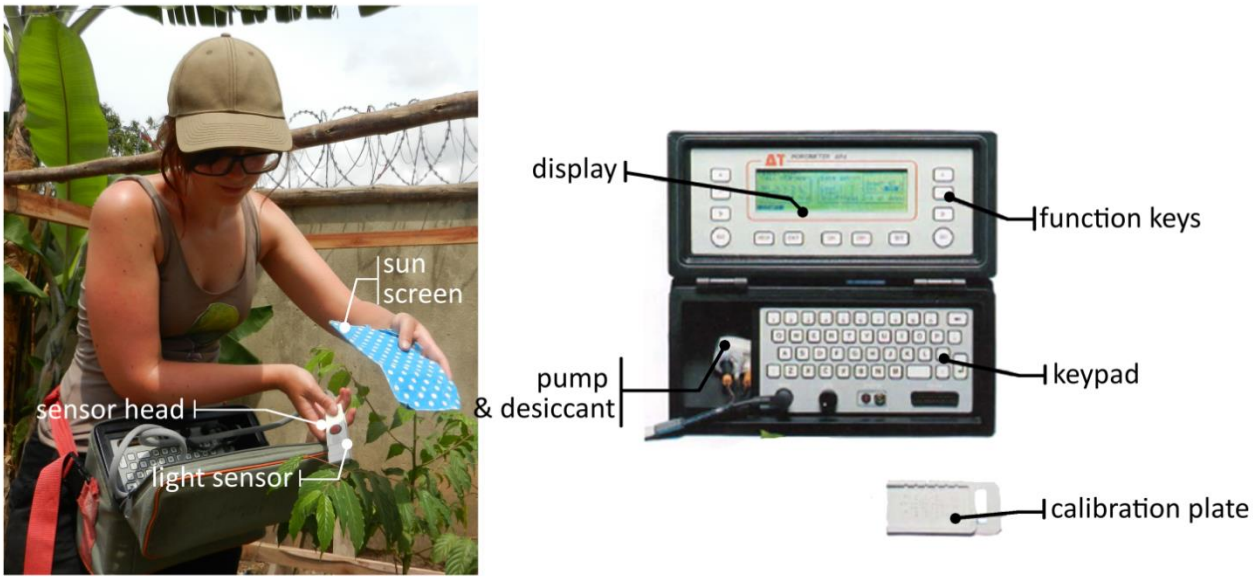

Figure 2.8 AP4 porometer, components and the use in an outside field experiment. The sensor head contains the leaf chamber with RH and temperature sensors. A light sensor measures the incoming PAR. The sensor head needs to be protected from direct sunlight to avoid to high temperature in the leaf chamber. Settings and measurements can be read from the display. Navigation through the software is possible with left and right handed function keys. Notes can be made with the QWERTY keypad. The air is pumped through a tube that contains self-indicating silica gel crystals (from yellow to white when they become wet) to remove moisture before it enters the leaf chamber.

2.3.5 PHOTOSYNTHETIC RATE

Photosynthesis is the key process of primary production in most plant species. Plants capture light and use it as energy source to transform water and carbon dioxide molecules into more complex molecules (Blankenship 2002). And that is where life starts. Animals, fungi and non-photosynthetic bacteria depend on this primary produced biomass (Blankenship 2002). The biomass is used primarily as nutrition but also for many other purposes. For example in a tree such as *Maesopsis eminii* photosynthesis is the first step in biomass production of diverse tissues including wood formation. Obviously, the latter is a very important process in a timber species. Nevertheless, not all of the CO_2 converted by photosynthesis is built in new tissue. A great amount is expended by respiration processes and released back to the atmosphere (Amthor and Baldocchi 2001). Respiration is necessary for growth and maintenance (Saveyn et al. 2007). The photosynthesis and respiration processes are largely influenced by the plant water status (Porporato and Laio 2001, Saveyn et al. 2007). Therefore CO_2 exchange at leaf level was monitored when drought stress was imposed to evaluate the effect on these processes for *Maesopsis eminii.*

The portable LI-6400 photosynthesis system was used to evaluate the capacity of the leaves to extract CO_2 from the atmosphere during the course of the drought experiment (LI-6400, LI-COR Inc., Lincoln, NE, USA). There are three basic types of gas-exchange systems: closed gas exchanged systems, open differential gas exchange systems and open compensating gas exchange systems. For an elaborated explanation and comparison of the techniques is referred to Field et al. (1989). The LI-6400 system calculates photosynthesis from CO_2 measurements in an open differential gas exchange system. Diverse components of the portable LI-6400 system are presented on Figure 2.9. Measurement of CO_2 and H_2O exchange between the leaf and the atmosphere were obtained by

enclosing part of the leaf in a leaf chamber. The apparatus was set to track environment temperature so that temperature in the leaf chamber could approach this temperature. Temperature in the leaf chamber was controlled by Peltier coolers and a thermocouple connector. The LED light source in the chamber had a photosynthetic active radiation that approached the incoming radiation detected by the light sensor. Air from the atmosphere was sucked into the system where-after the CO_2 and H_2O concentrations can be adjusted by scrubbing. For the experiment all CO_2 was filtered out whereas H_2O was scrubbed just until RH in the leaf chamber approximated 60%. Next, a constant CO_2 concentration could be obtained in the airstream by injecting CO_2. Concentration of the air flow was chosen close to ambient CO_2 concentration which corresponded with a fixed concentration of 600 ppm. Part of the air stream is passed through the leaf chamber whereas the other part of the stream goes directly to the gas analysers. The air leaving the chamber is depleted or enriched in CO_2 when leaves are using or producing CO_2 during the photosynthesis or respiration process respectively. Thus, basic equation for net photosynthesis can be formulated as equation [17] (Qubit Systems Inc. 2009).

$$P_n = \frac{([CO_2]_{out} - [CO_2]_{in}) \cdot \text{flow rate}}{\text{leaf area}} \qquad [17]$$

where P_n is the net photosynthesis, which is negative when respiration takes place. The flow rate is the fixed flow through the chamber. The stream passing the leaf chamber had a fixed flow rate of 300 µmol s^{-1}. Leaf area is the surface of the leaf captured in the chamber. The leaf chamber had a standard surface of 6 cm^2. $[CO_2]_{in}$ and $[CO_2]_{out}$ are the concentrations of the air entering and leaving the chamber, respectively. CO_2 concentrations are measured using infrared gas analysers (IRGA) in the sensor head. The analyser consists of two tubes, one through which the reference stream flows and another through which the sample stream flows. IR radiation passes through the tubes alternatively and is absorbed by the CO_2 that is present in the tube. The IR beam then enters the detector that has a separate chamber after each tube. The chambers are separated by a flexible membrane and filled with CO_2. The CO_2 in the chambers expands proportional to the IR that is not absorbed in the tube. As a consequence the membrane vibrates. The vibrations are detected and via standard gas concentrations the analyser was calibrated.

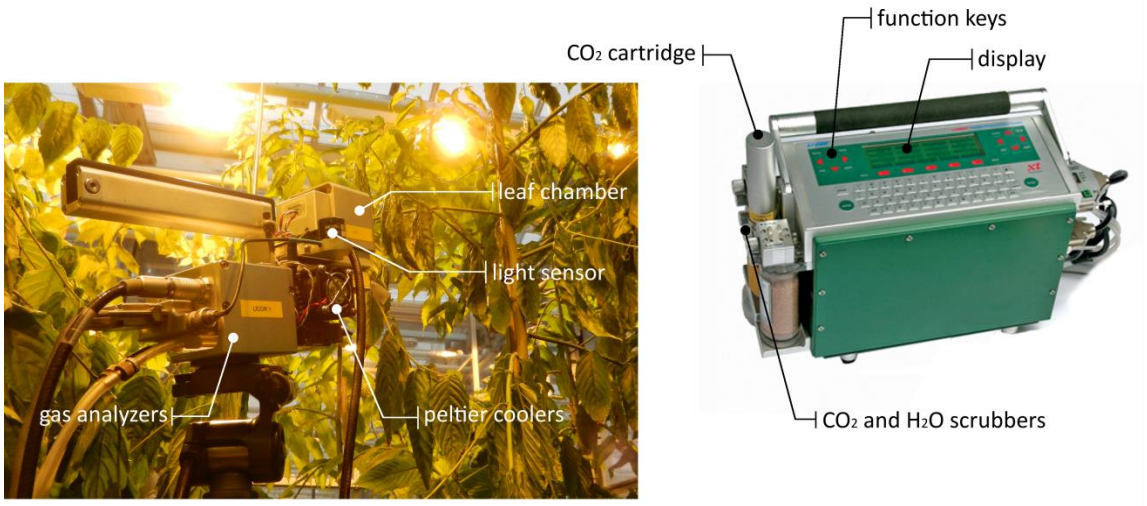

Figure 2.9 LI-6400 sensor head and console

Four leaves (1 at the bottom, 2 at the centre and one at the top of the crown) were labelled on the four plants that had continuous sensors (tree 3, 5, 11 and 12). Photosynthesis measurements were taken throughout the day (when assimilation lights were activated) on DOY 323, 324, 325, 326, 329 and 332. Measurements where focused on the drought treatment (11 and 12). The leaf labelled as leaf 1 on tree 11 was inserted in the leaf chamber. After stabilisation, photosynthesis was measured during two minutes and logged every 5 seconds. This routine was repeated on the other three leaves on tree 11. Next, photosynthesis was measured on the four leaves of tree 12 and thereafter on one of the control trees, tree 3. Then measurements were taken anew on tree 11 and 12 before going to tree 5. This sequence was continued throughout the rest of the day.

2.4 LINK TO WOOD ANATOMICAL MEASUREMENTS

2.4.1 PINNING

As described in the literature review, the pinning method allows examining the wood that is developed in a specific time period. Since no literature was found on *Maesopsis eminii* wound formation it was recommended to test the effect of cambial wounding prior to the actual experiment. A small tree that had been growing in the same greenhouse but was not included in the experimental setup (Figure 2.1) was selected to be pinned on DOY 296. The location on the stem where the needle was inserted was marked with white correction fluid (Tipp-ex). Because no obvious external effects of the pinning were observed, pinning was executed on the trees of the experiment as well.

Eight plants were pinned. As indicated in Figure 2.1 four trees were pinned in the drought treatment group and four in the control group. In order to prevent that collateral damage caused by the pinning would influence the physiological measurements there was only one tree in each group that both carried sensors and was pinned. If pinning would have an important effect, this could be noticed during analysis.

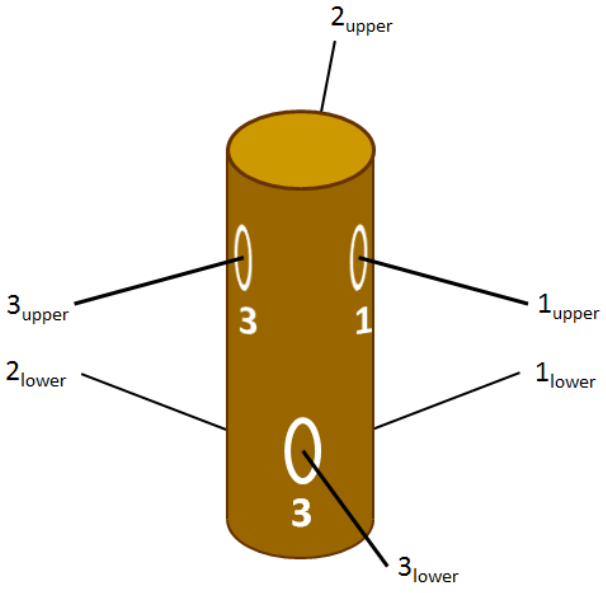

Figure 2.10 Schematic drawing of the positions of the pinnings. Numbers indicate the number of the pinning which refers to the date of pinning: 1. DOY 302; 2. DOY 324; 3. DOY 338

The position of the pinnings is illustrated in Figure 2.10. The first pinning was performed on DOY 302 to mark the start of the experiment. At 1 m height on the stem a needle with a thickness of 500 µm was inserted in the bark and removed immediately (1_{upper}). This was repeated 10 cm lower and 30° counter clockwise (1_{lower}). The second series of pinnings were executed on the day that irrigation was turned off for the trees allocated to the drought treatment (DOY 324). The third pinning coincides with the reactivation of the irrigation on DOY 338. All pinnings were marked and numbered with Tipp-ex. Diameters were measured with a calliper (± 0.05 mm) in the direction of the pinning at the time of pinning.

2.4.2 WOOD AND PINNING ANALYSIS

2.4.2.1 X-RAY TOMOGRAPHY

At the end of the experiment (DOY 63) all trees were felled and stem sections including the pinnings were excised. The samples were immediately wrapped in low density polyethylene (LDPE) plastic to prevent dehydration. Stem discs were unwrapped and sawn 1 cm above and 1 cm below the pinning at the workshop of the Laboratory of Wood Technology (Woodlab). The samples were wrapped in LPDE once more and were scanned fresh/green with the multi-resolution X-ray tomography scanner developed at the Centre for X-ray Tomography of the Ghent University (UGCT). Next, samples were conditioned at 20 °C and 65% RH for 14 days. The conditioned samples were scanned as well because they are expected to reveal more details of the wood structure.

X-ray tomography scanning uses the technique of radiography where X-rays illuminate an object. X-rays are created by electrons by hitting the target of the X-ray tube (Grider et al. 1986) and these X-rays are emitted in the direction of the object. Depending on the density and chemical composition of the object, the latter absorbs the X-rays partially, as such shadowing the detector that is placed behind the object, and thus revealing the internal structure of the object (Figure 2.11). The resolution that can be obtained depends on the distance from the object to the X-ray source and the detector, the pixel size of the detector and the size and type of the X-ray source (Wildenschild et al. 2002). Smaller spot size tubes allow higher resolutions and more detailed image. Large objects need to be placed further away from the source in order to remain within the conic light bundle and within the field of view of the scanner. Therefore less detailed images can be obtained from large objects. In this experiment it was required to implement pinnings 1 to 3 on the same scan. Therefore the entire stem discs were scanned and hence a lower resolution was obtained than if only one pinning canal could be isolated and extracted.

Computed tomography (CT) extents the possibilities of standard radiography by using 2D radiographic images of the object made under different angles (Herman 2009) and mathematically reconstructing the internal 3D structure.

Nanowood, the UGCT X-ray scanner, has two X-ray tubes and two X-ray detectors and a sample stage mounted on a rotation motor, in total resulting in an 8-axis motorized system. The sample can be translated and rotated and is placed as close to the source as possible while still fitting within the field-of-view of detector (Figure 2.11). The detector consists of a scintillator that converts incoming X-rays to optical photons that can be detected with a photomultiplier tube or a photodiode. High absorption, meaning dense tissue or a specific high absorbent material, results in a low signal since few X-rays reach the detector. Images are converted from negative to positive to create logical images where the presence of tissue is light and the background is dark (Figure 2.11). The correction

fluid used to mark the pinnings absorbed a considerable amount of X-rays which resulted in bright white marks on the positive image. This was very helpful to frame the pinnings on the screen.

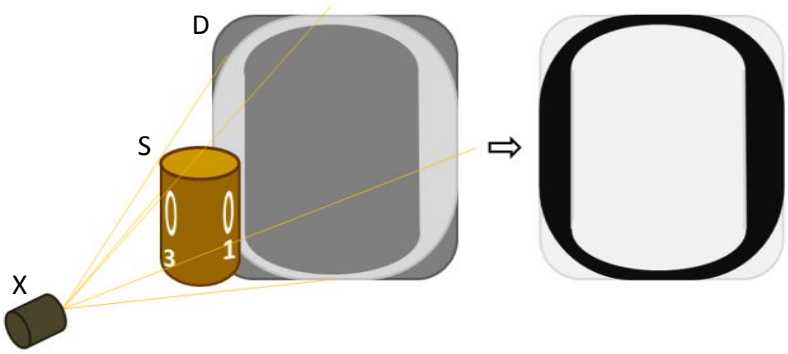

Figure 2.11 Schematic drawing of sample positioning in X-ray tomography and the conversion to a positive image. The sample (S) is placed between the X-ray tube (X) and the detector (D). The axis of the cone beam coincides with the centre of the detector. The negative is converted to a positive.

The stem sections were placed on a custom made holder and scanned with a rotation step size of 0.18°. The average voltage was 90 kV at a current of 70 µA. Flat field (projection without object) and dark field (projection without X-ray beam) images were taken to correct for the beam fluctuations, scintillator imperfections and readout noise. Reconstruction of the images was rendered using the software package Octopus (Vlassenbroeck et al. 2007; distributed by Inside Matters, Aalst, Belgium). The reconstruction pipeline included normalization (using the flat and dark field images), spot filtering and shift correction. The latter corrects possible movement artefacts during scanning. For each sample a scan at maximal resolution was obtained which depended on the allowable maximal total scan time and the size of the sample. Total scan time of the green samples was kept as short as possible to prevent drying, limiting allowable scan time per sample and hence reducing maximal resolution. Final scans had an intermediate resolution with voxel size ranging from 3.5 x 3.5 x 3.5 µm to 15 x 15 x15 µm. 3D images were stored as cross-sectional stacks. Further processing of the volumes was executed in the image processing package Fiji (Schindelin et al. 2012). Brightness and contrast levels were adjusted to have a clear image of the anatomical features. Reslicing of the stacks allowed viewing the stem sections in all three orthogonal orientations.

2.4.2.2 QUALITATIVE ANALYSIS OF THE TEST SAMPLE

On 2D cross-sections of the reconstructed tomographic test sample the pinning canal was located. Abnormal tissue around the wounding area was demarcated and examined in the three wood anatomical directions: transversal, radial and tangential. The extent of the effect of cambial wounding on *Maesopsis eminii* could be estimated as well as characterized to facilitate recognition on the other samples. Based on Yoshimura et al. (1981), the inner boundary of the formed wound was considered as the location of the cambial initials at the time of pinning.

2.4.2.3 QUANTITATIVE ANALYSIS

Pinning canals were located on the cross-sectional views of the conditioned samples. The actual samples were used to label the individual pin marks. Dimensions were determined by measuring specific distances on the image as indicated on Figure 2.12a. Lengths could be expressed in mm using the resolution of the image.

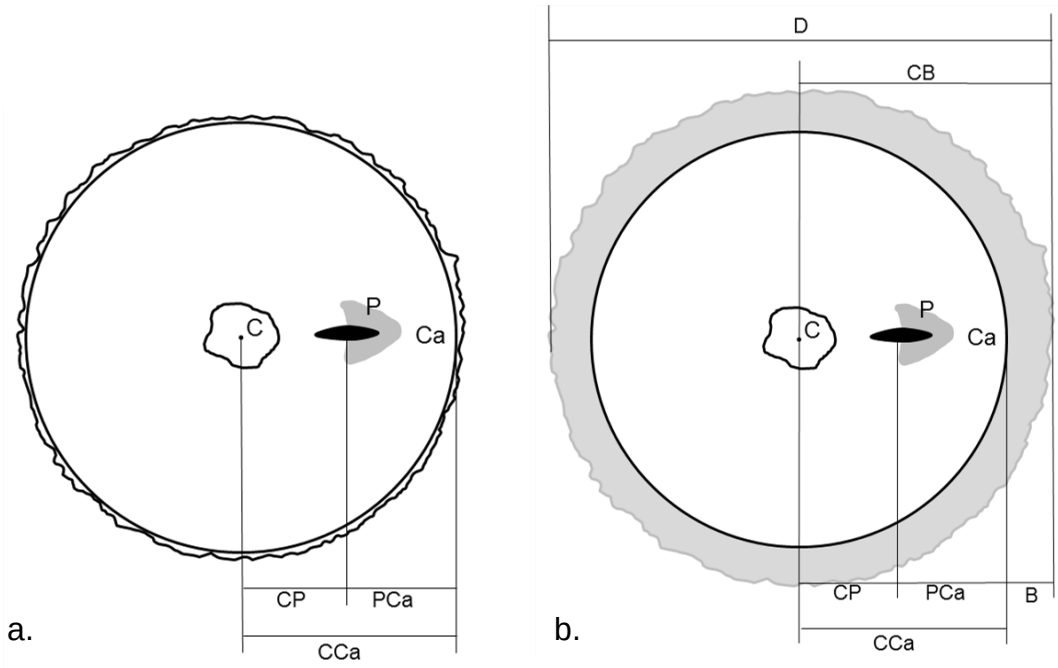

Figure 2.12 Schematic drawing of cross-section micro CT slices. **a.** Conditioned sample; **b.** identical sample in green condition. Spacing between wood anatomical features is measured on the digital images. C = centre of the sample; P = pin mark; Ca = cambium; B = bark. Letter combinations represent spacing between the features concerned. D = the outer bark diameter; B = bark thickness.

The wood formed prior to the pinning could be determined by measuring the length between the edge of the pith and the inner boundary of the wound. However, because of the irregular shape of the pith it was decided to measure this distance (CP) from the centre of the sample to the inner boundary of the wound wood. Xylem formed after the pinning event was measured from the wound wood boundary to the cambial ring (PCa). The inner-bark radius on the conditioned samples was measured between the centre and the cambium (CCa). Due to possible eccentric growth it was not preferable to compare absolute lengths measured at different angles (Seo et al. 2007). Therefore relative growth was expressed as the ratio of absolute growth before or after the pinning and the total radius (equation [18] and [19]).

$$\mathrm{CP}' = \frac{\mathrm{CP}}{\mathrm{CCa}} \qquad [18]$$

$$\mathrm{PCa}' = \frac{\mathrm{PCa}}{\mathrm{CCa}} \qquad [19]$$

where CP’ and CCa’ are the relative growth before and after the pinning, respectively.

Figure 2.12b shows the measurements obtained on the micro CT images of the fresh samples. On these images the bark could be included in the analysis. In analogy with the analysis on the conditioned samples, growth before the pinning was determined as the length between the centre and the inner wound wood boundary (CP). The wood formed after the pining was once more measured as the length between the inner wound wood boundary and the cambial ring (CCa).

Additionally the thickness of the bark was measured (B). Relative lengths were expressed relative to the over-bark radius (equation [20], [21] and [22]).

$$\mathrm{CP}' = \frac{\mathrm{CP}}{\mathrm{CB}} \quad [20]$$

$$\mathrm{PCa}' = \frac{\mathrm{PCa}}{\mathrm{CB}} \quad [21]$$

$$\mathrm{B}' = \frac{\mathrm{B}}{\mathrm{CB}} \quad [22]$$

Outer bark radii at the time of pinning were estimated using the measurements obtained from the green micro CT images. As described, the inner-bark radius at the time of pinning was measured as the length between the centre of the stem and the inner boundary of the abnormal tissue. A low variation of bark thickness was assumed during the time span of a few months. Therefore outer-bark radius was determined as the sum of pre-pinning wood and final sample bark thickness (Figure 2.13).

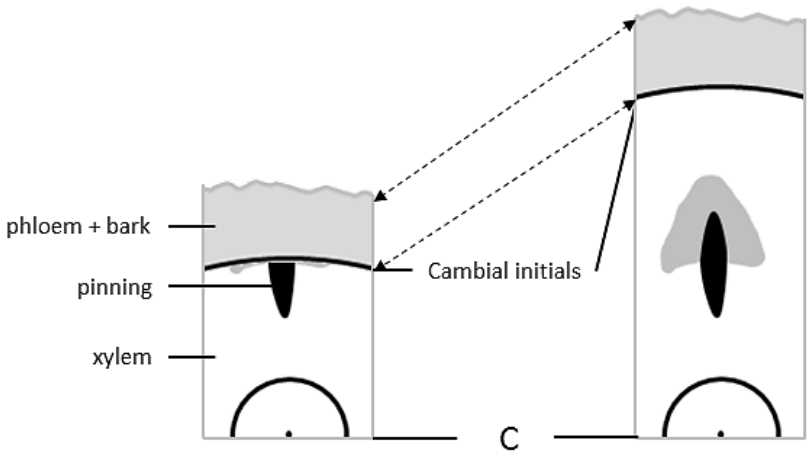

Figure 2.13 Schematic explanation of the localisation of the site of cambial initials and the estimation of the outer bark radius estimation at the time of pinning.

To enable comparison with the calliper measurements at the time of pinning, the radius estimations needed to be converted to diameter estimations. To account for possible eccentric growth, the inner-bark diameter at the time of pinning is estimated by multiplying the relative amount of wood before pinning (CP' in eq. [20]) with the total over-bark diameter (D on Figure 2.12). It was not possible to observe the inner-bark diameter on the scans because no estimation of the localisation of cambial initials at the time of pinning opposite to the side of pinning could be made. By implementing the total outer-bark measurement in the estimation (and not simply doubling the radius at the side of the pinning) a factor is used that includes the growth opposite to the pinning side. Finally the total outer bark diameter ($D_{estimated}$) at the time of pinning is derived by adding two times the bark thickness (eq. [23])

$$D_{estimated} = \mathrm{CP}' \cdot \mathrm{D} + 2\mathrm{B} \quad [23]$$

3 RESULTS

Since the objective of the experiment was to evaluate the effect of drought induced stress, this section will largely focus on those days where drought was imposed. This time span will be referred to as the "drought period". The irrigation of the plants allocated to the drought treatment was switched off on the 20th of November (DOY 324) and was reset to the initial irrigation scheme on the 4th of December (DOY 338). The "drought period" includes three days before the implementation of drought and five days after rewatering. A detailed overview of the plant physiological response to drought will be presented from DOY 321 till DOY 342 whereas sap flow rate and stem diameter variation will also be shown over a longer period to investigate the ability of *M. eminii* to recover after drought. In the latter case an overview of three months will be shown (DOY 321 2013 to DOY 55 2014). The results will be presented as averages per treatment in order to unambiguously and correctly interpret the effect of drought. For most measurements each treatment consisted of only two individuals which may result in relatively high uncertainties. Nevertheless, obvious trends and significant differences between treatments were observed.

3.1 AMBIENT PARAMETERS

3.1.1 AMBIENT PARAMETERS DURING THE DROUGHT PERIOD

During the drought period meteorological parameters in the greenhouse fluctuated around stable averages (Figure 3.1). Most of incoming photosynthetic active radiation rates (PAR) fluctuated between 100 and 200 µmol m^{-2} s^{-1} during daytime. Integration of the radiation over 24 hours reveals two periods of higher radiation (DOY 225-231 and DOY 335-337). During the day relative humidity (RH) was between 50 and 60%. At night RH rose to values between 70 and 80%. Daily average RH gradually decreased from 80% to 65% during the drought period. Averages of night time and daytime temperatures were around 21 °C and 26 °C, respectively, resulting in a daily average around 24 °C. Air temperature was stable during the whole drought period. As described in the materials en methods section RH and air temperature determine the water demand of the greenhouse atmosphere. This vapour pressure deficit (VPD) and is shown in Figure 3.2. Whole day average VPD increased from 0.5 kPA at the beginning of the drought period to 1 kPa at the end. Daytime averages reached 1.5 kPa. At night VPD dropped to values around 0.5 kPa in the beginning of the experiment but did not descent below 0.6 kPa at the end of the period (Figure 3.2a). This indicates that the atmospheric conditions became drier towards the end of the drought period. Soil water potential (SWP) in the pots of the trees subjected to the control treatment decreased throughout the day with strong increases when irrigation was supplied, fluctuating around -0.01 MPa. The SWP in the pots of the drought treatment followed the same pattern before drought was imposed. From the morning of DOY 324 no irrigation was supplied and SWP decreased as usual but did not increase anymore. During that day SWP decreased reaching -0.04 MPa at sunset. The following days SWP further decreased, reaching values lower than -0.08 MPa at DOY 329. Due to the severe drought in the dried out soil, one of the tensiometers was empty and the estimated data as shown in Figure 3.1 are those of the other tensiometer. At DOY 331 the other tensiometer was empty as well and values were estimated to be as low as or even lower than the lowest measured value. At DOY 338 irrigation was switched back on but on the same moment both tensiometers were not yet refilled so no accurate data is available for this time span. SWP is estimated to increase linearly from the minimum value during drought just before rewatering to the first reliable measured value.

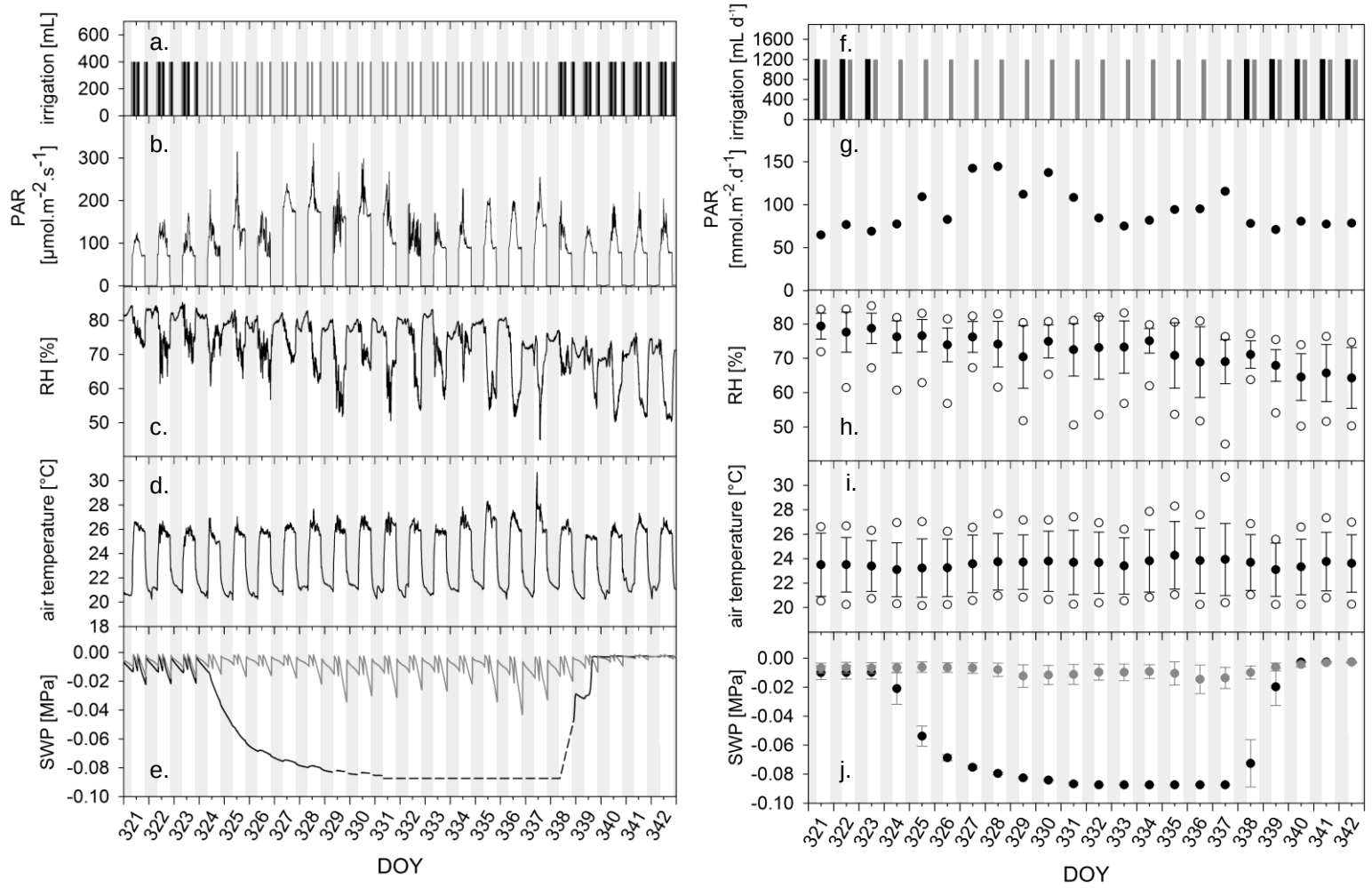

Figure 3.1 Ambient parameters during the drought period. On the left side (a-e) time series are represented and all data are included whereas on the right side (f-j) daily averages and totals are shown. Shaded bars represent night time and white bars represent daytime (8h-20h). Measurements on the control treatment are represented by dark grey symbols. Irrigation supplied to each pot is showed at each irrigation session (**a**) or per day (**f**) Five minute measurements of photosynthetic active radiation (PAR) measured above the crowns of the plants are shown (**b**). On the right graph (**g**) radiation is integrated over the whole day (0h-24h). Relative humidity (RH) was measured at crown height between the two rows of plants (**c**). On the right side (**h**) daily averages with standard deviation are represented by black dots. The upper and lower white dots represent maximum and minimum relative humidity. Air temperature was measured between the crowns as well (**d**), daily averaged, maximum and minimum values on the right graph (**i**). Soil water potential (SWP) was measured in the pots of the trees. Black and grey solid lines on the left graph (**e**) represent average SWP for drought and control treatment respectively. The dashed line represents the estimated values for SWP when SWP was outside the measurement range of the sensor. Daily averages are presented on the right handside graph (**j**).

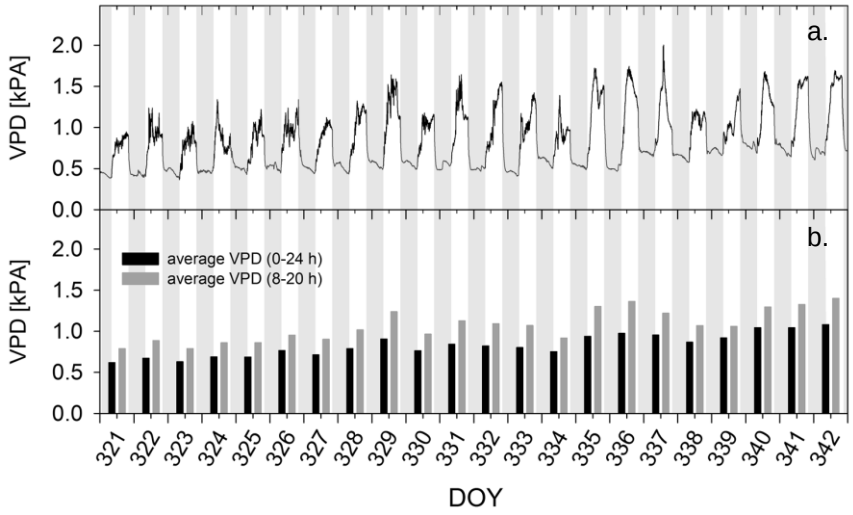

Figure 3.2 Vapour pressure deficit (VPD) during drought stress (DOY 224-337). **a**. All five minute data are included **b**. Average VPD including whole day data (0-24h) or only day time data (8-20h) in black and grey respectively. Shaded bars represent night time and white bars represent daytime (8h-20h).

3.1.2 AMBIENT PARAMETERS DURING DROUGHT AND RECOVERY

Figure 3.3 shows meteorological and soil moisture conditions during the period that drought was imposed and the period after rewatering until the end of the experiment. During this period the trees were monitored to establish the picture of recovery after drought stress. In order to create the full picture of recovery, external (non-plant) parameters should be included in the interpretation of this phase. Figure 3.3a depicts that total daily PAR was relatively higher during the drought period and declined around DOY 365 to stagnate around 40 $mmol.m^{-2}.d^{-1}$. Relative humidity was decreasing during the drought period and continued to decrease during the recovery phase. Daily average of RH reached a minimum of 50% at DOY 351 after which it increased. Air temperature was stable during the entire experiment. Except for a few colder days, air temperature fluctuated around 24 °C. Figure 3.3d illustrates that the atmosphere in the greenhouse became drier from DOY 321 to DOY 351. Water potential of the soil was stable around - 0.002 MPa during the recovery period.

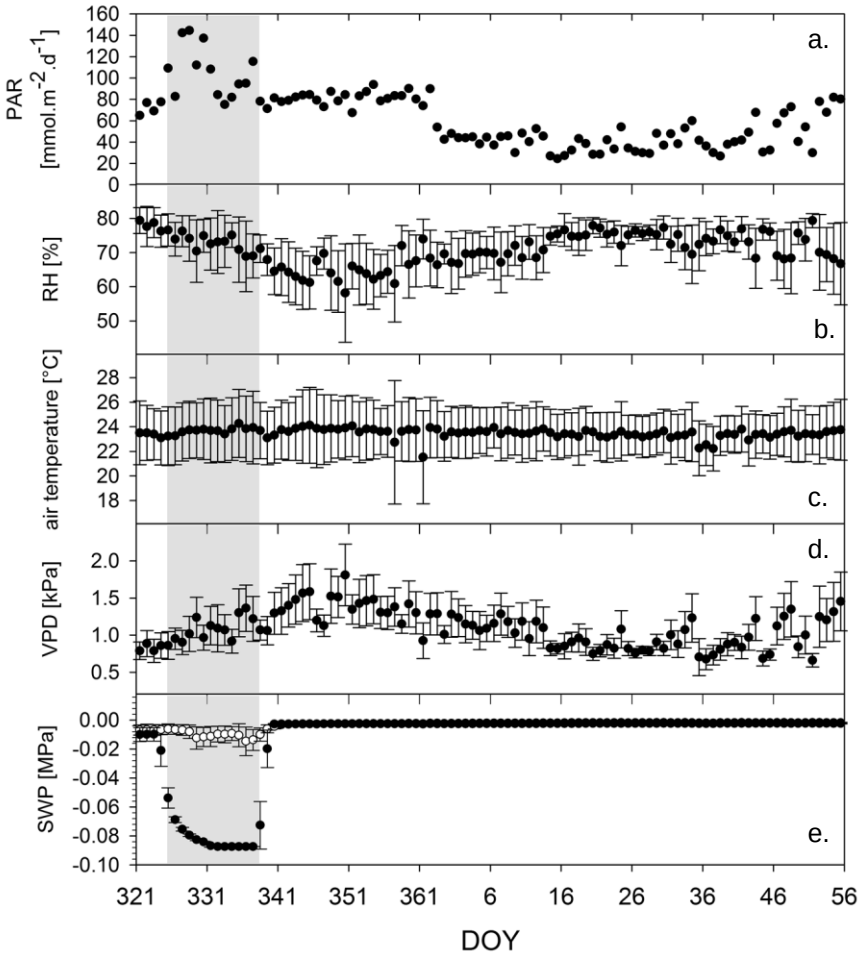

Figure 3.3 Meteorological and soil conditions during and after the period of imposed drought (grey shaded). **a.** Total daily photosynthetic active radiation (PAR) **b.** Daily average relative humidity (RH) **c.** Daily average of air temperature **d.** Daily averages of calculated vapour pressure deficit (VPD) **e.** Black dots represent daily average of soil water potential (SWP) measured in the pots of the drought treatment. White dots represent the control treatment. Error bars represent standard deviations.

3.2 SAP FLOW RATE AND STEM DIAMETER

3.2.1 SAP FLOW RATE AND STEM DIAMETER DURING DROUGHT PERIOD

Sap flow rates of the control treatment reach 100 g h^{-1} around midday (13:00) at the beginning of the drought period (DOY 321) and slightly decreased to 60 g h^{-1} at the end of the drought period (Figure 3.4). On Figure 3.5a these rates are integrated over 24 hours. With a total daily sap flow approaching 1200 g at the beginning of the drought period, trees of the control treatment took up almost the entire amount of supplied irrigation. Analogous with sap flow rate, there is a small decrease in total daily sap flow for the control treatment towards the end of the drought period. Figure 3.5b shows the deviation in stem diameter to the initial diameter (17.3 mm ± 0.5). As shown on Figure 3.5b diameters of the control treatment increased to 19.0 mm (± 0.8). Tree height of the control treatment at the end of the drought treatment was 234 cm (±11).

The drought treatment already had slightly lower sap flow rates and total daily sap flow than the control treatment at the beginning of the experiment. On Figure 3.4 can be observed that while no irrigation was supplied on DOY 324, sap flow was still initiating in the morning, reaching the same maximum as on the previous days at midday (13:00). But on this first day of imposed drought, sap

flow rate dropped rapidly after reaching this maximum. The next morning sap flow was initiated as well but considerably lower rates were reached. Sap flow further decreased on DOY 326 and 327 and seemed to have come to a completely standstill between DOY 328 and 337. A small revival could be observed on the day of rewatering. From DOY 399 on no sap flow was observed.

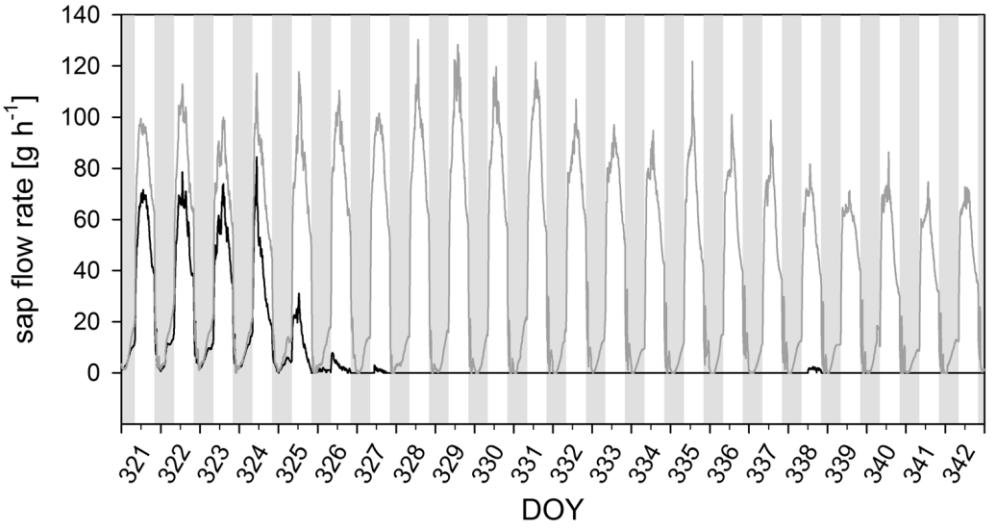

Figure 3.4 Sap flow rate during drought stress (DOY 324-337). The black line represents drought treatment and the dark grey line represents the control treatment. Shaded bars represent night time and white bars represent daytime (8h-20h).

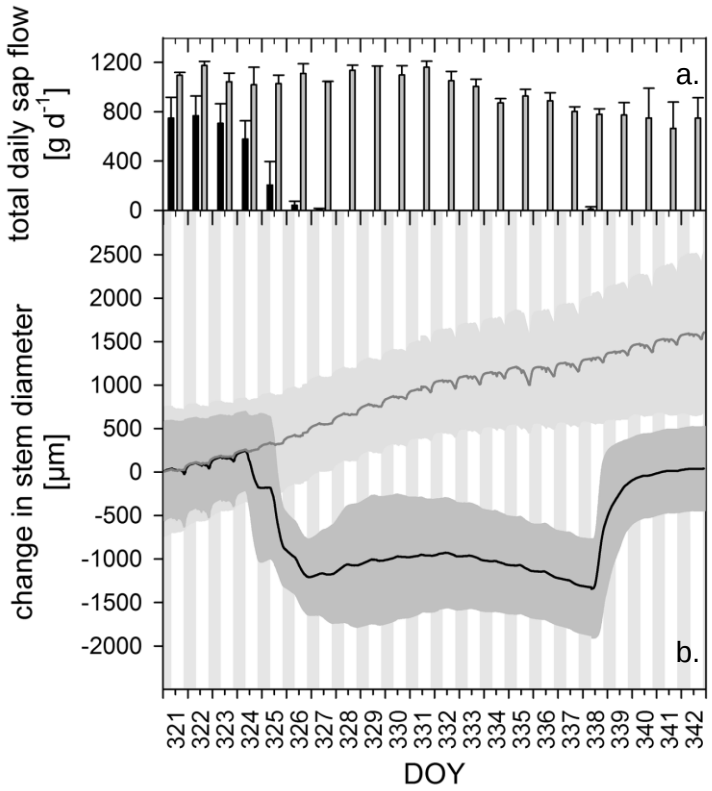

Figure 3.5 a. Total daily sap flow during drought stress (DOY 324-337). Black bars represent the drought treatment and grey bars represent the control treatment. **b.** Stem diameter variation during drought stress. Black line with dark grey standard error band represents the drought treatment. Grey line with light grey standard error band represents control treatment. Shaded bars represent night time and white bars represent daytime (8h-20h). At DOY 321 diameter of the drought treatment was 18.0 mm (± 0.4) and diameter of the control treatment measured 17.3 mm (± 0.5).

Figure 3.5b shows the stem diameter variation which is set to zero at the start of the drought period. At that moment (DOY 321) stem diameter of the drought treatment was 18 mm (± 0.4). The first days, when irrigation was supplied, diameter variation of both treatments had similar growth rates and followed the same diurnal pattern. When drought was imposed, stem diameter of the drought treatment rapidly decreased on DOY 324 to 326. After sunset on DOY 326 stem diameter increased again and continued to increase the following days. The net growth was thus positive and almost parallel with the control treatment between DOY 226 and 332. Thereafter diameter shrinkage was observed from DOY 332 until the moment of rewatering on DOY 338. That day, diameters strongly increased but did narrowly reach their original dimensions (18.1 mm ± 0.3). The height of the trees that had been treated with drought stress was 232 cm (± 17).

On Figure 3.6 the diurnal patterns of sap flow rate and stem diameter variation under normal irrigation routine are shown. Sap flow already initiated at 3:00 and reached 20 g h^{-1} before sunrise. At sunrise sap flow rates quickly rose and continued to rise steadily to a maximum around 13:00. In the afternoon sap flow rates slowly decreased and dropped to just above zero at sunset. Swelling of stems could be observed between 21:00 and 15:00 where stem diameters sharply increased during the first hours of the night. From 2:00 to sunrise diameter continued to increase progressively. During the day the stem diameter fluctuated and subsequently increased until 15:00. Contraction of the stems was observed between 15:00 and 21:00. Positive increment resulting in net growth of the stem diameter was seen between 22:00 and 15:00.

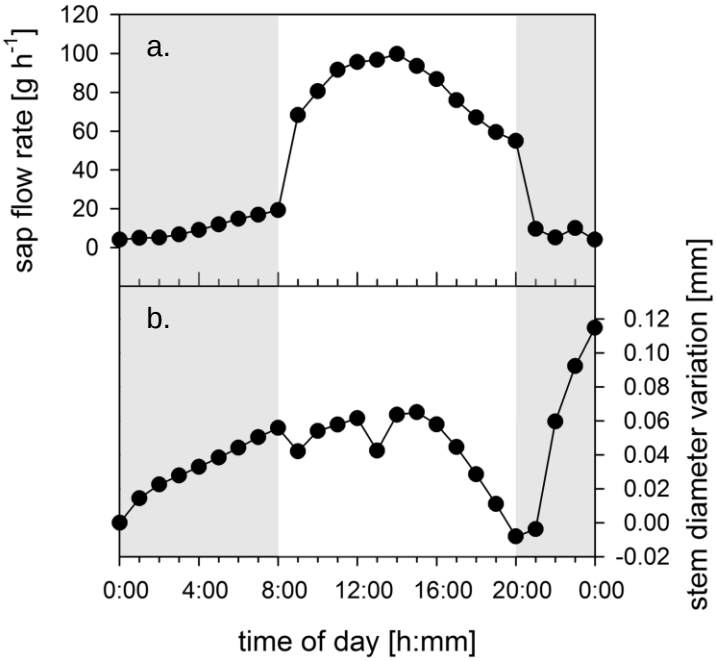

Figure 3.6 Diurnal patterns of the control treatment based on DOY 321-342. **a** Average hourly sap flow; **b.** cumulated average hourly stem diameter variation of the days included. Shaded bars represent night time and white bar represent daytime (8h-20h).

In order to fully assess sap flow during the drought period, elaboration of the stem heat balance with all its components was evaluated in detail. The different components are presented in Figure 3.7.

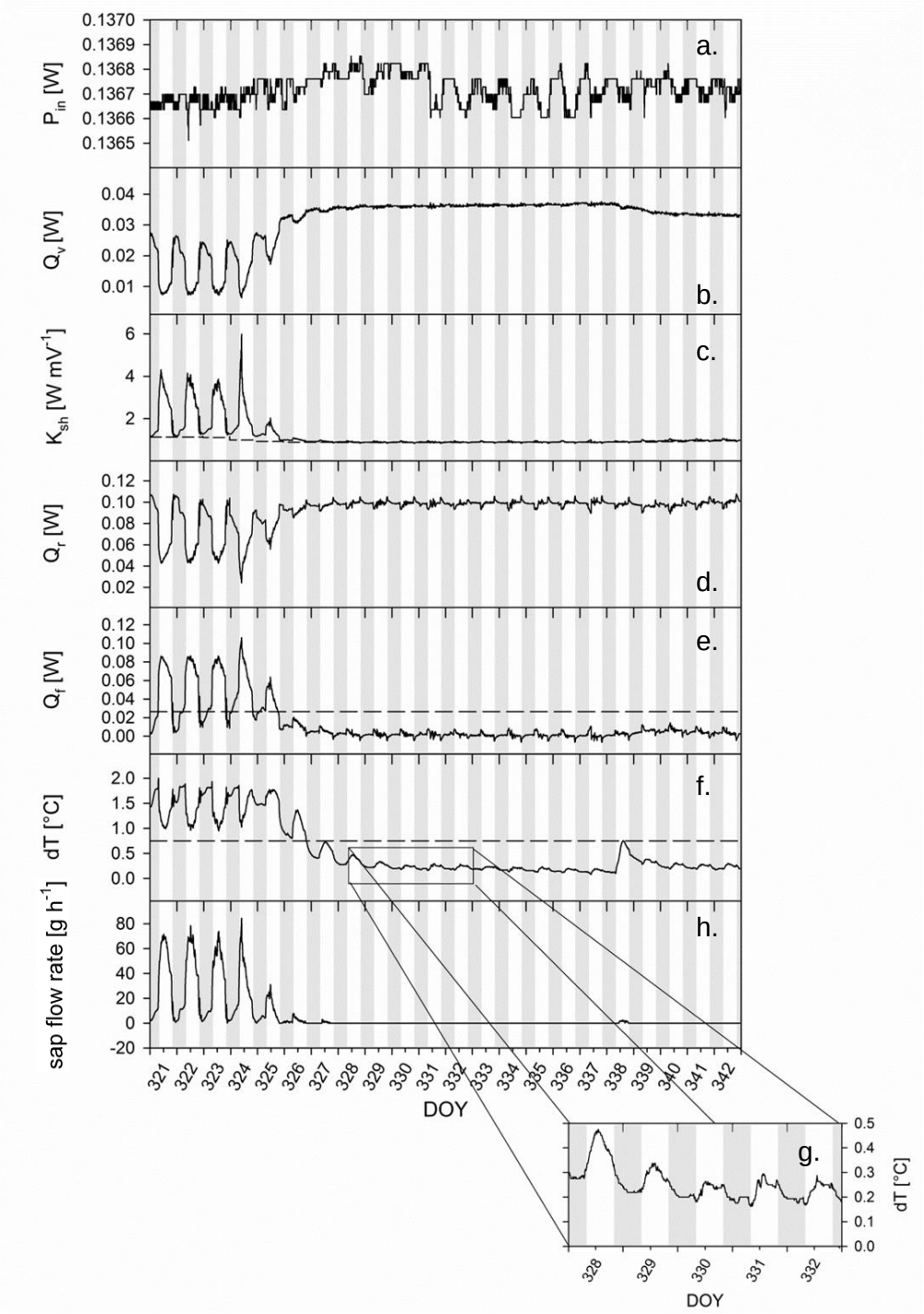

Figure 3.7 Presentation of stem heat balance calculation of the drought treatment during the drought period. No irrigation was supplied from DOY 324 to DOY 337. **a.** Power supplied to the heater (P_{in}); **b.** heat dissipated through vertical conduction (Q_v); **c.** apparent thermal conductance for the gauge installation (Ksh, solid line) and minimum thermal conductance (dashed line); **d.** heat dissipated through radial conduction (Q_r); **e.** heat dissipated by the sap flow through convection (Q_f, solid line) and the threshold for low sap flows (20% of P_{in}, dashed line); **f.** Vertical temperature difference over the heater (dT, solid line) and the threshold for low temperature differences due to low sap flow rates (0.75 °C; dashed line); **g.** close-up of the temperature difference dT on DOY 328-332; **h.** Sap flow rate as calculated by the stem heat balance method described in the material and methods section.

Although the power supply fluctuated it could be considered constant since the fluctuations were marginal. Vertical conductance (Q_v) increased when drought was imposed (DOY 324). Diurnal

dynamics could still be observed on DOY 324 to 326. After that, Q_v remained constant during drought stress. On the day of rewatering Q_v slightly decreased after which it stagnated again. Radial conduction Q_r increased after drought induction. Small but quick rises and steep decreases were observed when assimilation lights were switched on and off respectively. The remaining factor of the heat balance is the heat dissipated by the sap flow through convection (Q_f). This heat dropped under the pre-set threshold on the second day of drought (DOY 325). The vertical temperature difference over the heater (dT) is shown on Figure 3.7 f and g. On the days before drought was imposed similar diurnal patterns were observed which can be interpreted by the hyperbolic relationship with sap flow (Figure 3.8). After drought was imposed, dT decreased and an undulating pattern was observed with maxima during the day and minima at night. During the entire period of drought stress these daily dynamics were seen. In many applications a linear relation between temperature difference and low sap flow velocity is found. This also applied for the sensors of this experiment. For each sensor the linear relation at low sap flow rates and the hyperbolic relation at high sap flow rates are presented on Figure 3.8. The linear relationship could be used to connect the diurnal pattern of dT to a diurnal pattern in sap flow during drought stress. Therefore regression analysis for the sensors of the drought treatment was computed (Figure 3.9 and Table 2).

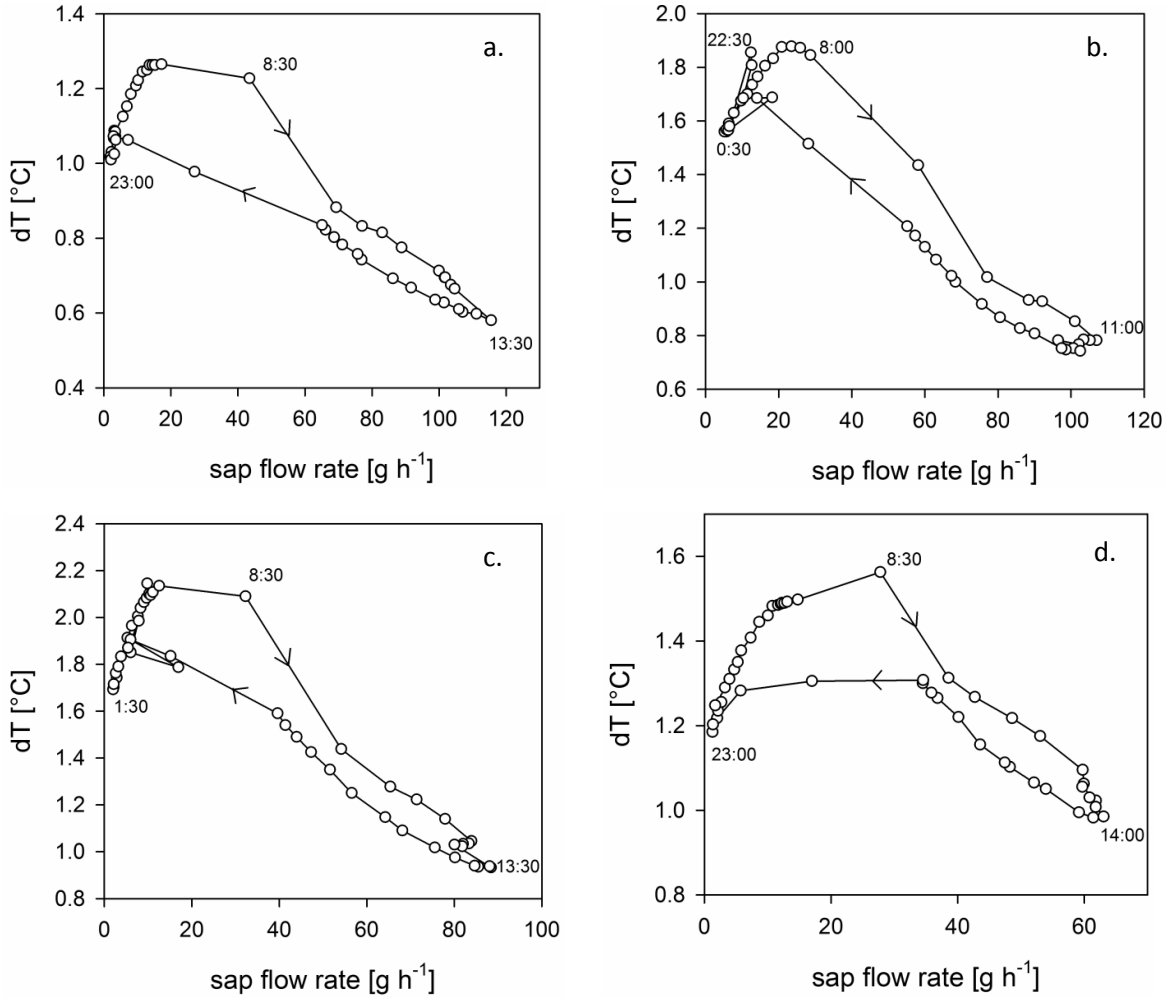

Figure 3.8 Linear and hyperbolic dependence of the flow rate on the temperature difference dT. Diurnal course of temperature difference is indicated by the arrows and the timestamps. Only measurements from DOY 319 to 323 are included so that all trees received the control irrigation regime. **a.** tree 3; **b.** tree 5; **c.** tree 11; **d.** tree 12

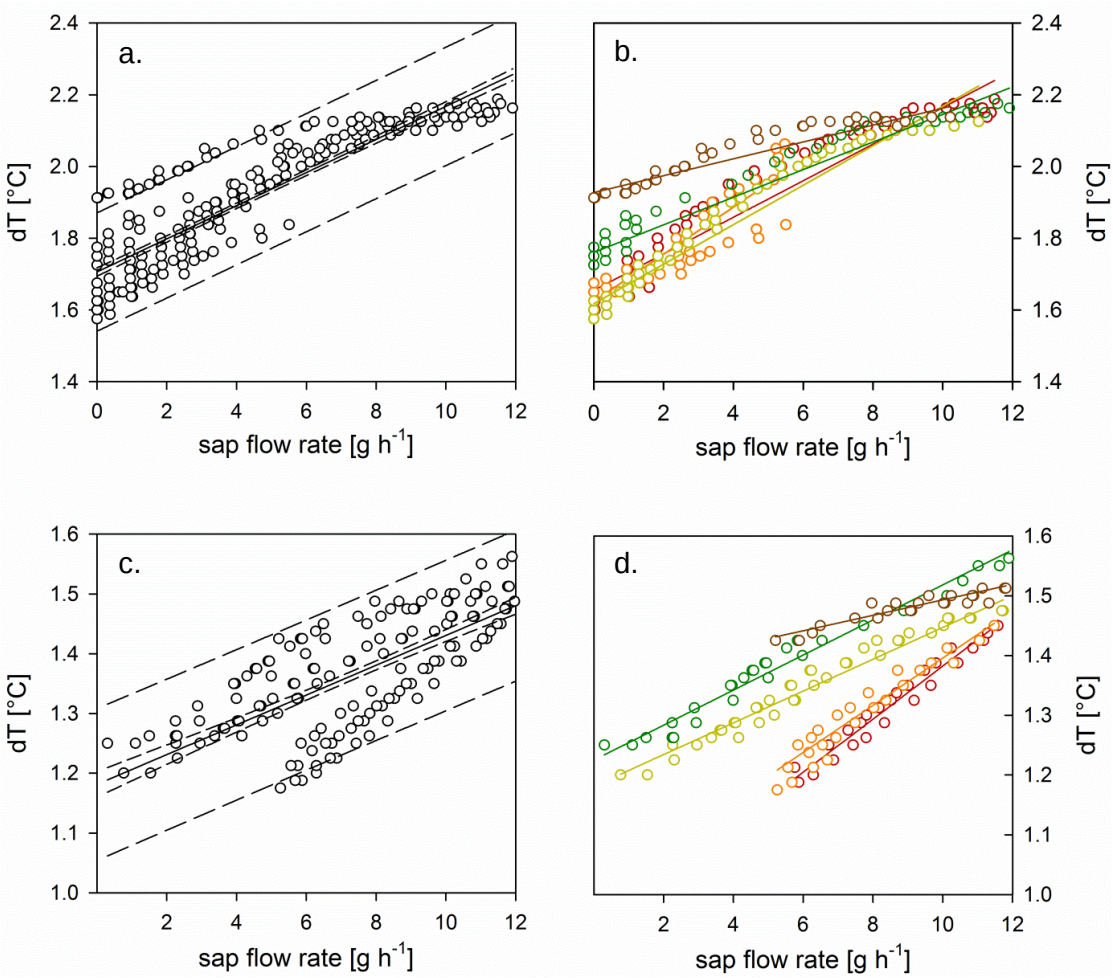

Figure 3.9 Linear regression between low sap flow rates and temperature difference over the heater (dT) for the drought treatment. Only measurements from DOY 319 to 323 are included. **a.** tree 11, linear regression analysis with all data included; **b.** tree 11, separate regression analysis per day; **c.** tree 12, linear regression analysis with all data included; **d.** tree 12, separate regression analysis per day. Results from the regression analyses are presented in Table 2.

Table 2 Linear regression between low sap flow rates and temperature difference over the heater. Equation: $dT = y_0 + a.SF$. Linear regression curves are plotted in Figure 3.9. ($P<0.0001$ for all coefficients)

Tree	DOY	y_0	a	R^2	Figure 3.9
11	319-323	1.7061 ± 0.0059	0.0462 ± 0.0010	0.8218	a
	319	1.6548 ± 0.0089	0.0509 ± 0.0013	0.9424	b
	320	1.6242 ± 0.0068	0.0657 ± 0.0023	0.8974	
	321	1.6177 ± 0.0063	0.0550 ± 0.0011	0.9633	
	322	1.7606 ± 0.0061	0.0385 ± 0.0009	0.9621	
	323	1.9275 ± 0.0045	0.0235 ± 0.0007	0.9235	
12	319-323	1.1812 ± 0.0108	0.0249 ± 0.0014	0.5467	c
	319	0.9381 ± 0.0125	0.0444 ± 0.0015	0.9536	d
	320	1.0007 ± 0.0121	0.0395 ± 0.0015	0.9302	
	321	1.1809 ± 0.0035	0.0266 ± 0.0005	0.9743	
	322	1.2249 ± 0.0055	0.0293 ± 0.0010	0.9602	
	323	1.3639 ± 0.0061	0.0129 ± 0.0007	0.8951	

To re-evaluate the thresholds used in the SHB method, sap flow was recalculated while the threshold of 0.75 °C was set to zero and gradually increased with steps of 0.05°C. In this empirical way the lowest threshold was selected for which dividing by small temperature differences did not result in excessive sap flow rates. Eventually the threshold was set at 0.3 °C and sap flow was recalculated. The result is shown on Figure 3.10.

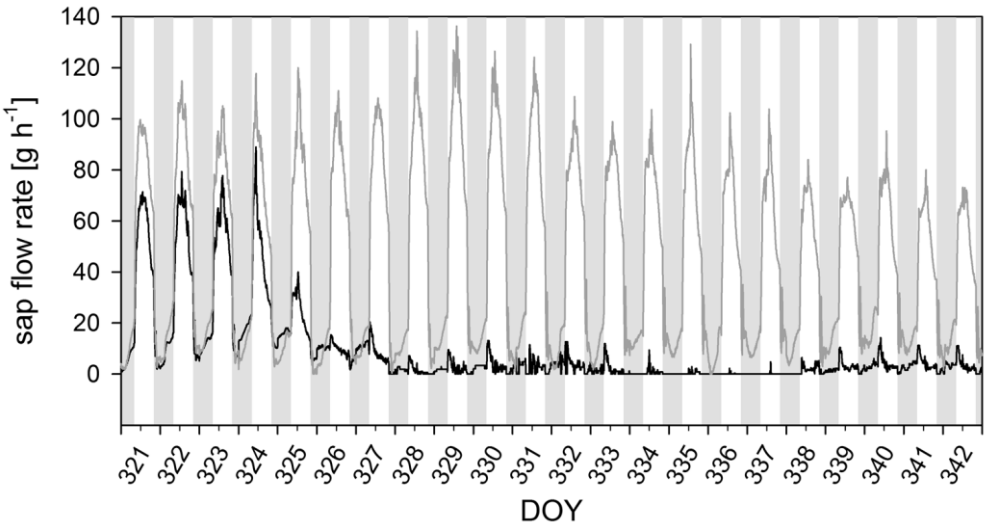

Figure 3.10 Recalculated sap flow rate during drought stress (DOY 324-337). The black line represents drought treatment and the dark grey line represents the drought treatment. Shaded bars represent night time and white bars represent daytime (8h-20h).

3.2.2 SAP FLOW RATE AND STEM DIAMETER VARIATION DURING DROUGHT AND RECOVERY

Stem diameters did not increase during two months after rewatering (Figure 3.11). Also the diurnal dynamics, *i.e.* daily diameter contraction and expansion, only returned approximately 60 days after irrigation was supplied again. Sap flow progressively rose after rewatering. The variation between the two plants of the drought treatment was large. Figure 3.11b shows that tree 11 almost fully recovered, with sap flow rates as high as the sap flow rate at the start of the experiment. After the long period of stagnation diameter of tree 11 started to grow on the last days of the experiment. Tree 12 on the contrary still had no considerable recovered sap flow rates at the end of the experiment. Although diurnal dynamics of stem diameter variation returned, a net shrinkage of the stem was observed during the last weeks of the experiment.

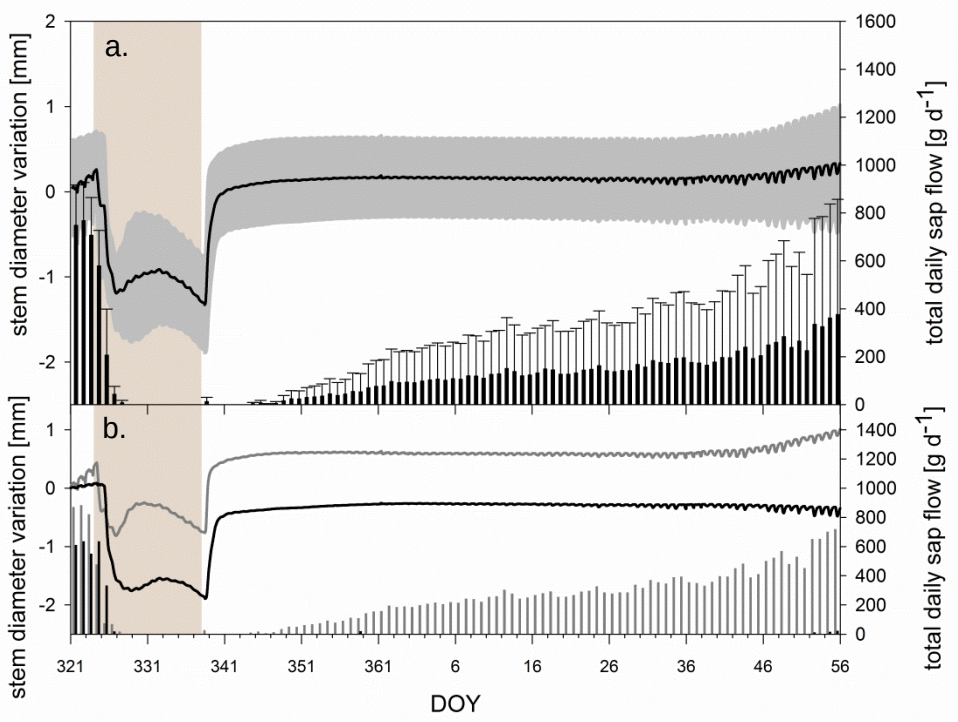

Figure 3.11 Total daily sap flow and stem diameter variation of the drought treatment during and after the period of imposed drought (beige shaded) **a.** Results represented as an average for the control treatment. Stem diameter variation is represented by the black line. Standard deviation on stem diameter variation is represented by the grey error band. Bars represent total daily sap flow. Standard deviation is represented by the error bars; **b.** Results are presented for the two trees of the drought treatment separately. Tree 11 is represented in grey and tree 12 is represented in black.

3.3 TOTAL LEAF AREA AND LEAF WATER POTENTIAL

3.3.1 TOTAL LEAF AREA AND LEAF WATER POTENTIAL DURING DROUGHT PERIOD

At the beginning of the experiment the number of leaves was comparable for all four trees with sensors. Control trees carried 1156 leaves per tree (± 18) and trees selected for the drought treatment had 1160 leaves per tree (± 131). The average surface of one leaf throughout the drought period was 34.6 cm² (± 13.6). Figure 3.12a showed a decline in total leaf area of the trees subjected to drought. Leaf shedding commenced between DOY 326 and 329. At DOY 326 leaves of the drought treatment visually lost most of their turgor (Figure 3.13). Figure 3.12b shows that the apoplastic pressure potential of the leaves declined even faster. During the day before drought was implemented (DOY 323) leaf water potential was between -0.2 and -0.6 MPa , apart from two plants that had ψ_l of -0.8 and -1.0 MPa in the afternoon. Around midday on the first day of drought (DOY 324) the leaf water potential of the drought treatment dropped to -1.1 MPa (± 0.4) whereas leaves of the control trees had a water potential of -0.5 MPa (± 0.1). Leaf water potential of the drought treatment continued to decrease reaching values of -5.5 MPa (± 1).

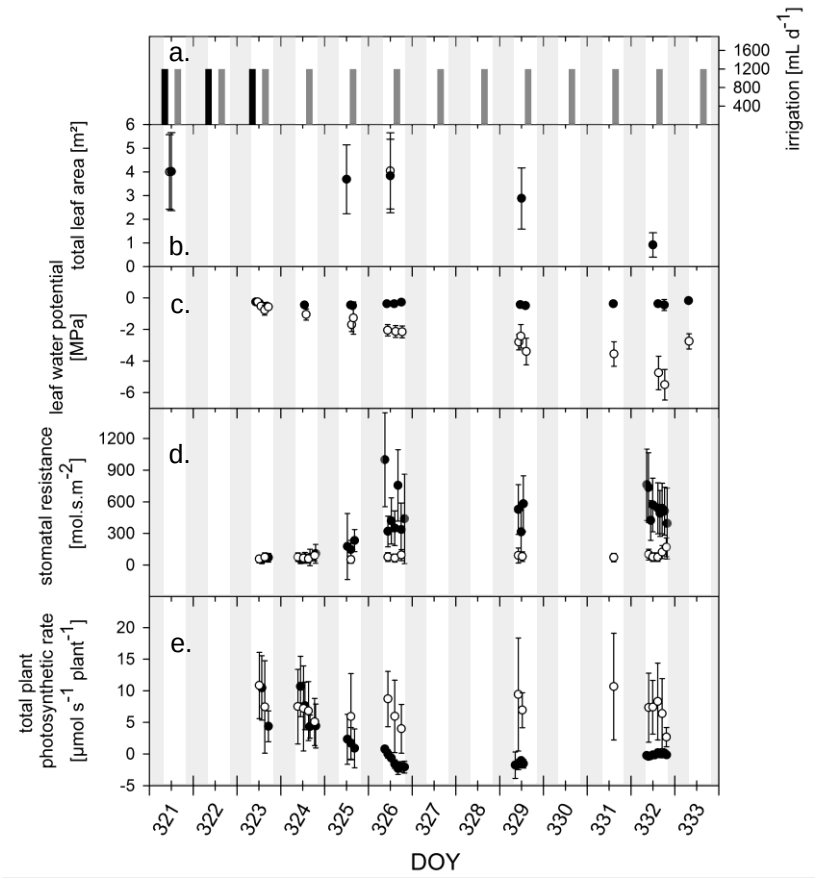

Figure 3.12 leaf properties **a.** total daily irrigation of drought (black bars) and control (black bars) treatment; **b.** total tree leaf area; **c.** leaf water potential; **d.** stomatal resistance; **e.** total plant photosynthetic rate; Black dots represent drought treatment, white dots represent control treatment. Shaded bars represent night time and white bars represent daytime (8h-20h).

Figure 3.13 Pictures of leaves during different stages of the drought treatment. Turgor loss and wilting can be clearly observed.

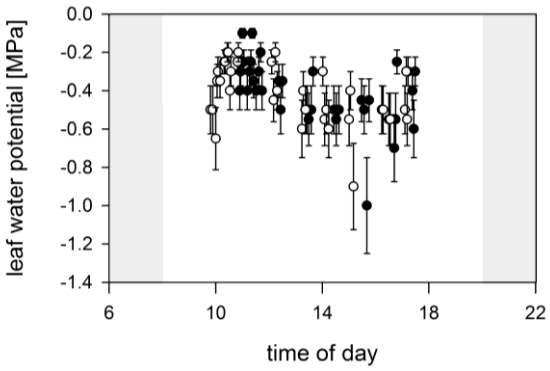

Figure 3.14 Leaf water potential on DOY 323. Black dots represent the seven trees (8-14) of the drought treatment. The control treatment (1-7) is represented by white dots. Shaded bars represent night time and the white bar represents daytime (8h-20h).

3.3.2 LEAVES DURING RECOVERY

A few days after rewatering of the plants, buds on the stem of some trees started bursting. Two weeks after rehydration, a couple of sprouts could be observed on the stem of tree 11 (Figure 3.15). In addition, in the top of tree 11 a considerable amount of green branches and leaves had developed. Whereas on tree 12 little growth of new leaves was observed (Figure 3.16).

Figure 3.15 Sprouting of fresh branch with leaves on the stem of tree 11 on DOY 352

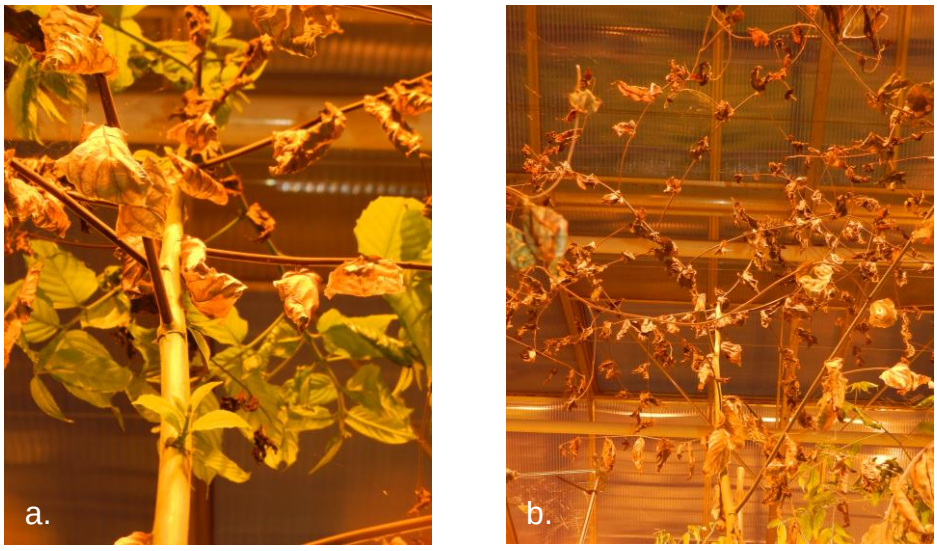

Figure 3.16 Tree tops of on DOY 353 **a.** tree 11 **b.** tree 12

3.4 STOMATAL RESISTANCE

Leaf stomatal resistance was measured periodically with the AP4 porometer (Delta-T Devices) between 12 and 16 h on the day before drought was imposed (DOY 223) and intensively throughout the day on the first day of drought (DOY 324). In addition to those measurements, leaf conductance measurements were logged by the LI-6400 photosynthesis apparatus during the drought period. While using the LI-6400 photosynthesis system to measure carbon uptake by the leaves, H_2O-exchange of the leaves was measured simultaneously. Stomatal conductance was calculated by the instrument in real time. Since it was not the initial intention to measure stomatal conductance with the LI-6400, user settings on the parameters for this calculation were not adjusted for the species. Neither the slope and offset of the boundary layer as a function of leaf area nor the stomatal ratio (K) to convert one-sided boundary layer conductance to effective boundary layer conductance were adjusted. Therefore data obtained with the porometer were considered as more accurate. To compare the measurements simultaneously taken with both instruments on DOY 323 and 324, they were converted to the same units since porometer readings were in velocity units and LI-6400 measurements in mol units of conductance.

Porometer measurements were converted from velocity to mol units of resitance using the following formula (eq. [24]) as described in the AP4 Porometer User Manual (Webb et al. 1990).

$$r' = r \cdot V_0 \cdot \frac{T}{T_0} \cdot \frac{P_0}{P} \qquad [24]$$

where r' is the resistance in m² s mol^{-1}, r is the resistance in s m^{-1} and V_0 (22.7·10^{-3} m²mol^{-1}) is the molar volume of air at T_0 (273 K) and P_0 (1000 hPa). T is temperature in K and is derived from the meteodata. P is atmosphere pressure in hPa and was measured during each calibration phase of the resistance measurements.

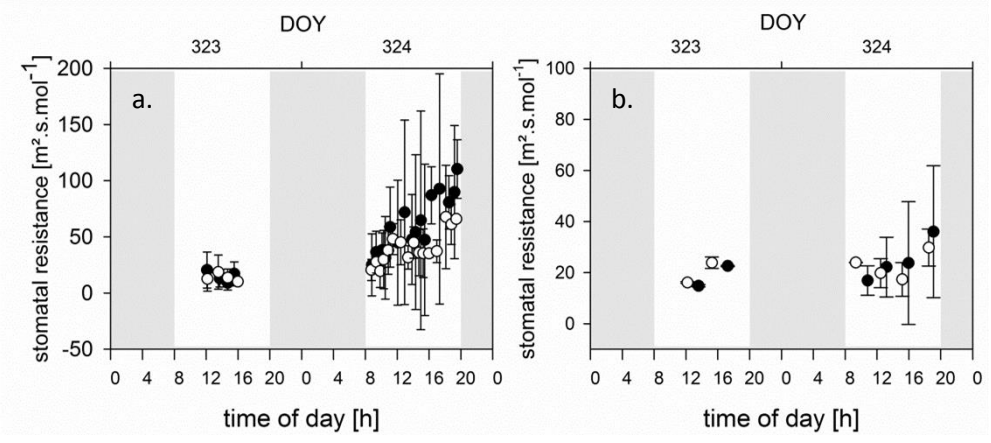

Figure 3.17 Stomatal resistance on DOY 323 and 324. Black dots represent drought treatment, white dots represent control treatment. a. stomatal resistance obtained with a dynamic diffusion porometer. b. Stomatal resistance derived by taking the reciprocal of conductance measurements executed using a portable LI-6400 photosynthesis system. Shaded bars represent night time and white bars represent daytime (8h-20h).

The results presented on Figure 3.17a showed a stomatal resistance around 20 m² s mol^{-1} on the afternoon of DOY 323. On the first day of drought (DOY324), r_s of trees exposed to drought increased

at a higher rate than trees of the control treatment. It can be observed that all resistances of the drought treatment increased more than those of the drought treatment. It should be noted once more that great uncertainty probably resulted from low replication (n = 2) and biological variation. This is illustrated by Figure 3.18. This graph shows that r_s of tree 11 increased significantly more than r_s of the other three trees including tree 12 which did not received irrigation either.

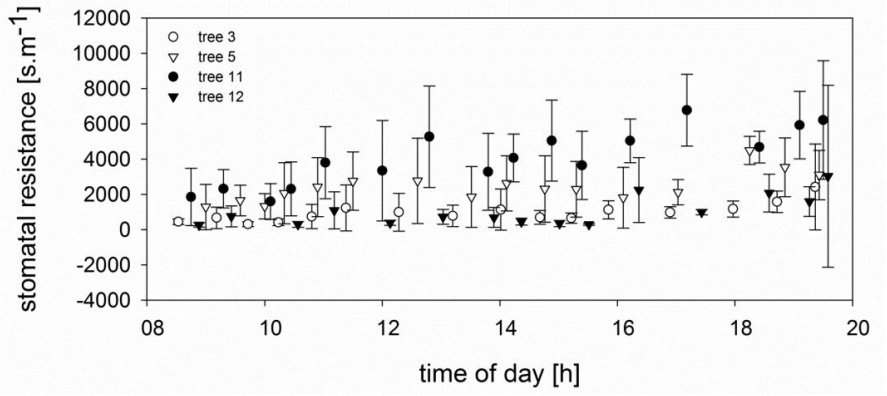

Figure 3.18 Stomatal resistance measured with the AP4 Porometer per tree on DOY 324. Trees 3 and 5 were irrigated at 9 h, 13 h and 21 h. Trees 11 and 12 received no water.

Figure 3.17b shows a similar trend as Figure 3.17a. That is why was decided to use the conductance measurements obtained with the LI-6400 photosynthesis system for the entire drought period. Since measurements with both instruments were taken simultaneously on DOY 323 and 324, it was possible to make a calibration curve in order to transform the LI-6400 measurements to effective resistance values. In this way, stomatal resistance could be evaluated over the entire drought period.

For each LI-6400 measurement on DOY 323 and 324 a measurement that was taken on the same moment was selected from the porometer data. Regression analysis was performed using R 3.1.0 for Windows. The resistance measured with the porometer was the independent variable and the LI-6400 dataset was the dependent variable. In order not to interfere with the effect of drought, for each treatment separately a linear model was fit using the method of least squares. R^2 was 0.5509 and 0.624 for the control and drought treatment respectively. Hence, LI-4600 measurements made during the entire drought period were transformed using the fitted regression equations (eq. [25])

$$r_p = a \cdot r_l + b \qquad [25]$$

with r_p the effective resistance in $m^2.s.mol^{-1}$, r_l the resistance (reciprocal conductance) measured with the LI-6400 in $m^2.s.mol^{-1}$, a the slope of the regression line and b the intercept. The effective leaf stomatal resistance is shown on Figure 3.12d.

3.5 PHOTOSYNTHETIC RATE

In Figure 3.12e photosynthetic rate of the total plant is presented in µmol CO_2 per second. In Figure 3.19 the results are presented on the scale of one day. On DOY 323, the day before drought was imposed, measurements on both treatments indicated the same photosynthetic activity for all trees. On the first day of drought (DOY 324) there was no difference between treatments either. The second day of drought, a decline in net photosynthesis was observed for the drought treatment. From DOY 326 to 329 negative photosynthetic rates were registered on leaves of the drought

treatment. On DOY 332 net photosynthesis on the drought treatment was zero. Throughout the whole day the leaves did not use CO_2 for photosynthesis nor produced CO_2 by respiration.

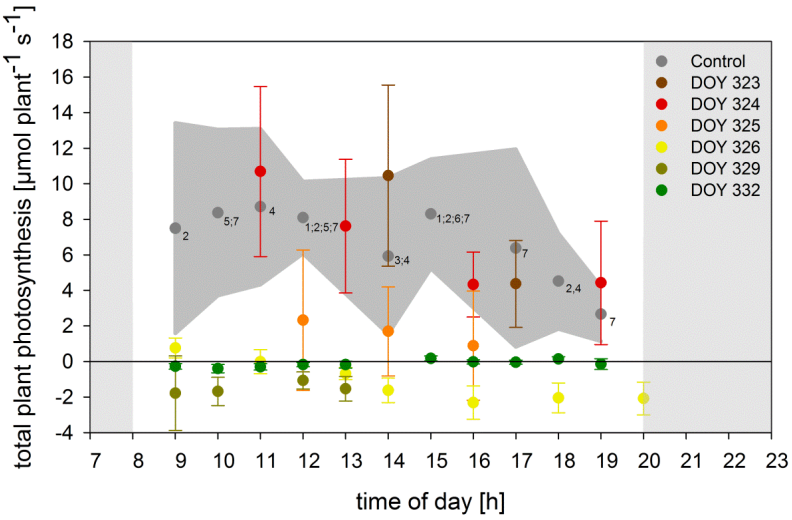

Figure 3.19 Total plant net photosynthesis. Grey dots represent daily photosynthesis of the control treatment. The number indicates which days are included in the average photosynthesis rate: 1. DOY 323; 2. DOY 324; 3. DOY 325; 4. DOY 326; 5. DOY 329; 6. DOY 331; 7. DOY 332. The uncertainty on the control averages is indicated by the grey area. Coloured dots represent total plant net photosynthesis of trees which received no water on DOY 324-337.

3.6 Wood anatomical features

3.6.1 Test sample

Cross-sections of the *M. eminii* test sample were obtained by X-ray CT scanning (Figure 3.20). Grey areas in the green and wet sample (Figure 3.20a) concealed the more detailed structures. After drying the sample, more details were resolved. It can be observed that the sample had shrunk during drying. While the diameter at the height of the pinning was 12 mm on the green sample, it was only 10.9 mm on the dried sample. Shrinkage occurred mostly in the outer band of the stem section.

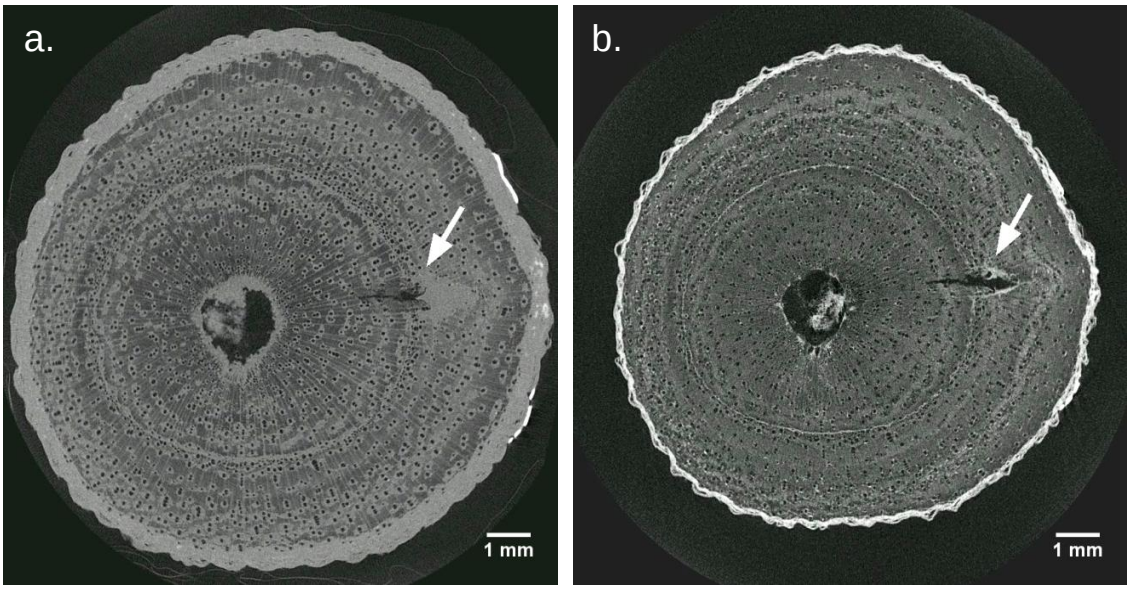

Figure 3.20 Micro CT transverse section of the test sample. **a**. green; **b.** conditioned. Arrows indicate the location of the pinning. Resolution = 15 µm, Scale bars = 1 mm

On Figure 3.21, scanned at higher resolution, it can be observed that a different type of wood tissue had formed around the pinning. The mechanical damage of the pinning on this sample, a hole in the wood, extended 1.5 mm in radial, 0.5 mm in tangential and 2 mm in longitudinal direction. The three-dimensional effect of pinning is illustrated in Figure 3.22.

Figure 3.23 shows that the location of the cambial initials at the time of pinning could be estimated by evaluating successive transverse sections at the level of the pinning. There was a clear inner border of the modified tissue. Since the border remained constant along the longitudinal axis, this was regarded as the position of the cambium cells at the moment of pinning.

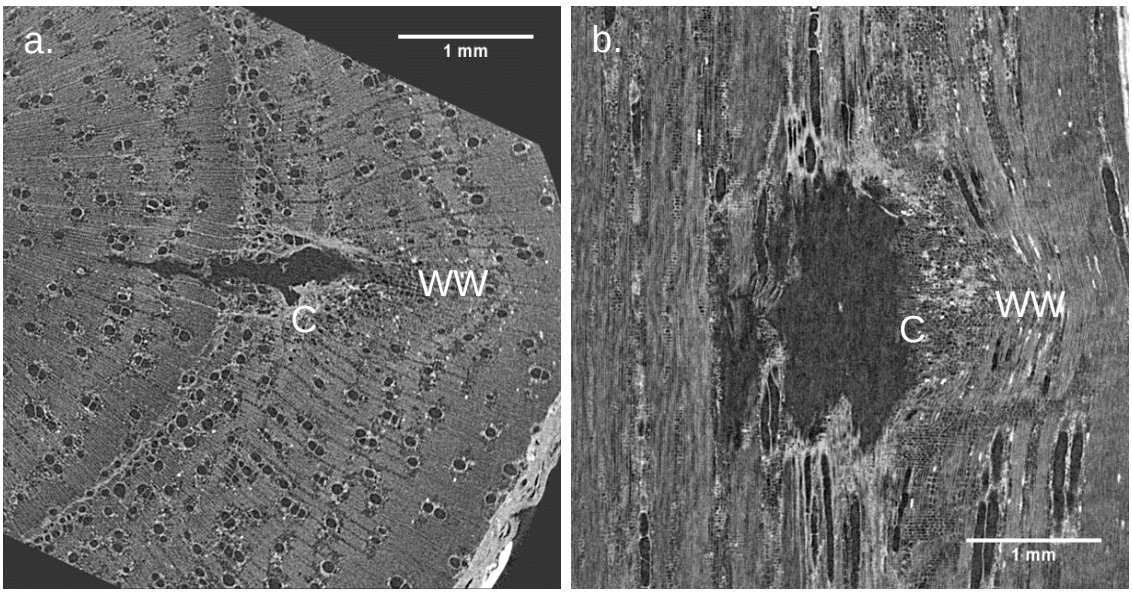

Figure 3.21 Conditioned micro CT slice of the pinning on the test sample. Callus (C) and wound wood (WW) were formed as a response to wounding. **a**. transverse section; **b**. radial section. Resolution = 3.5 µm, Scale bars = 1 mm

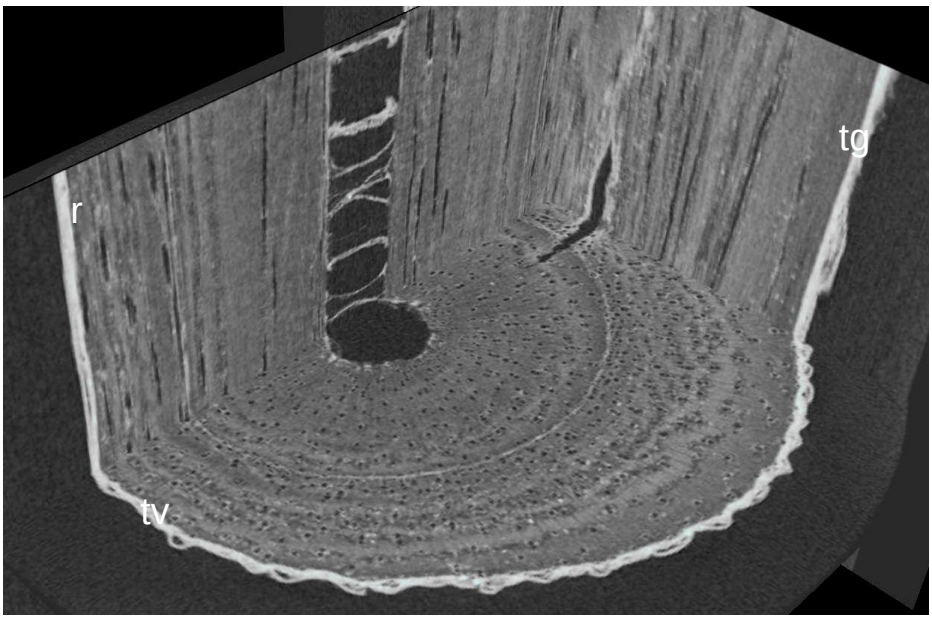

Figure 3.22 3D reconstruction of radial (r), transversal (tv) and tangential (tg) micro CT slices of the pinning on the test sample. Resolution of the slices = 15 µm

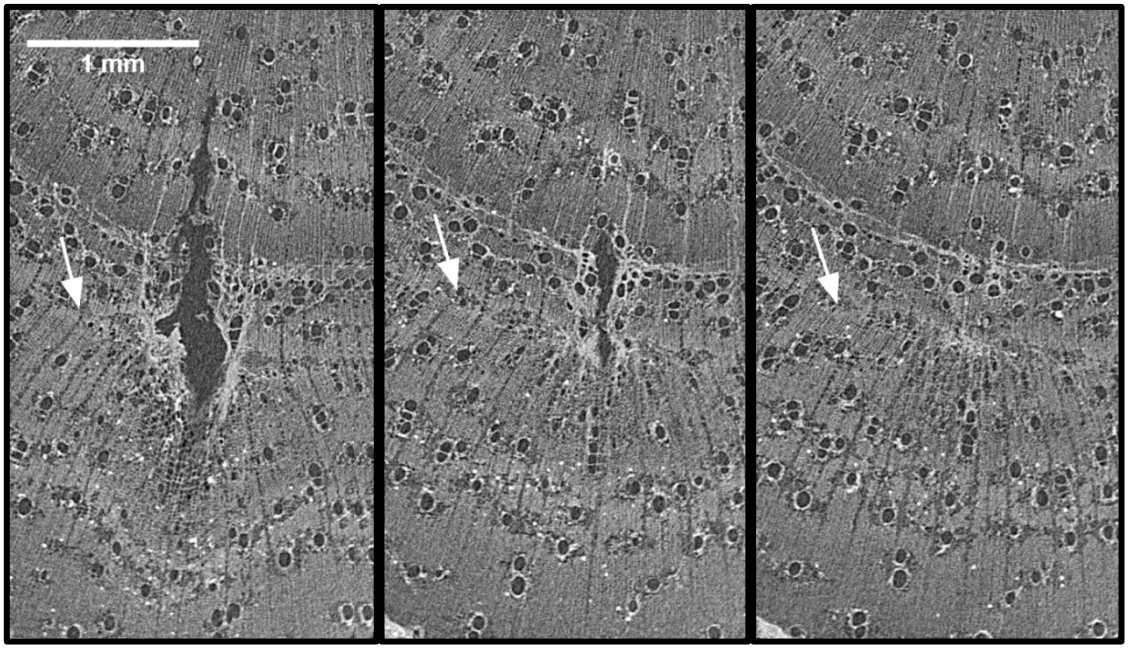

Figure 3.23 Conditioned micro CT cross sections of the pinning on the test sample on different longitudinal locations. Probable location of the cambium at the moment of pinning is indicated with an arrow. The centre of the stem is situated above the top of the images. Resolution = 3.5 µm, Scale bar = 1 mm

The stem sections of the trees used in the experiments had larger dimensions than the test sample and contained 3 pinnings each. Therefore scanning at high resolution (3.5 µm) was not an option given the relative long scan times required and the fact that only a single pinning could be visualized at this high resolution while quantitative analysis required the full cross-section. Therefore the test sample was scanned at high resolution as well as low resolution to evaluate image quality. Figure 3.24 shows that a resolution of 15 µm was sufficient to recognise the wound wood subsequent to the pinning. Scans of the samples from the experiment had resolutions ranging from 7 to 11 µm depending on the size of the sample and the allowable scan time (see section 2.4.2.1).

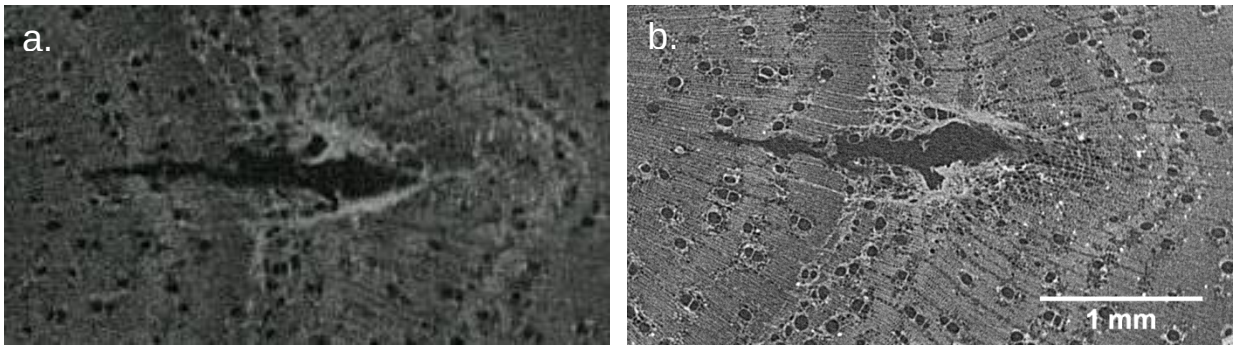

Figure 3.24 Micro CT transverse section of the test sample. **a**. Resolution = 15 µm; **b.** Resolution = 3.5 µm. Scale bar = 1 mm

3.6.2 MICRO CT IMAGES AND ANALYSIS

The response to pinning of the trees used in the experiment was similar to that of the test sample. Pinning locations could be easily pointed out and the position of the cambium could be estimated by delineating the wound tissue. It was convenient to recognise the wound tissue in consequence of the

cambium injury on the trees of the control treatment. As illustrated in Figure 3.25b the pinnings on the drought treatment just before (2) and just after (3) the drought period were located close to the bark, which made it difficult to demarcate the wound tissue and consequently difficult to locate the position of the cambium at the time of pinning.

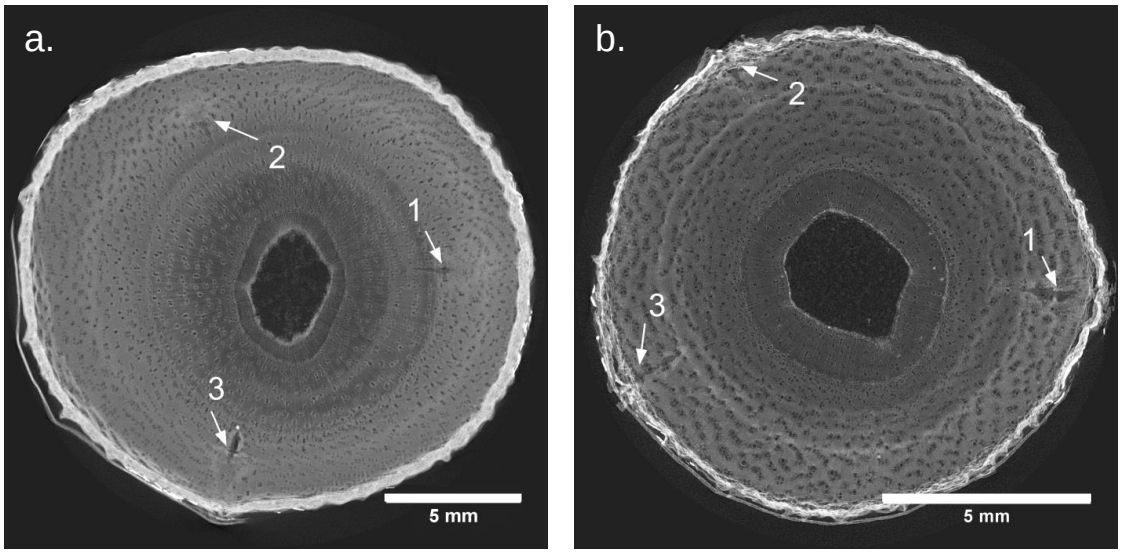

Figure 3.25 Conditioned micro CT transverse section from **a**. the upper pinning on tree 3 of the control group (Resolution = 11 µm); **b.** the upper pinning on tree 8 of the drought group (resolution = 7 µm). Arrows indicate the location of the pinning. Numbers indicate the number of the pinning which refers to the date of pinning: 1. DOY 302; 2. DOY 324; 3. DOY 338. Scale bars = 5 mm

An overview of the timing, location, naming and numbering of the pinnings is given in section 2.4.1. The first pinning indicated the start of the experiment on DOY 302. Figure 3.26a shows that for the trees from the control group, the absolute distance from the centre of the trees to the first pinning was smaller than the absolute distance from the centre to the later pinnings. This was true for the control treatment as well as for the drought treatment. The second pinnings were executed on the same day (DOY 324) that irrigation was turned off for the trees allocated to the drought treatment. The third pinning indicated the reactivation of the irrigation. Between the second and the third pinning no wood was formed in the drought treatment. The control trees did form wood between pinning 2 and 3 and there was a considerable amount of wood formed after the pinnings. This amount is declining from pinning 1 to 3 because the tree had more time to grow between the first pinning and harvesting than between the third pinning and harvesting. For the drought treatment there was only wood formation after the first pinning but this was a much smaller amount of wood. To take in account a possible deviation from perfect concentricity and circularity, relative lengths were shown (Figure 3.26b). The same trends could be observed and thus confirmed on this graph. Note that the total lengths of the stacks on Figure 3.26a were larger for the control treatments. This means that inner-bark radii after harvest and drying of all drought treatment trees were on average 3 mm shorter than those of the control treatment after harvest and drying. On the other hand, the amount of wood formed before the first pinning on the trees of the drought treatment and the trees of the control treatment (the first brown and black bars respectively on Figure 3.26 and Figure 3.28) was the same. Hence, the trees of both treatments had comparable dimensions at the beginning of the treatment. This was also confirmed by the dendrometer data (see section 3.2.1).

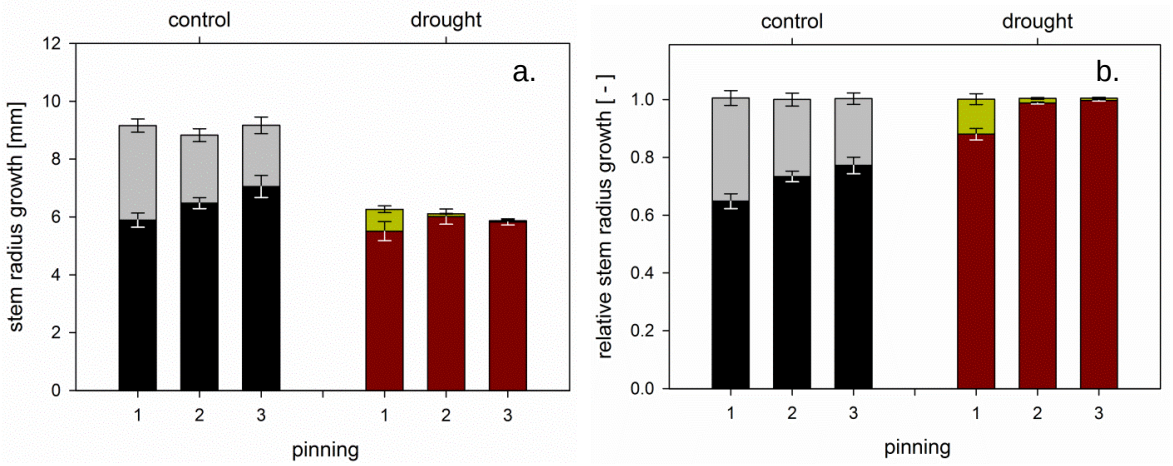

Figure 3.26 Stem radius growth of the conditioned samples**. a.** absolute lengths **b.** lengths relative to the total inner-bark radius. Black and grey stacks represent the lengths measured on the control group. Black represents the distance between the centre of the pith to the pinning. Grey represents the distance between the pinning and the interior of the bark. Coloured stacks represent the drought treatment. Brown bars represent the distance between centre and pinning, green bars represent distance between pinning and interior of the bark. The number of the pinning refers to the date of pinning: 1. DOY 302; 2. DOY 324; 3. DOY 338

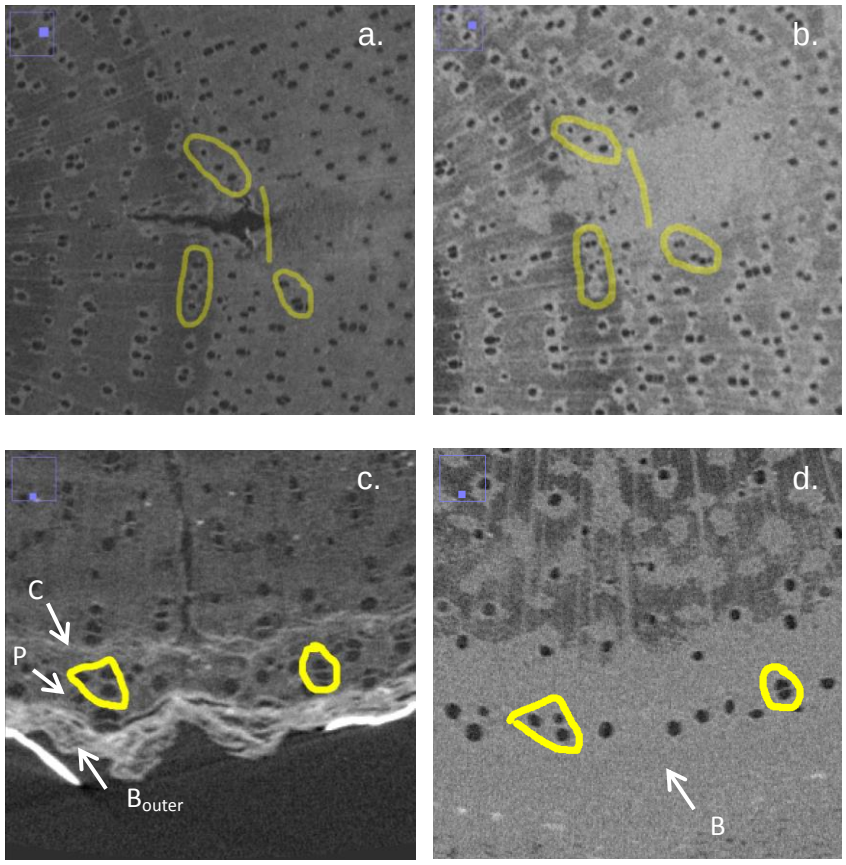

Figure 3.27 Comparison of micro CT images of dry and green samples. Anatomical features that are found in both images are encircled. **a.** Conditioned micro CT transverse section of a pinning. The yellow line indicates the location of the cambial initials at the time of pinning; **b.** The same pinning on a green micro CT transverse section The yellow line indicates the estimation of location of the cambial initials at the time of pinning, adopted from a; **c.** conditioned micro CT transverse section of the bark. Cambium initials (Ca), secondary phloem (Ph) and the shrivelled outer bark (B_{outer}) can be identified. **d.** Green micro CT transverse section of the same location. The inner border and the subdivisions of the wet bark (B) cannot be distinguished.

In order to study the same features on green samples, delineation of wound-tissue needed to be estimated on the green micro CT images. As shown on Figure 3.27a and b the location of the cambium at the time of the pinning could be estimated by comparing the green images with the conditioned images. Patterns in anatomical features could be identified on both images. In this way the delineation of wound wood could be copied from the dry to the green images. As described in the material and methods section (section 2.4.2.3), measurements on cross section images of the green samples required delineation of the bark. This could be done similarly, by identifying the cambial initials on the conditioned sample and transferring the location to the green image (Figure 3.27c and d). The grey area on Figure 3.27d, most likely indicating high water content, extended to the outer layers of the xylem contributing to the uncertainty in delineating the bark.

In Figure 3.28 is shown that in the measurements on the green samples, the same trends as on the oven dry samples could be observed. There was no growth during and after the drought period for the drought treatment. Although it seems that a small amount of wood was formed between and after pinning 2 and 3, it should be noted that error flags are large and overlap. This was due to the before mentioned uncertainty of the bark delineation. So it could not be stated with certainty that wood was formed between or after pinnings 2 and 3. It can be observed that wood was formed after the first period. However, this is a much smaller amount of wood than on the control sample. The control trees did form wood between and after all three pinnings. The absolute thickness of the bark was smaller for the drought treatment (Figure 3.28a) whereas the relative thickness of the bark was similar for both treatments (Figure 3.28b).

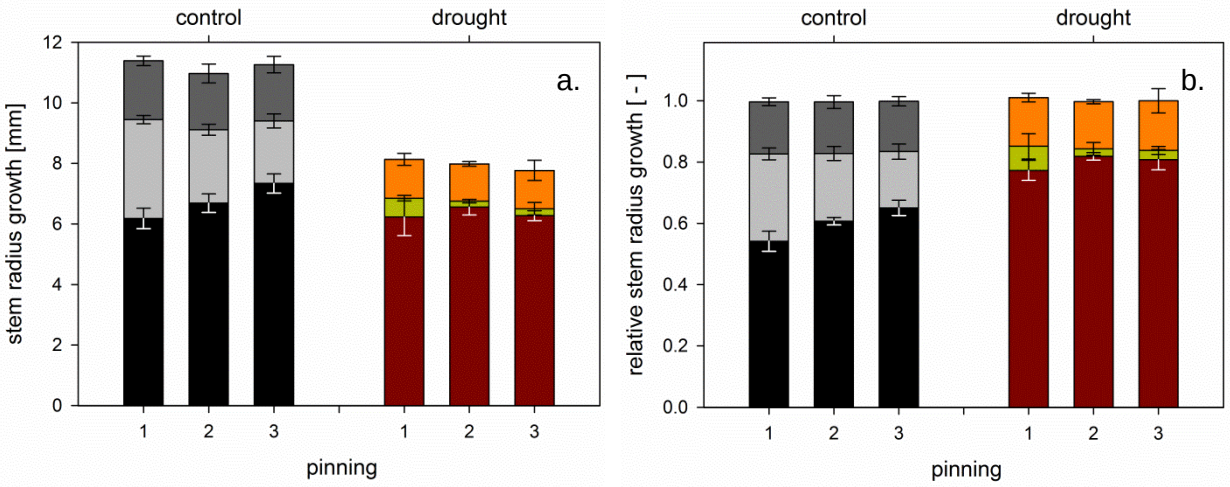

Figure 3.28 Stem radius growth of the green samples**. a.** absolute lengths **b.** lengths relative to the total over bark radius. Black and gray stacks represent the lengths measured on the control group. Black represents the distance between the centre of the pith to the pinning. Light grey represents the distance between the pinning and the interior of the bark. Dark grey represents the thickness of the bark. Coloured stacks represent the drought treatment. Brown represents the distance between the centre of the pith to the pinning. Green represents the distance between the pinning and the interior of the bark. Orange represents the thickness of the bark. The number of the pinning refers to the date of pinning: 1. DOY 302; 2. DOY 324; 3. DOY 338

Calliper measurements of diameters at the height of the pinning were obtained at the time of pinning. These diameters were compared with diameter estimations based on the radii measured on the micro CT images. Figure 3.29a shows that for 27 of the 30 measurements the results based on the micro CT images were larger than the calliper measurements. The average difference between the two methods was 0.8 mm. On Figure 3.29 diameters are grouped and averaged per pinning and per treatment. The larger diameters measured on the micro CT images could be observed for each pinning on each treatment. Nevertheless, the same trends in diameter growth could be observed for both methods.

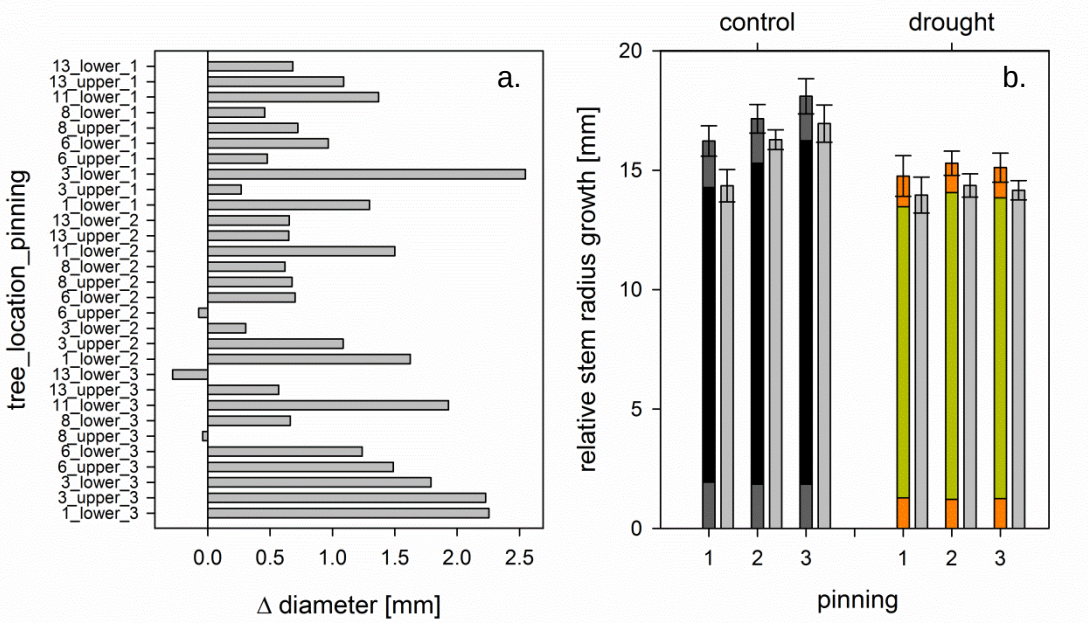

Figure 3.29 Comparison of diameters obtained from direct measurements and estimated from micro CT images. **a.** All measurements are displayed with their label. The label contains the number of the tree, the longitudinal location of the pinning and the number of the pinning. Trees 1, 3 and 6 were control trees and trees 8, 11 and 13 were allocated to the drought treatment. Δ diameter = estimated diameter – measured diameter. **b.** Average diameters per treatment per pinning. Black and grey stacks represent the control treatment with the xylem diameter (black) and the bark (dark grey) at both ends. Coloured stacks represent the control treatment with the xylem diameter (green) and the bark (orange) at both ends. Light grey bars represent the corresponding measured diameters.

4 DISCUSSION

4.1 REMARKABLE DIAMETER PATTERN AFTER DROUGHT INDUCEMENT

The first eye-catching result of the experiment is the extraordinary course of stem diameter a few days after imposing drought (Figure 3.5). Other studies mostly observe only a net decline in dimensions from the start of imposed drought until rewatering (Zweifel and Häsler 2001, Gallardo et al. 2006, Saveyn et al. 2007, De Swaef et al. 2009, 2013a, Nalevanková et al. 2013). Yet, in this experiment, after a sharp decline, a revival of stem diameter was observed a few days after drought inducement while no water was supplied (DOY 227-332). To be able to understand this occurrence, it is essential to know which plant dynamics are contained in the diameter measurements. Therefore, a brief overview of the theories and models that have been developed to link the non-destructive diameter measurements to plant physiological dynamics is be given. Also the notable deviations of *Maesopsis eminii* to these classical patterns and courses is be pointed out.

4.1.1 INTERMEZZO: LINKING STEM DIAMETER VARIATION TO GROWTH AND PLANT WATER RELATIONS

Variation in stem growth is dual, namely irreversible growth and changes in water content (Kozlowski and Winget 1964). Herzog (1995) related stem radius to the sap flow to use it to estimate transpiration. The theory is based on the diurnal use and replenishment of the stem water reservoir in the bark (Figure 4.1a and Figure 4.2). During the day internal water reserves are used and water content of the stem decreases, resulting in a lower (more negative) osmotic potential in the storage tissue in the evening. Osmotically active photosynthetic assimilates in the phloem may also attribute to the more negative potential in the storage tissue. Additionally, the rise in xylem water potential due to the time lag of sap flow towards transpiration and the corresponding ceasing of the negative tension pressure, contributes to the potential gradient driving water towards the storage tissue.

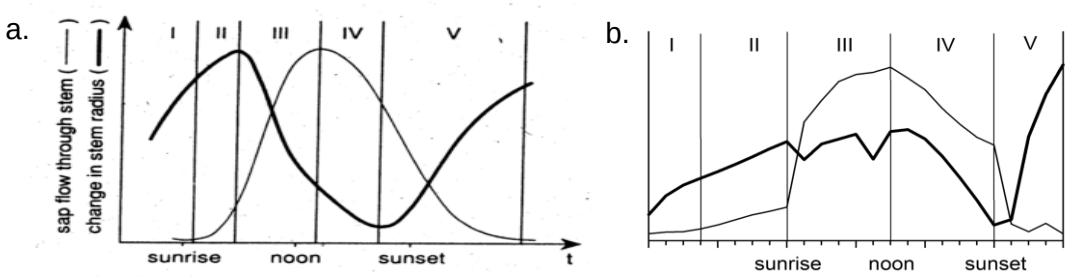

Figure 4.1 a. Theoretical course of characteristics of diurnal sap flow and radius variation. I. Nightly resaturation without measurable sap flow. II. Delay in sap flow rising and stem shrinking. III. Strong concave decrease in stem radius until maximum flow rate is reached. IV. Delay between maximum flow rate and smallest radius. V. Decline in sap flow and fast increase in stem radius (Herzog et al. 1995) **b**. Averaged diurnal course of sap flow and stem diameter for the *Maesopsis eminii* seedlings.

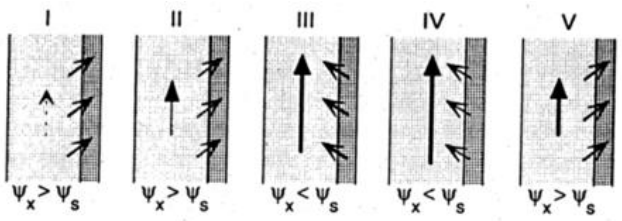

Figure 4.2 Schematic drawing of the diurnal upwards axial flow and radial flow which is the exchange of water between the conductive xylem tissue (light) and the storage tissue (dark). Flow towards the storage tissue results in radius increment. The phases correspond with the consecutive phases described on Figure 4.1a. Water flows towards the lowest water potential. Ψ_x is the xylem water potential and Ψ_s is the storage water potential. Intensity of the axial sap flow is indicated by the thickness of the arrows. (Herzog et al. 1995)

Figure 4.1b shows the phases of diurnal course of diameter variation and sap flow described by Herzog et al. (1995) applied to the measurements on *M. eminii* during control treatment (see also Figure 3.6). Some obvious deviations of the classical pattern could be observed. However, one should keep in mind that stem shrinkage and swelling can considerably vary from day to day (Zweifel et al. 2000). On sunny days maximum daily shrinkage (MDS) can be extensively greater than on cloudy days due to higher transpiration rates (Zweifel et al. 2000). The patterns on Figure 3.6 and Figure 4.1b were generated from a dataset of 20 days during which incoming radiation fluctuated (Figure 3.1g) and therefore should be interpreted with caution. Nevertheless, it is noteworthy that although the sap flow course of *M. eminii* generally followed the theoretical course, the timing was remarkably different. Sap flow initiated around 2:00 and reached a rate of 20 g h^{-1} before sunrise. Figure 3.1b shows that no radiation was observed during these early hours. Phase II was elongated and initiated earlier for *M. eminii* compared to the typical pattern. Also a more distinct effect of sunset was observed. Though, this could originate from the shorter time span in which the assimilation lights reach their maximal radiation (Figure 3.1b) compared to natural dawn. Also the stem diameter pattern remarkably differed from the classic course. While phase III usually corresponds with a steep decrease in stem radius, diameters of *M. eminii* only fluctuated during this phase according to water supply by irrigation (9:00, 13:00 and 21:00). A steep but not even concave decrease occurred only from noon to sunset.

Zweifel (2000) related stem radius variations to changes in water content of the specific locations of water storage. He found that if the xylem water potential (ψ_x) is above a phase-transition point, water content (WC) of the stem can be calculated from continuous stem radius measurements. Above this point water is withdrawn almost solely from the elastic living bark tissue. This insight was derived by drying cut stem sections while monitoring their weight, volume and microscopic cross-section. Until the phase-transition point was reached, contraction occurred mostly in the living tissues of the bark (cambium, phloem and parenchyma). In this phase the difference in weight (ΔW) was linearly correlated to the volume decrease (ΔV). When ψ_x falls below the threshold value, the rigid xylem tissue becomes depleted. During this inelastic phase decreasing water content and associated weight loss is less expressed in a volume change. Indeed, in the young *Maesopsis eminii* trees contraction of the stem tissue after cutting and drying mostly occurred in the outer, living layers of the stem section. This could be observed visually on Figure 3.20 and Figure 3.27 (c,d). Moreover, the total radius of the xylem tissue on Figure 3.26a (total stacks) was equal to the dimension of the xylem on the green samples on Figure 3.28 (total stack without the dark grey bark

section). If the inelastic drying phase occurs in living plants, air is sucked into the vessels and the water column breaks, *i.e.* cavitates. Zweifel (2000) concluded that since fluctuations of xylem only marginally contribute to diurnal changes in stem diameter, stem dimensions can be used to describe the water status of the plants. Within the range of available water depletion, the dendrometer measurements can be directly coupled with the stem water content. Bark water content can be determined by evaluating water potential gradients. These gradients can be coupled with water uptake, sap flow through the stem and transpiration in flow and storage models (Zweifel and Häsler 2001, Zweifel et al. 2001, Steppe et al. 2006).

As mentioned at the beginning of this section, diameter variations are composed both of diurnal dynamics of water storage and tree growth. To extract the latter, different approaches have been described that can be divided into two categories (Deslauriers et al. 2007). The daily approaches extract one value per day whereas the stem cycle approach is a reduction of the five phases course by Herzog et al. (1995) into a three phases cycle (Deslauriers et al. 2007). The cycle consists of a contraction phase, an expansion phase and a phase of stem radius increase which can be separated and analysed independently (Deslauriers et al. 2007, 2011). As described in the literature review, adequate hydrostatic pressure is an indispensable condition for tree growth (Lockhart 1965). A threshold can be determined above which irreversible growth can take place (Proseus et al. 1999, Steppe et al. 2006, De Swaef et al. 2013a). As such, growth rate is determined by biochemical reactions to support cell wand expansion that contain a turgor-sensitive step (Proseus et al. 1999).

Recently, Steppe et al. (2006) developed a dynamic flow and storage model that includes both the diurnal water dynamics and stem growth. As described in 1.2.1.2, this model is an enhancement of the van den Honert concept (1948). If a proper calibration is performed, the mathematical model can predict stem diameter variation and dynamic water transport with whole tree leaf transpiration as the only input. Moderations of the model have led to practical applications such as efficient irrigation systems (Steppe et al. 2008b) and improved models (De Pauw et al. 2008). In particular, adjustments were made to be able to use the model under dry conditions (Baert and Steppe 2013). The models are mentioned in this intermezzo, mostly to complete the overview of how stem diameter data can be analysed and interpreted. Although not yet implemented on these data, it is possible that with the use of models, valuable and even more profound insights will be gained.

With this background, the dendrometer results gathered in this experiment can be put into a larger perspective.

4.1.2 UNRAVELING THE DIAMETER AND SAP FLOW RESPONSE TO DROUGHT OF *M. EMINII*

When the average diameter course is studied (Figure 3.5), it can be argued that the diameter variation of the separate trees could follow another course within the uncertainty band. However, the same course of decline-revival-relapse-increase was confirmed for both trees as can be seen in Figure 3.11. It needs to be ruled out if the ostensibly extraordinary response of the stem diameter to drought can be declared by a sensitivity of the sensor to environmental factors. In particular temperature is known to possibly cause inaccuracies in the use of precision dendrometers (Drew and Downes 2009). Therefore it was verified if similar trends were found in the course of temperature, VPD and radiation and in the course of dendrometer data, but no evidence for such an influence was found.

The revival of the diameter starts on DOY 327, the fourth day of drought, while sap flow rates were approximately zero (Figure 3.4 and Figure 3.5) and the wilting process had already commenced. Thus, it can be assumed that there was water shortage and the turgor of the cells was minor. Therefore, as described in the intermezzo (4.1.1), according to the model of Lockhart (1965), stem diameter variation was unlikely to be caused by wood formation and should be caused by a change in water content. But where did this water come from during water shortage?

A possibility of downward water redistribution within the plant was put forward. In this theory, water from the upperparts of the tree would be withdrawn and stored in the trunk base. However, the availability of top water appeared to be very low. On the days concerned (DOY 227-332), leaf water potential with values of -2 to -6 MPa exerted a strong tensile force on the water molecules (Figure 3.12c). On DOY 333, leaf water potential was measured before sunrise in order to assure that predawn equilibrium in water potential could be assumed where the potential of the leaves approaches stem water potential. Thus, it can be expected that on that morning both in the leaves and the branches a low water potential of -2.75 MPa was prevalent (Figure 3.12c). Hence, a very strong tensile force had to be overcome to obtain downward water movement. It can be excluded that the gravitational component of the water potential could surmount these negative potentials since the water potential of water molecules in the top of the trees, approximately 230 cm above reference level, is only 0.023 MPa. Another proposition was a type of active hydraulic redistribution where osmotic assimilates were transported into the water storage pool of the trunk base as a response to drought. However, this was very doubtful to occur. First of all, the photosynthesis process in the leaves already came to a standstill at DOY 326 so assimilation of osmotic active molecules is doubtful. Also, assumed that very negative water potential is built up in the living cells of the bark, this water would not be easily available for resumption of sap flow after the drought period. Therefore the hypothesis of redistribution of crown water towards the trunk was rejected.

If the water was not coming from above, the next step is to assume that new water was entering the roots and transported upwards. This hypothesis raises three main questions: Where and how did the roots find water while soil water potentials indicated that no more available water was present in the pots (Figure 3.1e)? If there is an upward transport of water, what is the mechanism driving it? If there is a kind of sap flow, should it not be observed by the sap flow sensor?

Where and how did the roots find water?

The ability of roots to grow towards higher moisture content is called hydrotropism (Eapen et al. 2005, Cassab et al. 2013). Although many studies have been elaborated on the long known role of the root cap in the mechanism of gravitropism, where the roots grow in the direction of gravitation, remarkably little is known about the hydrotropic response of roots (Eapen et al. 2005). Nonetheless, it is believed that gravitropic growth of roots is strongly influenced by the microenvironment and thus driven by water concentrations, nutrient distribution, obstacles, temperature, light and the availability of oxygen (Takahashi 1997, Eapen et al. 2005, Takahashi et al. 2014). In analogy with gravitropism, the root cap has the leading role in hydrotropism, since it is the first to encounter the soil conditions while moving through it (Eapen et al. 2005). The exact mechanism is still mysterious and subject to research. A clear synopsis of the already deciphered sensing and response mechanisms in the root growth response to water is given by Eapen et al. (2005) and updated by (Cassab et al. 2013). Probably *Maesopsis eminii* trees used hydrotropism as a strategy to escape

drought. In Figure 4.3 it can be seen that some of the roots escaped the pots through the bottom holes when drought was imposed. They managed to reach the water that was stagnated in the drainage troughs. Furthermore, it was observed that trees that had produced more roots outside the pots were able to longer maintain their turgor and greenness.

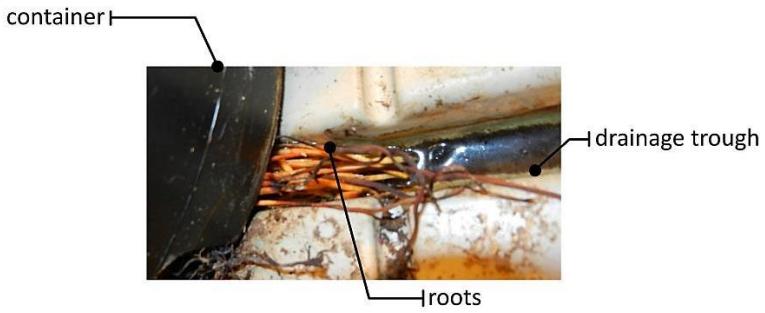

Figure 4.3 Roots of tree 11 from the drought treatment outside the container.

What causes or drives the presumed sap flow during DOY 227-332?

At first, it was thought that water uptake by the roots during DOY 227-332 was driven by transpiration as described in the literature review (section 1.2.1.2). The leaf water features at that time revealed however that it was unlikely that transpiration was still able to exert a lifting force on the water molecules as is the mechanism in the standard cohesion-tension theory. Transpiration considerably declined during that period because of leaf shedding (Figure 3.12b and Figure 3.13). It can also be assumed that at the remaining leaf surface, transpiration was limited if not nonexistent. During DOY 227-332 leaf water potential dropped from -2 to -6 MPa while ψ_l of the control treatment and ψ_l of the drought treatment, before drought was imposed, were between -0.2 and -0.6 MPa (Figure 3.12c). Therefore it can be expected that most of the leaves were beyond the threshold for plasmolysis where turgor drops below zero and the leaves become permanently wilted (Boyer 1968, Slatyer 1969, Porporato and Laio 2001). The assumption of zero transpiration is clearly confirmed by the extremely high stomatal resistance rates (Figure 3.12d). When these values are compared to initial r_s and r_s of the control treatment (Figure 3.12d and Figure 3.17) it can be concluded that the stomata were closed during DOY 227-332. Possibly, the answer to the unidentified low sap flow mechanism can be found in the other unexpected observation of sap flow rates: as depicted in Figure 3.4 and Figure 3.6 and stated before, there is predawn sap flow on all days of the experiment for the control group and for all trees before drought was imposed. Also here it needs to be verified whether this sap flow was driven by transpiration. Sadly, no stomatal resitance measurements were made before sunrise or long enough after sunset. In the summer of 2013 an outside experiment with comparable setup was conducted in south Uganda in the framework of this dissertation. The results of the experiment were not implemented in the final work. An exception is the series of stomatal resistance measurements that are shown here solely to supplement this part of the discussion (Figure 4.4). Here also, most resistance measurements were performed during the day. However some resistances were registered before sunrise and after sunset. The high resistance values suggest that stomata were closed both in the morning and in the evening. However, these resistance values were still relatively low compared to the resistance at the moment of midday stomatal closure. Hence, the degree of stomatal closure at midday was higher than at night and at night stomatal closure may not have been absolute. This may indicate that the species does have a

trait for night time transpiration. Nonetheless, since the details of the experiment are not included and conditions were different, interpretation should be done carefully.

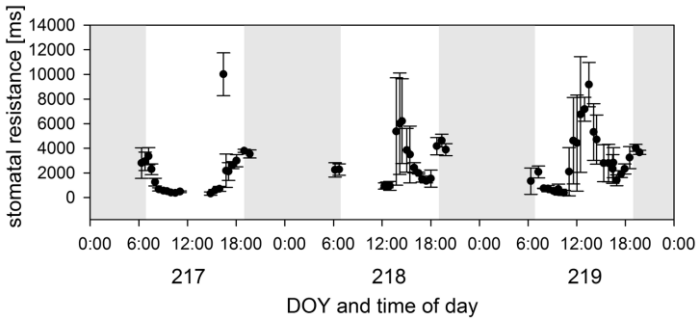

Figure 4.4 Stomatal resistance on young *M. eminii* trees in an outside pot experiment in Uganda. Black dots represent the average resistance of three trees. Error bars represent standard deviation. The trees received irrigation. Shaded bars represent night time and white bars represent daytime (6:52-18:59).

At this stage night time transpiration cannot be ruled out for *Maesopsis eminii*. Dawson et al. (2006) described this phenomenon for many tree species in different ecosystems. To correctly evaluate the existence of night time transpiration in this species, transpiration itself should be measured. Transpiration rates can be evaluated by using the mass balance method (Vermeulen et al. 2007) or by applying the stem heat balance on a crown branch, by up-scaling with the ratio of total leaf area/leaf area upstream of the sensor (Steppe et al. 2006) or by the ratio of the daily sum of stem sap flow/branch sap flow (Saveyn et al. 2007). However, although normally higher water demand of the atmosphere is related to higher sap flow rates (Dawson et al. 2007), a decline in vapour pressure deficit during the increase in predawn sap flow was found (respectively Figure 3.2 and Figure 3.4). Hence, it can be assumed that VPD was not triggering transpiration during the night which could drive sap flow. From these findings it could be concluded that transpiration was not the (only) parameter generating predawn sap flow. Presence of an osmotic driving force resulting in an upward positive pressure, known as root pressure (Henzler et al. 1999), was suggested. Due to an indirect active uptake of water into the root vessel a positive pressure is build up in the stem xylem (Mohr and Schopfer 1994). In some plants, root pressure can be observed by guttation droplets at the tips of the serrations of the leaf margins (Mohr and Schopfer 1994, Kramer and Boyer 1995c). Kramer and Boyer (1995a) describe tree groups of theories for root pressure: secretion (non-osmotic) theories, electro-osmotic theories, osmotic theories. The latter is considered as the most acceptable and therefore briefly explained. In the roots the apoplastic pathway is interrupted by the hydrophobic Casparian strip (Figure 4.5) and water transport is forced to follow the symplastic route through semi-permeable membranes. Hence, this root zone can be considered as an osmotic pump. It is known that solutes can cumulate in the root xylem by an active distribution of mineral nutrient ions, disintegration of protoplasts in maturing xylem vessels and nutrients that are absorbed by the transpiration stream. Hence, an osmotic gradient is present over the semi-permeable membranes, causing the diluted solution (apoplastic water) to move towards the root xylem. The osmotic pressure pushes the water into the xylem vessels of the stem. When the plant is transpiring, root pressure is neutralized by the tensile strength and the nutrient concentration in the root system is lowered by increased water flow. When transpiration is limited however, it can be of great influence on the plant-water relations. For example, it is believed to play a role in the refilling of cavitated xylem vessels (Sherwin and Pammenter 1998). The occurrence and relevance of root pressure is still a topic of active research.

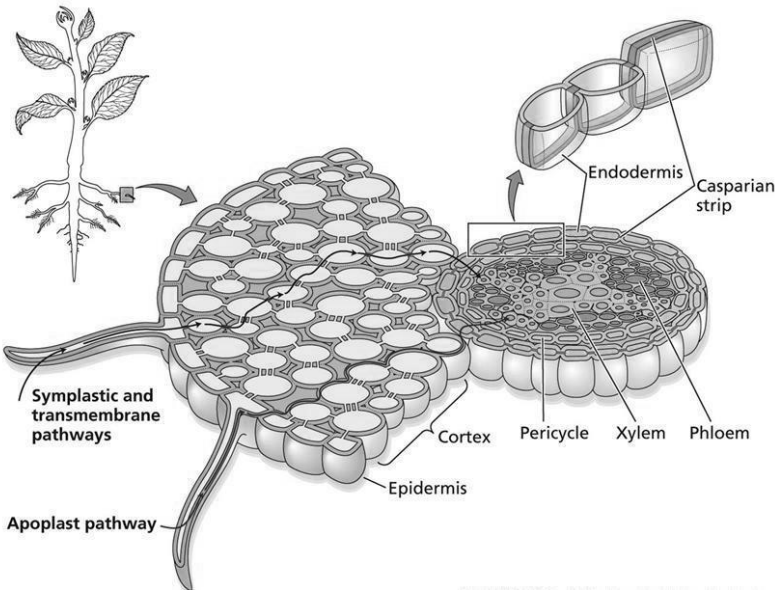

Figure 4.5 Root structure and intracellular (symplastic) and intercellular (apoplastic) transport of water in roots (Taiz and Zeiger 2010)

When reviewing the typical diurnal course of sap flow and diameter in Figure 3.6 or Figure 4.1b, the assumption of the capacity of *Maesopsis eminii* to build up an osmotic pressure in its root system ccould be confirmed from the fact that predawn sap flow increased while there was no shrinkage in stem diameter. If the sap flow was caused by increasing transpiration rates, this would have resulted in a decrease in stem diameter. Indeed, the latter was observed when sap flow rates were augmented by a plausible boost in transpiration when the lights were turned on but not during predawn conditions when on the contrary increment of stem diameter was observed. De Swaef et al. (2013b) also observed an increase in stem diameter during the morning, which they related to root pressure. The existence of root pressure and the presumed capacity of *Maesopsis eminii* to produce root pressure thus suggested water uptake through the roots during the last hours of the night and during drought stress, both with limited transpiration. In the first case, water was easily available for the roots for predawn root pressure ($\psi_{soil} > -0.015$ MPa, Figure 3.1e). Hence, the water forced into the stem xylem could cause sap flow rates high enough to be picked up by the sensor. In the latter case, drought stress limited the available water for the roots. The remaining water in the drainage gutters was relatively low and depleting. It is assumed that the water that was pressed upward from the root system immediately moved radial towards the storage compartments causing the increase in stem diameter variation (De Swaef et al. 2013b). In order to allow this radial transport and storage, adequate amounts of living tissue should be present. The CT scans confirmed that parenchyma was reasonably abundant around the vessels and in the rays. This was also described by Ani and Aminah (2006).

Could the presumed sap flow be observed with the SHB method and why (not)?

Although sap flow rates during drought were constrained due to limited water supply, it was interesting to find out whether the diameter dynamics were completely lacking in the sap flow measurements or whether they could be detected in the sensor signals. As described in the material and methods section (2.3.1.1), sap flow rates presented in Figure 3.4 were calculated according to the Dynagage sap flow sensors manual. The end result of the stem heat balance depends on the

determination of many parameters such as K_{sh}, dT threshold and Q_f threshold and valuable signals may be wrongly excluded. Therefore the stem heat balance was re-evaluated in detail. The intermediate steps are presented in Figure 3.7. During most of the drought period both Q_f and dT were below the pre-set thresholds and sap flow was set to zero. The course of the temperature difference (Figure 3.7f) revealed that the sensor did detect diurnal dynamics. The course of dT during the period of increasing diameters has been enlarged in Figure 3.7g so that the diurnal pattern can be clearly observed. The dT pattern follows a smooth and recurring undulating pattern with maxima during the day and minima at night, in contrary to the sudden changes in the raw CH signal (incorporated in the calculation of radial conduction, Q_r on Figure 3.7 by eq. 13) exactly at the moment of on and off switching of the assimilation lights caused by warming of the outside of the sensor. The pattern of dT during the drought period could be interesting if it truly could be related to sap flow instead of being set to zero. From the diurnal course of temperature diference in function of sap flow that is presented in the the Dynagage sap flow sensors manual (Figure 4.6) it could be seen that there is a linear relation between dT and low sap flow rates in red cedar (*Thuja plicata*). It was tested whether the same linear relation could be expected for the sap flow measurements on *Maesopsis eminii*.

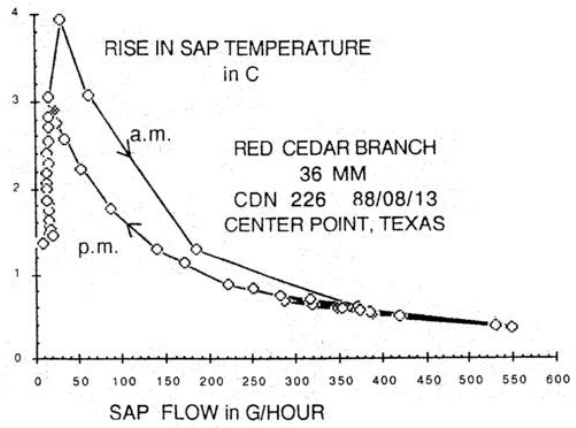

Figure 4.6 Rise in sap temperature in function of sap flow (Dynamax Inc 2005)

The diurnal courses of dT in function of sap flow rates are presented in Figure 3.8 and their calculation is based on the 5 days prior to drought induction. All sensors were evaluated separately because the correlation would probably be sensor-specific. Indeed, for each sensor linear correlation could be assumed within a specific range of sap flow rates and within a limited time of day. These limits were derived from Figure 3.8 for the sensors on the drought treatment with the intention to acquire a linear relation that could be used to relate the dT measurements during drought to sap flow rates. In Figure 3.9a and c and in Table 2 it is shown that for both sensors a different linear relation could be assumed. However, low R^2 values indicated weak regressions. When the five days were analysed separately, much better linear models could be fit. Hence, could be decided that correct (daily) calibration and validation would be necessary to allow using the linear relation on days different from the ones that were used to create the relation. Figure 3.8 and the regression analysis showed that the precondition for linear dependency of dT not only included low sap flow rates. Moreover, the linear relation required temperature differences between 1.7 and 2.2 °C for tree 11 and between 1.18 and 1.45 °C for tree 12. However, temperature differences over the heater did not exceed the threshold that was set for the calculation of the heat balance (0.75 °C) starting from

DOY 327 (Figure 3.7). Therefore linear relations could not be used. The fact that dT values of the control treatment and before drought was imposed were considerately larger could be explained by the remark on the stem heat balance in the material and methods section (last paragraph in 2.3.1.1). Sap flow was set to zero each time that minimal K_{sh} is determined. However it could be possible and according to the assumption of relevant root pressure that sap flow of the control treatment was never zero at night. A modest sap flow could absorb a small amount of heat from the heater and warm up the thermocouples that were above the sensor (A and B, Figure 2.4). A little less heat is dissipated through conduction so that the temperature difference over the sensor increases. Only if there is absolute zero sap flow, upwards and downwards heat dissipations will be equal leading to zero dT. During drought sap flow rates are more likely to approach zero sap flow and hence lead to a very small dT. However, the dynamics in dT may thus indicate a very low sap flow rate. Unfortunately these dynamics are filtered out since at the time of drought, both the convection flow and temperature differences are below their threshold and sap flow is set to zero (Figure 3.7e and f). As described in the material and methods setting, the reasoning behind this filter is to exclude unrealistic excessive sap flow rates that result from dividing by too small dT values. For different species, different dT thresholds are chosen with 0.75 °C as the standard setting. To evaluate if a lower threshold could be used, sap flow was recalculated while the threshold of 0.75 °C was set to zero and gradually increased. Figure 3.10 shows recalculated sap flow with a threshold of 0.3 °C. It should be kept in mind that by limiting the effect of the filters, other artefacts may have been included in the calculation. The sudden rises in calculated sap flow when the light were switched on could have been the result from AC response as described before. Nonetheless, Figure 3.10 was an extra indication that it would be premature to assume that sap flow declined to zero and there were no dynamics in the water transport after drought implementation. Moreover, the same pattern (although on a smaller scale) that raised the presumption of root pressure in the control treatment could be observed on some of the drought days (e.g. the morning before DOY 329, 330 and 338, 340). It can be stated that there are convincing indications of low night time sap flow and considerable predawn sap flow, driven by root pressure. Although night time sap flow rates may be relatively small compared to daytime rates, low sap stream during the night is of extreme importance for the survival of the plant (Nadezhdina 1999).

4.2 RESPONSE OF *MAESOPSIS EMINII* TO DROUGHT AND ITS SURVIVAL STRATEGY

The response of plants to drought consists of a complex of diverse and interacting mechanism and differs from plant to plant (Ritchie 1981, Porporato and Laio 2001). Besides, the effect of drought is hard to predict since it not only depends on the variety of inherent plant responses but also on the character and severity of the drought itself. The severity of drought is influenced by many factors such as rainfall frequency and distribution, moisture-holding capacity of the soil and vapour pressure deficit of the atmosphere (Farooq et al. 2009). Figure 4.7 shows that soil water deficit directly affects the plant water potential. Next, all plant processes have different sensitivities to the declining water potential. A typical sequence of plant physiology decay caused by the decrease in cell water potential is given in Figure 4.8.

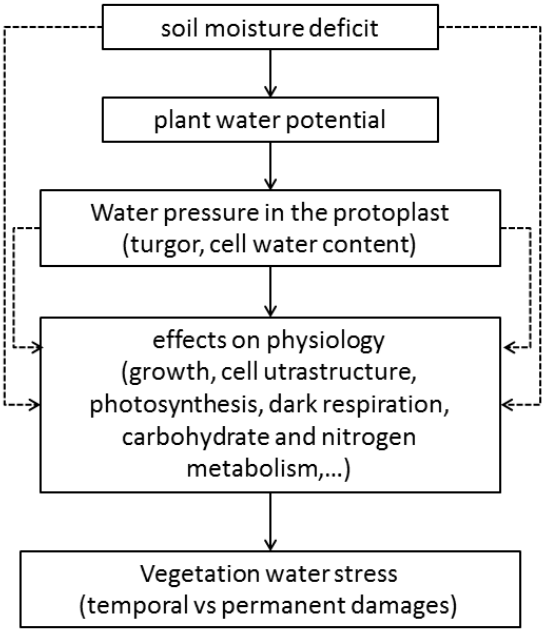

Figure 4.7 Processes linking soil moisture conditions to plant and vegetation status (after Porporato and Laio (2001)).

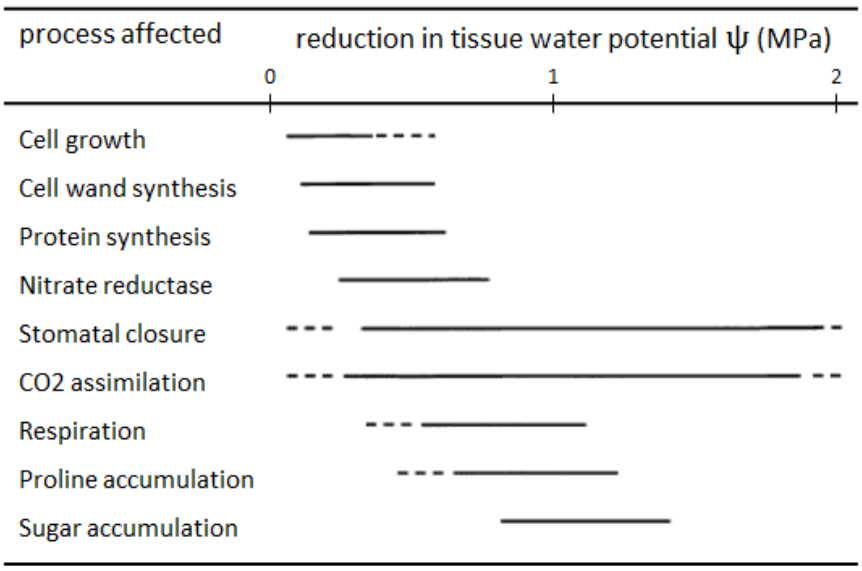

Figure 4.8 Effect of reduction in tissue water potential on physiological processes. Lines represent the range of reduction in water potential (relative to water potential of irrigated plants under mild VPD) that disturbs the process in question (Hsiao and Acevedo 1974, Porporato and Laio 2001).

The first process to be affected by water deficit often is the expansion growth followed by cell wand synthesis (Ritchie 1981, Porporato and Laio 2001, Farooq et al. 2009). The CT images revealed that no wood was formed after the induction of drought (Figure 3.26 and Figure 3.28). It can thus be stated that drought stress leaded to impaired mitosis, cell elongation and expansion which severely hampered tree growth. At leaf level, the first response to water deficit was observed in the leaf water potential. At the day when drought was imposed (DOY 324), ψ_l of the drought treatment was lower than the control treatment. The following days, ψ_l rapidly decreased and quickly reached the

level where plasmolysis is expected to occur, leading to wilting (ψ_l < -1,5 MPa, Boyer 1968; Slatyer 1969; Porporato and Laio 2001). Increasing stomatal resistance indicated a rising degree of stomatal closure (Figure 3.12d). Stomata of tree 11 were already closing on the first day of drought (DOY 324, Figure 3.18) and the other drought treated tree start closing its stomata on the second day. It can be assumed that absolute stomatal closure followed on the third day. Drought stress hinders the photosynthesis through stomatal and non-stomatal limitation of which the former could be relatively small (Farooq et al. 2009). It could be seen that on DOY 325 total net photosynthetic rate (respiration – gross photosynthetic rate) was only a fraction of the initial rate or the rate of the control treatment (Figure 3.12e and Figure 3.19) while stomatal closure was not yet complete. However, to correctly assign stomatal and non-stomatal limits of drought stress, extensive monitoring of the photosynthetic apparatus and its biochemical pathways is required. The negative photosynthetic rate from DOY 326 to 329 indicated net respiration. Hence, it could be assumed that the respiratory processes were only affected by the water deficit after the photosynthetic processes already diminished, which is in agreement with the sequence proposed by Hsiao and Acevedo (1974) and Porporato and Laio (2001) (Figure 4.8). When leaf water potential dropped below -2 MPa, leaves had lost their turgor and the leaf shedding process started (Figure 3.12 and Figure 3.13). Leaves became dry and the total leaf area rapidly decreased. After 9 days, the trees had shed most of their leaves and some of their branches.

Although it may seem that drought stress shuts down the life functions of plants one by one without the trees having any control over the occurrence and sequence, plants have developed various strategies to cope with and survive under suboptimal water supply. Different responses of drought as categorized by Farooq et al. (2009) are represented on Figure 4.9.

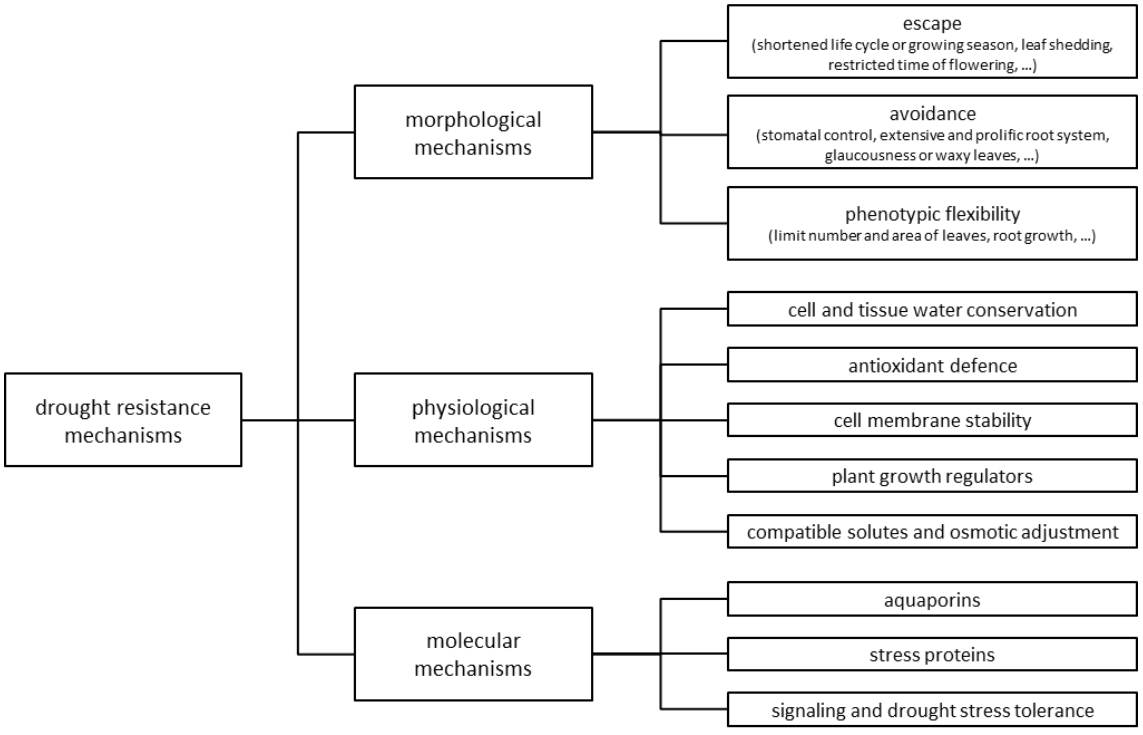

Figure 4.9 Mechanisms of plant drought tolerance at morphological, physiological and molecular levels (based on Farooq et al. (2009)).

The effects of drought stress on the *M. eminii* trees as described above were mostly morphological changes but could be driven by physiological mechanism (e.g. water content) and molecular mechanisms. In the case of *M. eminii* leaf shedding could be one of avoidance mechanisms. Indeed, *M. eminii* is known to be drought deciduous (Hall 1995). One could speak of an escape mechanism if the trees adjust their life cycle so that they don't have to face drought during the vulnerable life stages. Leaf shedding in this experiment could be seen as an avoidance mechanism where the plants avoid water loss if the initial avoidance mechanism of stomatal closure is not sufficient. Even when stomata are closed as a first response to drought and although transpiration through the epidermis is limited by the hydrophobic cutin layer, under severe drought and great water demand of the atmosphere, water may still be lost through the cuticula. By shedding their leaves, trees can limit the amount of water that can be lost to the atmosphere and which cannot be replaced by the uptake of soil water through the roots. Reducing the amount of leaves may be a key component of the plants adaptation of drought as a part of its phenotypic flexibility towards drought (Tyree et al. 1993, Farooq et al. 2009). The negative pressure gradient over the conductive system strongly increases under drought stress. Under such a high tension the water column can be broken by the nucleation of a micro-void which will expand explosively (Tyree and Ewers 1991). The cavitation fills the conduit component. Cavitation mostly is stopped at the pit membrane separating the conductive cells. Interruption of the pathway forces faster water transport in the remaining conduits, causing more vessels to cavitate. This runaway embolism can only be prevented or limited by lower transpiration rates. Once the conduit system is filled with air, they are not easily repaired to participate again in the water transport. Therefore it is often preferred to confine cavitation to the easily replaceable parts to safeguard the larger parts that represent long periods of investment in biomass production and growth (Tyree and Ewers 1991). The ability to reject distal, expendable organs such as leaves and small branches in favour of the larger organs is inherent to the plants hydraulic structure. Zimmermann (1983) proposed the hypothesis of hydraulic segmentation that states that segmentation is caused by declining diameter and proportionally more vessels ends in junctions. Hence, greater resistances cause a large potential gradient in shoots and leaves. The mechanism of hydraulic segmentation can only confine cavitation to distal organs if there is significant transpiration and larger stems are not more vulnerable to cavitation than distal branches and leaves (Tyree and Ewers 1991). The latter made that Tyree and Ewers (1991) proposed the hypothesis of vulnerability segmentation. If distal parts are more vulnerable (cavitate at a smaller decrease in water potential) the hydraulic segmentation is unnecessary. To determine the exact mechanism that caused *M. eminii* to shed leaves and small branches, water potentials should be evaluated together with transpiration rates and conductivities so that vulnerability curves (loss of conductivity of the segment in function of water potential) can be determined (Tyree et al. 1993).

The leaf shedding process and the root pressure occurrence suggested that the trees tried to maintain optimal water status in their trunk as if they were in a state of dormancy. Indeed, the trees could rapidly respond to rehydration when irrigation was supplied on DOY 338. Except for sap flow rate and stem diameter variation there were no extra measurements made during the recovery period. However, after two weeks (DOY 252), new leaves were observed on the stem and at the top of tree 11 (Figure 3.15 and Figure 3.16). The ability to produce new biomass after a period of drought without normal photosynthetic carbon assimilation indicated the presence of considerable amounts of living tissue containing plant reserves. As suggested earlier, intermediate abundance of parenchyma cells could be confirmed by the CT scans and the literature. The sprouting of new leaves

and branches coincided with the resumption of sap flow. That is, as is shown on Figure 3.11, only for tree 11. It seemed that tree 12 did not recover from the water deficit, in any case not before the end of the experiment. At the end of the experiment tree 11 resumed its sap flow to the same rates as the beginning of the experiment whereas for tree 12 no considerable sap flow could be observed. There was very little diurnal shrinkage and swelling observed for both trees until DOY 326. This could be an indication that stem water storage could not be sufficiently replenished until then. The first net stem diameter increment can be observed for tree 11 from DOY 38 (2014). Although the diurnal dynamics of tree 12 returned as well, a net shrinkage was observed from DOY 38 (2014). Zweifel et al. (2001) described how depletion of living tissue is reversible as long as the water potential of the cell water does not decrease below a cell-damaging level. It is possible that water potential of the storage cells of tree 12 was low enough to cause irreversible damage. Maybe even, the xylem tissue was cavitated to some extent so that resumption of the water transport was hindered. The return of diurnal dynamics could be declared by reactivating or renewing of the living tissue, maybe driven by root pressure. In order to fully assess the recovery of the trees after drought, a more quantitative analysis of the period after rewatering is required. The contradictious observations on tree 11 and 12 put forward that *M. eminii* may be resilient to drought but not guaranteed. Above that, even though tree 11 seemed to be fully recovered, the duration of recovery, approximately 75 days, was much longer than the drought period itself which lasted only 14 days.

4.3 WAS IT POSSIBLE TO PIN-POINT OUT THE LINK TO WOOD ANATOMY?

As a first attempt to simultaneously assess the physiological and wood anatomical effects of drought on *Maesopsis eminii*, the outcome was satisfying. We have established that *Maesopsis eminii* does form a distinguishable and demarcated amount of morphological modified wood in response to cambial wounding with a fine needle. Hence, *M. eminii* proved to be a suitable species to investigate cambial dynamics through the pinning method. X-ray tomography allowed easy study of the pinning regions in three dimensions. Extracting the wood fragment just around the pin mark and longer scan time would result in very high resolution and probably lead to an even more complete assessment of wound wood formation in the species. However, as described in section 3.6.1, the location of cambial initials at the time of pinning could be estimated at lower resolutions. The mechanical and morphological damage was confined to the area around the pinning (Figure 3.19). Therefore, it could be assumed that the spacing between pinnings used in this work was adequate to prevent converging effects of the pinnings. At first sight it can be stated that the pinnings did not strongly influence any physiological features or their measurements. With X-ray scanning the sample is not destructed, which was a strong advantage since the same samples could be scanned green and conditioned. On the scans of the conditioned samples of the control treatment (Figure 3.26) it was possible to allocate wood formation to specific periods, being the period before drought was imposed (difference between pinning 1 and 2), the period that the other trees received the drought treatment (pinning 2 to 3) and the recovery period (3 to bark). Using the relative measurements, the amount of wood formed in the drought period was less clearly identifiable. However, to compare wood formation in different samples and at different locations in the samples it is preferred to use the relative measurements that take into account the possible eccentricity of the stems. The drought period lasted only to weeks. It can be assumed wood formation during this short period actually was small and that the observation of little wood formation is logically. From the scans of the conditioned samples of the drought treatment clearly could be observed that the drought treatment had a distinct effect on wood formation. There was no difference between the second and the third

pinning, indicating no wood formed during the drought treatment. Also, no wood was observed anterior to the pin marks, indicating that there was no wood formed during the recovery period. This may contradict the net positive stem diameter variation that was observed during the last two weeks before harvest (DOY 44 - 56 2014, Figure 3.11). However, it was already suggested that the recovery of the trees was very variable from tree to tree and limited in general. The wood anatomical findings could confirm that outcome. To adequately link physiological measurements to the wood anatomical measurements it is desired to obtain the anatomical measurements on samples that are in similar state as they were when the physiological data were taken, *i.e.* living tissue. Sadly, measuring on the green samples was cumbersome due to the high X-ray absorbance of the abundant water resulting in vague grey areas on the scans. Although it was possible to copy the rough delineation of wound wood and the bark from the conditioned to the green images (Figure 3.27), measurements were less accurate. Still, the results were valuable since they not only revealed the same pattern as on the dry scans, they also showed that the absolute thickness of the bark is larger for the control treatment (Figure 3.28). This may indicate that the control trees had more living tissue, hence more water storage capacity. This coincides with the findings on the physiological measurements on diameter and sap flow. This also indicates that the assumption of constant bark thickness that was made to estimate the over-bark diameter at the time of pinning (see section 2.4.2.3) was incorrect. The overestimation of bark thickness could have caused that estimations of the diameter were always larger than the calliper measurements at the time of pinning. Different results between the estimated and the measured diameters could also have originated from the positioning of the calliper. Although it was intended, calliper measurements probably were not made perfectly in the direction of the pinning. This was confirmed by measuring the dry diameter of the dry samples in the directions of the pinning which mostly differed from the diameter measurements on the dry scans. However, as presented in Figure 3.29, estimation of the diameter on the scans always exceeded the calliper measurements, confirming that the difference could be considered as an overestimation. In large trees, a wood sample can be taken left and right from the pinning at the time of pinning to determine the thickness of the bark. This could be easily executed using a Pressler bore. If estimation of the diameter could be improved, anatomical features could be properly linked to stem diameter variations leading to a more precise timing of wood formation so that it can be evaluated at the same time of physiological measurements. For now, in this experiment, the broad timing of growth could be determined and the growth measurements did confirm the findings of the physiological research.

The *M. eminii* trees proved to be resilient to drought. Therefore, as drought resilient species, they could become of great importance in regions where longer and more severe periods of droughts are predicted due to climate change. However, drought clearly had an effect on the *M. eminii* trees. During and a long time after the drought period no wood could be formed because the plant had poor water conditions and there was no photosynthetic assimilation to sustain biomass production. Since *M. eminii* is regarded as a timber species, poor wood formation is very undesirable. In this research, wood anatomical analysis confined to growth measurement. More detailed study of the anatomy and evaluation of macroscopic features (e.g. mechanical tests) are required to determine the effect on the quality of the timber. Also the ecosystem service of carbon sequestration can be jeopardized by minor wood formation due to longer droughts occurs at large scale.

5 CONCLUSIONS

Maesopsis eminii showed interesting physiological behaviour. Diurnal courses of both sap flow rate and stem diameter variation deviated from the expected patterns that are described in the literature. The occurrence of low night time sap flow, most likely driven by root pressure, was put forward. Considerable sap flow rates could be observed several hours before sunrise. This night time sap flow is of great importance in the daily plant-water relations. Above that, root pressure is considered as one of the key resistance mechanisms to drought of *M. eminii*. The stem heat balance to measure sap flow rates was not suitable to measure the proposed low sap flow rates and monitored no sap flow during drought. However, re-evaluation of the SHB calculations, exposed strong indications of the existence of low sap flow dynamics during drought stress. Rapid leaf shedding after drought inducement prevented irreversible damage to the xylem conduction system. Together with the capacity of root pressure, it assured that the trees could maintain optimal water and reserves status in their trunk. After rehydration, trees responded by the production of new leaves, which allowed the resumption of water dynamics and growth.

It was possible to identify and demark wound formation caused by the pinnings on micro CT slices of the stems. This was used to investigate the difference in growth between the control and the drought treatment. On the scans of the control treatment it was possible to distinguish all three pinnings and the wood that was formed between them. The analysis of the drought treatment showed that no wood was formed during and after the drought period. The trends observed in the growth patterns, thus confirmed the physiological findings. Precise localisation of the cambial initials at the time of the pinning could be improved but as a first attempt to establish the link between the two perspectives on plant responses to drought, the outcome was very satisfactory since the pinning-method was suitable to link the physiological outcomes to wood formation.

Maesopsis eminii was limitedly resistant to the drought that was imposed. During drought, the water conditions of the plants were poor and there was no wood formation during and after the drought. However, some of the trees managed to resume sap flow and produce new biomass (leaves, branches) after the drought period.

6 FURTHER RESEARCH

The pot experiment was very interesting and useful to gain fundamental knowledge on the plant-water relations, the growth and the link between them on a tropical tree species. However, a pot experiment is not completely representative for real field conditions. Actual field conditions are considerably more complex, especially under drought stress which is the simultaneous reaction of water limitation, increased temperature (heat waves) and increased radiation intensity due to the absence of clouds. As appeared from the assessment, roots probably have a major role in the drought resistance of *Maesopsis eminii*. Although, they did manage to escape and seek water, the root development was strongly restricted by the pots. Hence, it would be interesting to repeat the experiment in a natural environment for example on mature trees in a forest ecosystem. In this way the effect of actual droughts can be monitored to validate and complete the outcomes of the greenhouse experiment. Natural root development could be observed to examine the actual hydrotropic capacity of *Maesopsis eminii* and the influence on the root pressure. The advantage of performing the experiment on mature trees would not only be the representation towards natural forests and plantations. Also, it would have some inherent advantages to perform the measurements. Pinning on large trees is more convenient and has less influence on the plant. Also, it would allow determination of the bark thickness at the time of pinning. A direct application of the pot experiment could be the intentional droughts in *Maesopsis eminii* nurseries as a hardening treatment. In hardening management drought is used to force modification of functional characteristics to improve the avoidance mechanisms and adaptive changes of the plant so that it is more resilient to drought when it is transplanted. To predict the success and functioning of this management, the second part of this experiment should be extended. Plants should be more closely monitored during and after recovery by evaluating the same broad range of physiological and anatomical features. In addition the morphological changes of the plants could be interesting. Did the new leaves were smaller than the leaves before drought? How did the root system develop during and after drought?

The intesntion of this dissertation was to explore if uniting physiological and wood anatomical perspectives would lead to a better understanding of plant behaviour to drought. In this initial stage, the anatomical analysis was limited to observation of growth. In further research, this could be extended by an overall assessment of anatomical features in function of drought (e.g. the course of density, vessel width and abundance of parenchyma). Also the physiological measurements could be enhanced. By including transpiration measurements and monitor low sap flow rates using different sensors, the understanding of the plant water relations of *Maesopsis eminii* could be enhanced. The combination of the improved physiological and anatomical methods could lead to the unique possibility to correlate hydraulic relevant properties of transport cells to plant-water relations, providing a foundation for better predictions of tree behaviour towards changing environments.

REFERENCES

Allen, C. D., A. K. Macalady, H. Chenchouni, D. Bachelet, and N. Mcdowell. 2010. A global overview of drought and heat-induced tree mortality reveals emerging climate change risks for forests. Forest Ecology and Management 259:660–684.

Allen, R. G. R., L. S. L. Pereira, D. Raes, and M. Smith. 1998. Crop evapotranspiration-Guidelines for computing crop water requirements-FAO Irrigation and drainage paper 56. FAO, Rome 300:1–15.

Alley, R. B., T. Berntsen, N. L. Bindoff, Z. Chen, A. Chidthaisong, P. Friedlingstein, J. M. Gregory, G. C. Hegerl, M. Heimann, B. Hewitson, B. J. Hoskins, F. Joos, J. Jouzel, V. Kattsov, U. Lohmann, M. Manning, T. Matsuno, M. Molina, N. Nicholls, J. Overpeck, D. Qin, G. Raga, V. Ramaswamy, J. Ren, M. Rusticucci, S. Solomon, R. Somerville, T. F. Stocker, P. A. Stott, R. J. Stouffer, P. Whetton, R. A. Wood, and D. Wratt. 2007. IPCC, 2007: Summary for Policymakers. In: Climate Change 2007: The Physical Science Basis. Contribution of Working Group I to the Fourth Assessment Report of the Intergovernmental Panel on Climate Change [Solomon, S., D. Qin, M. Manning, Z. Chen, M. Marqu. Cambridge, United Kingdom and New York, NY, USA.

Amthor, J., and D. Baldocchi. 2001. Terrestrial higher plant respiration and net primary production. Pages 33–54 Terrestrial global productivity. Academic Press, Orlando, Florida, US.

Anderson, D. B. 1936. Relative Humidity or Vapor Pressure Deficit. Ecology 17:277–282.

Ani, S., and H. Aminah. 2006. Plantation Timber of Maesopsis Eminii. Journal of Tropical Forest Science 18:87–90.

Arend, M., and J. Fromm. 2007. Seasonal change in the drought response of wood cell development in poplar. Tree physiology 27:985–92.

Baert, A., and K. Steppe. 2013. Putting Two Water Transport Models to the Test under Wet and Dry Conditions. Acta Horticulturae 991.

Baranga, D. 2007. Observations on resource use in Mabira Forest Reserve , Uganda. African Journal of Ecology 45:2–6.

Bauch, J., and O. Dunisch. 2000. Comparison of growth dynamics and wood characteristics of plantation-grown and primary forest carapa guianensis in central amazonia. IAWA Journal 21:321–333.

Bell, C. J., and G. R. Squire. 1981. Comparative Measurements with Two Water Vapour Diffusion Porometers (Dynamic and Steady-State). Journal of Experimental Botany 32:1143–1156.

Blankenship, R. E. 2002. The Basic Principles of Photosynthetic Energy Storage. Pages 1–10 Molecular mechanisms of photosynthesis. Blackwell Science Ltd, Oxford, UK.

Boko, M., I. Niang, A. Nyong, C. Vogel, A. Githeko, M. Medany, B. Osman-Elasha, T. R., and Y. P. 2007. Africa. Climate Change 2007: Impacts, Adaptation and Vulnerability. Contribution of Working Group II to the Fourth Assessment Report of the Intergovernmental Panel on Climate Change, M.L. Parry, O.F. Canziani, J.P. Palutikof, P.J. van der Linden and C.E. Pages 433–467.

Bonan, G. B. 2008. Forests and climate change: forcings, feedbacks, and the climate benefits of forests. Science 320:1444–1449.

Boyer, J. S. 1968. Relationship of Water Potential to Growth of Leaves. Plant Physiology 43:1056–1062.

Bryukhanova, M., and P. Fonti. 2012. Xylem plasticity allows rapid hydraulic adjustment to annual climatic variability. Trees 27:485–496.

Buchholz, T., A. Weinreich, and T. Tennigkeit. 2010. Modeling heliotropic tree growth in hardwood tree species—A case study on Maesopsis eminii. Forest Ecology and Management 260:1656–1663.

Bush, M. B., J. R. Flenley, and W. D. Gosling. 2011. Tropical Rainforest Responses to Climate Change. Page 454 (M. B. Bush, J. R. Flenley, and W. D. Gosling, Eds.), 2nd edition. Praxis Publishing, Chichester, UK.

Cassab, G. I., D. Eapen, and M. E. Campos. 2013. Root hydrotropism: an update. American journal of botany 100:14–24.

Cochard, H., S. Forestier, and T. Améglio. 2001. A new validation of the Scholander pressure chamber technique based on stem diameter variations. Journal of Experimental Botany 52:1361–1365.

Collatz, G. J., J. T. Ball, C. Grivet, and J. A. Berry. 1991. Physiological and environmental regulation of stomatal conductance, photosynthesis and transpiration: a model that includes a laminar boundary layer. Agricultural and Forest Meteorology 54:107–136.

Coruzzi, G., and D. R. Bush. 2001. Nitrogen and carbon nutrient and metabolite signaling in plants. Plant physiology 125:61–4.

Cowan, I. R. 1965. Transport of water in the soil-plant-atmosphere continuum. Journal of Applied Ecology 2:221–239.

Dawson, T. E., S. S. O. Burgess, K. P. Tu, R. S. Oliveira, L. S. Santiago, J. B. Fisher, K. A. Simonin, and and A. R. Ambrose. 2007. Nighttime transpiration in woody plants from contrasting ecosystems. Tree Physiology 27:561–575.

Deslauriers, A., S. Rossi, and T. Anfodillo. 2007. Dendrometer and intra-annual tree growth: What kind of information can be inferred? Dendrochronologia 25:113–124.

Deslauriers, A., S. Rossi, A. Turcotte, H. Morin, and C. Krause. 2011. A three-step procedure in SAS to analyze the time series from automatic dendrometers. Dendrochronologia 29:151–161.

Dixon, H. H., and J. Joly. 1894. On the ascent of sap. Philosophical transactions of the Royal Society of London. Series B, Biological sciences 186:563–576.

Drew, D. M., and G. M. Downes. 2009. The use of precision dendrometers in research on daily stem size and wood property variation: A review. Dendrochronologia 27:159–172.

Dynamax Inc. 2005. Dynagage sap flow sensors:107.

Eapen, D., M. L. Barroso, G. Ponce, M. E. Campos, and G. I. Cassab. 2005. Hydrotropism: root growth responses to water. Trends in plant science 10:44–50.

Edwards, G., and D. A. Walker. 1983. C3, C4: Mechanisms, and cellular and environmental regulation, of photosynthesis. Blackwell Scientific Publications, Oxford, UK.

Farooq, M., A. Wahid, and N. Kobayashi. 2009. Plant drought stress: effects, mechanisms and management. Agronomy for Sustainable Development 29:185–212.

Field, C., J. Ball, and J. Berry. 1989. Photosynthesis: principles and field techniques. Pages 209–253 *in* R. W. Pearcy, J. R. Ehleringer, H. A. Mooney, and P. W. Rundel, editors. Plant physiological ecology; field methods and instrumentation. Chapman and Hall, London, UK.

Food and Agriculture Organisation of the United Nations. 2012. State of the World 's Forests 2012. State of the World's Forests:60.

Gallardo, M., R. B. Thompson, L. C. Valdez, and M. D. Fernández. 2006. Use of stem diameter variations to detect plant water stress in tomato. Irrigation Science 24:241–255.

Goldstein, G., J. L. Andrade, F. C. Meinzer, N. M. Holbrook, J. Cavelier, P. Jackson, and A. Celis. 1998. Stem water storage and diurnal patterns of water use in tropical forest canopy trees. Plant, Cell and Environment 21:397–406.

Government of Uganda. 2007. Uganda National Adaptation Programmes of Acion:73.

Gricar, J., M. Zupancic, K. Cufar, and P. Oven. 2007. Wood formation in Norway spruce (Picea abies) studied by pinning and intact tissue sampling method. Wood Research 52:1–9.

Grider, D. E., A. Wright, and P. K. Ausburn. 1986. Electron beam melting in microfocus X-ray tubes. Journal of Physics D: Applied Physics 19:2281.

Hall, J. B. 1995. Maesopsis eminii and its status in the East Usambara Mountains. EUCFP Techincal Report 13:40.

Hamilton, A. C., and R. Bensted-Smith (Eds.). 1989. Forest Conservation in the East Usambara Mountains, Tanzania. IUCN, Gland, Switzerland and Cambridge, UK.

Henzler, T., R. Waterhouse, A. Smyth, M. Carvajal, D. Cooke, A. Schaffner, E. Steudle, and D. Clarkson. 1999. Diurnal variations in hydraulic conductivity and root pressure can be correlated with the expression of putative aquaporins in the roots of lotus japonicus. Planta 210:50–60.

Herawati, E. 2010. Performance of Glued-Laminatd Beams Made from Small Diameter Fast-Growing Tree Species. Journal of Biological Sciences 10:37–42.

Herman, G. T. 2009. Fundamentals of Computerized Tomography: Image Reconstruction from Projections. Page 300. Springer, London, UK.

Herzog, K., R. Häsler, and R. Thum. 1995. Diurnal changes in the radius of a subalpine Norway spruce stem: their relation to the sap flow and their use to estimate transpiration. Trees 10:94–101.

Van den Honert, T. H. 1948. Water transport in plants as a catenary process. Discussions of the Faraday Society 3:146–153.

Hsiao, T. 1973. Plant responses to water stress. Annual review of plant physiology 24:519–570.

Hsiao, T. C., and E. Acevedo. 1974. Plant responses to water deficits, water-use efficiency, and drought resistance. Agricultural Meteorology 14:59–84.

Kozlowski, T., and C. Winget. 1964. Diurnal and seasonal variation in radii of tree stems. Ecology 45:149–155.

Krabel, D. 2000. Influence of sucrose on cambial activity. Pages 113–126 *in* R. A. Savidge, J. R. Barnett, and R. Napier, editors. Cell and Molecular Biology of Wood Formation. BIOS Scientific Publishers, Oxford, UK.

Kramer, P. J., and J. S. Boyer. 1995a. Water Relations of Plants and Soils. Academic Press, London, UK.

Kramer, P. J., and J. S. Boyer. 1995b. Stomata and Gas Exchange. Pages 257–282 Water relations of plants and soils. Academic Press, Waltham, Massachusetts.

Kramer, P., and J. Boyer. 1995c. The absorption of water and root and stem pressures. Pages 167–200 Water relations of plants and soils. Academic Press, Waltham, Massachusetts.

Laurance, W. F., and C. A. Peres (Eds.). 2006. Emerging Threats to Tropical Forests. Page 563. University of Chicago Press, Chicago.

Lawlor, D. W. 1993. Photosynthesis: molecular, physiological and environmental processes. Page 318. Longman Scientific & Technical, Harlow, UK.

Leuning, R., A. Tuzet, and A. Perrier. 2004. Stomata as part of the soil-plant-atmosphere continuum. Page 304 *in* M. Mencuccini, J. Grace, J. Moncrieff, and K. G. McNaughton, editors. Forests at the Land-Atmosphere Interface. Oxon, UK.

Lhomme, J. P., a. Rocheteau, J. M. Ourcival, and S. Rambal. 2001. Non-steady-state modelling of water transfer in a Mediterranean evergreen canopy. Agricultural and Forest Meteorology 108:67–83.

Lockhart, J. a. 1965. An analysis of irreversible plant cell elongation. Journal of theoretical biology 8:264–75.

Mcneely, J. A. 1994. Lessons from the past: forests and biodiversity. Biodiversity and Conservaton 3:3–20.

Mohr, H., and P. Schopfer. 1994. Plant Physiology. Springer-Verlag, Berlin.

Montagnini, F., C. Jordan, and F. Products. 2005. Importance of Tropical Forests. Pages 1–17 Tropical Forest Ecology: The Basis for Conservation and Management.

Nadezhdina, N. 1999. Sap flow index as an indicator of plant water status. Tree physiology 19:885–891.

Nalevanková, P., K. Střelcová, Z. Sitková, and M. Ježík. 2013. Dynamics of stem diameter under soil drought 2012: Response of mature European beech trees. Šiška B. et al.: Environmental changes and adaptation strategies.

Newton-Fisher, N. E. 1999. The diet of chimpanzees in the Budongo Forest Reserve, Uganda. African Journal of Ecology 37:344–354.

Nicholson, S. E. 1989. Sharon (1989) Long-term changes in African Rainfall.pdf. Weather 44:46–56.

Nobel, P. S. 1983. Biophysical Plant Physiology and Ecology. Page 608. W.H. Freeman, San Francisco, US.

Orwa, C., A. Mutua, R. Kindt, R. Jamnadass, and A. Simons. 2009. Agroforestree Database: a tree reference and selection guide version 4.0. http://www.worldagroforestry.org/af/treedb/.

Den Ouden, J., B. Muys, F. Mohren, and K. Verheyen. 2010. Bosecologie en bosbeheer. Pages 1–680. Uitgeverij Acco, Leuven.

Pagel, W. 2002. Joan Baptista Van Helmont: reformer of science and medicine. Cambridge University Press.

De Pauw, D. J. W., K. Steppe, and B. De Baets. 2008. Identifiability analysis and improvement of a tree water flow and storage model. Mathematical biosciences 211:314–32.

Pearce, D., F. E. Putz, and J. K. Vanclay. 2003. Sustainable forestry in the tropics: panacea or folly? Forest Ecology and Management 172:229–247.

Pimm, S. L., G. J. Russell, J. L. Gittleman, and T. M. Brooks. 2013. The Future of Biodiversity 269:347–350.

Plumptre, A. J. 1995. The importance of " seed trees " for the natural regeneration of selectively logged tropical forest 74:253–258.

Porporato, A., and F. Laio. 2001. Plants in water-controlled ecosystems: Active role in hydrologic processes and response to water stress: III. Vegetation water stress. Advances in Water Resources 24:725–744.

Proseus, T., J. Ortega, and J. Boyer. 1999. Separating growth from elastic deformation during cell enlargement. Plant physiology 119:775–84.

Qubit Systems Inc. 2009. Plant CO2 Analysis Package. Kingston, Canada.

Ritchie, J. T. 1981. Water dynamics in the soil-plant-atmosphere system. Pages 81–96 Plant and Soil. ICARDA, The Hague, The Netherlands.

Robert, E. M. R., N. Schmitz, J. A. Okello, I. Boeren, H. Beeckman, and N. Koedam. 2010. Mangrove growth rings: fact or fiction? Trees 25:49–58.

Saveyn, A., K. Steppe, and R. Lemeur. 2007. Daytime Depression in Tree Stem CO2 Efflux Rates: Is it Caused by Low Stem Turgor Pressure? Annals of Botany 99:477–485.

Schindelin, J., I. Arganda-Carreras, E. Frise, V. Kaynig, M. Longair, T. Pietzsch, S. Preibisch, C. Rueden, S. Saalfeld, B. Schmid, J.-Y. Tinevez, D. J. White, V. Hartenstein, K. Eliceiri, P. Tomancak, and A. Cardona. 2012. Fiji: an open-source platform for biological-image analysis. Nature methods 9:676–82.

Schmitt, U., R. Jalkanen, and D. Eckstein. 2004. Cambium dynamics of Pinus sylvestris and Betula spp. in the northern boreal forest in Finland. Silva Fennica 38:167–178.

Schnitzer, S. A., and F. Bongers. 2002. The ecology of lianas and their role in forests. TRENDS in Ecology & Evolution 17:223–230.

Scholander, P. F., H. T. Hammel, E. A. Hemmingsen, and E. D. Bradstreet. 1964. Hydrostatic Pressure And Osmotic Potential In Leaves Of Mangroves And Some Other Plants. Proceedings of the National Academy of Sciences of the United States of America 52:119–25.

Schulze, E.-D., J. Čermák, M. Matyssek, M. Penka, R. Zimmermann, F. Vasícek, W. Gries, and J. Kučera. 1985. Canopy transpiration and water fluxes in the xylem of the trunk of Larix and Picea trees — a comparison of xylem flow, porometer and cuvette measurements. Oecologia 66:475–483.

Seo, J. W., D. Eckstein, and U. Schmitt. 2007. The pinning method: From pinning to data preparation. Dendrochronologia 25:79–86.

Sherwin, H., and N. Pammenter. 1998. Xylem Hydraulic Characteristics, Water Relations and Wood Anatomy of the Resurrection Plant Myrothamnus flabellifolius Welw. Annals of Botany 81:567–575.

Slatyer, R. O. 1969. Physiological Significance of Internal Water Relations to Crop Yield. Pages 53–88 *in* J. D. Eastin, F. A. Haskins, C. Y. Sullivan, C. H. M. Van Bavel, and R. C. Dinauer, editors. Physiological Aspects of Crop Yield: Proceedings of a symposium sponsored by the University of Nebraska, the American Society of Agronomy, and the Crop Science Society of America, and held at the University of Nebraska, Lincoln, Nebr., January 10-24. American Society of Agronomy & Crop Science Society of America, Madison, US.

Smith, D. M., and S. J. Allen. 1996. Measurement of sap flow in plant stems. Journal of Experimental Botany 47:1833–1844.

Steppe, K., and R. Lemeur. 2007. Effects of ring-porous and diffuse-porous stem wood anatomy on the hydraulic parameters used in a water flow and storage model. Tree physiology 27:43–52.

Steppe, K., R. Lemeur, and R. Samson. 2002. Sap flow dynamics of a beech tree during the solar eclipse of 11 August 1999. Agricultural and Forest Meteorology 112:139–149.

Steppe, K., D. J. W. De Pauw, and R. Lemeur. 2008a. Validation of a dynamic stem diameter variation model and the resulting seasonal changes in calibrated parameter values. Ecological Modelling 218:247–259.

Steppe, K., D. J. W. De Pauw, and R. Lemeur. 2008b. A step towards new irrigation scheduling strategies using plant-based measurements and mathematical modelling. Irrigation Science 26:505–517.

Steppe, K., D. J. W. De Pauw, R. Lemeur, and P. a Vanrolleghem. 2006. A mathematical model linking tree sap flow dynamics to daily stem diameter fluctuations and radial stem growth. Tree physiology 26:257–73.

Sunderlin, W. D., A. Angelsen, B. Belcher, P. Burgers, R. Nasi, L. Santoso, and S. Wunder. 2005. Livelihoods, forests, and conservation in developing countries: An Overview. World Development 33:1383–1402.

De Swaef, T., S. M. Driever, L. Van Meulebroek, L. Vanhaecke, L. F. M. Marcelis, and K. Steppe. 2013a. Understanding the effect of carbon status on stem diameter variations. Annals of botany 111:31–46.

De Swaef, T., J. Hanssens, A. Cornelis, and K. Steppe. 2013b. Non-destructive estimation of root pressure using sap flow, stem diameter measurements and mechanistic modelling. Annals of botany 111:271–282.

De Swaef, T., K. Steppe, and R. Lemeur. 2009. Determining reference values for stem water potential and maximum daily trunk shrinkage in young apple trees based on plant responses to water deficit. Agricultural Water Management 96:541–550.

Taiz, L., and E. Zeiger. 2010. Plant Physiology. Sinauer Associates Inc., Sunderland, USA.

Takahashi, H. 1997. Hydrotropism: The current state of our knowledge. Journal of Plant Research 110:163–169.

Takahashi, N., Y. Yamazaki, A. Kobayashi, A. Higashitani, and H. Takahashi. 2014. Hydrotropism Interacts with Gravitropism by Degrading Amyloplasts in Seedling Roots of Arabidopsis and Radish 1:805–810.

Tyree, M. 1997. The cohesion-tension theory of sap ascent: current controversies. Journal of Experimental Botany 48:1753–1765.

Tyree, M. T., H. Cochard, P. Cruiziat, B. Sinclair, and T. Ameglio. 1993. Drought-induced leaf shedding in walnut: evidence for vulnerability segmentation. Plant, Cell and Environment 16:879–882.

Tyree, M. T., and F. W. Ewers. 1991. The hydraulic architecture of trees and other woody plants. New Phytologist 119:345–360.

United Nations. 2009. State of the World ’s Indigenous Peoples. Economic & Social Affairs.

Vandegehuchte, M., and K. Steppe. 2012. Sap-flux density measurement methods: working principles and applicability. Functional Plant Biology 40:213–223.

Vermeulen, K., K. Steppe, K. Janssen, P. Bleyaert, J. Dekock, J. Aerts, D. Berckmans, and R. Lemeur. 2007. Technology and Product Reports. HortTechnology 17:220–226.

Viisteensaari, J., S. Johansson, V. Kaarakka, and O. Luukkanen. 2000. Is the alien tree species Maesopsis eminii Engl. (Rhamnaceae) a threat to tropical forest conservation in the East Usambaras, Tanzania? Environmental Conservation 27:76–81.

Vlassenbroeck, J., B. C. Masschaele, M. Dierick, V. Cnudde, Y. De Witte, K. Pieters, L. Van Hoorebeke, and P. Jacobs. 2007. Recent developments in the field of X-ray nano- and micro-CT at the Centre for X-ray Tomography of the Ghent University. Microscopy and Microanalysis 13:184–185.

Webb, N., T. Bragg, R. Spencer, J. Wood, C. Nicholl, and E. Potter. 1990. AP4 porometer user manual. Cambridge, England: Delta-T Devices Ltd.

Wildenschild, D., C. Vaz, and M. Rivers. 2002. Using X-ray computed tomography in hydrology: systems, resolutions, and limitations. journal of Hydrology 267:285–297.

Yoshimura, K., S. Hayashi, T. Itoh, and K. Shimaji. 1981. Studies on the Improvement of the Pinning Method for Marking Xylem Growth I.: Minute Examination of Pin Marks in Taeda Pine and other Species. Wood research: bulletin of the Wood Research Institute Kyoto University 67:1–16.

Zimmermann, M. H. 1983. Xylem Structure and the Ascent of Sap. Springer-Verlag, Berlin.

Zweifel, R., and R. Häsler. 2001. Dynamics of water storage in mature subalpine Picea abies: temporal and spatial patterns of change in stem radius. Tree physiology 21:561–9.

Zweifel, R., H. Item, and R. Häsler. 2000. Stem radius changes and their relation to stored water in stems of young Norway spruce trees. Trees 15:50–57.

Zweifel, R., H. Item, and R. Häsler. 2001. Link between diurnal stem radius changes and tree water relations. Tree physiology 21:869–77.